

14th International Conference  Physics of  
5th Autumn School  Advanced Materials

# Abstract Book PAMS-5



September 8-15, 2022  
Dubrovnik, Croatia  
[www.icpam.ro](http://www.icpam.ro)

# **PAMS-5**

**5<sup>th</sup> Autumn School on Physics of Advanced  
Materials**

**September 8-15, 2022, Dubrovnik, Croatia  
[www.icpam.ro](http://www.icpam.ro)**

## **Daily Program and Abstracts**

**Aurelian Rotaru**

**Daniel Moraru**

**Cover: Dragos Dutu**



The 14<sup>th</sup> International Conference on Physics of Advanced Materials (ICPAM-1) continues the tradition of the previous conferences organized by the Faculty of Physics of Alexandru Ioan Cuza University of Iasi at every four years, since 1980, and at every two years since 2012.

Beginning with 2012, the conference has as co-organizers prestigious institutions. Due to their contribution, the scientific quality of the conference increased, the conference papers being published in special issues in *Materials Science and Engineering: B*; *Applied Surface Science*, *Thin Solid Films* and *Material Today: Proceedings*.

In 2014 the first autumn school on Physics of Advanced Materials, PAMS-1 was held in parallel with ICPAM-10. This event is focused on providing interdisciplinary expert training, involving both fundamental knowledge and current research topics. The fact that the school is organized in parallel with the conference assures a better interaction between the conference participants involved in different fields of physics of advanced materials and the participants attending the school. In the same year we began the collaboration with the 4<sup>th</sup> International Festival of NanoArt, promoting the art and science interaction.

Since 2016, beginning with ICPAM-11, the conference and the events hosted by the conference became itinerant.

For the first time, the 13<sup>th</sup> edition, the 4<sup>th</sup> Autumn School on Physics of Advanced Materials (PAMS-4), and the 5<sup>th</sup> International Festival of NanoArt were organized in a hybrid form.

Over 180 participants contributed with around 200 abstracts (ICPAM-13 and PAMS-4) for plenary, invited, oral and poster presentations.

Beginning with 2021 these events will be organized every year. We invite participants to publish their results, presented in the conference, in the special issues of Coatings, Materials and Nanomaterials journals. These journals are partners and sponsors at the same time, sustaining the conference and the autumn school.

The special Issues are:

**New trends in Functional Materials and Devices**, published by Coatings

**New developments in physics of advanced materials**, published by Materials

**New Achievements in Nanostructured and Low Dimensional Materials and Systems**, published by Nanomaterials.

**Novel Materials with Target Functionalities** published in the open access journal Nanomaterials.

Manuscripts should follow the instructions and the deadlines given on <https://icpam.ro/papers-publication/>.

We would like to thank all participants for their important scientific contribution and the sponsors and partners for their support.

## ICPAM-14, PAMS-5 General Chairs

**Felicia IACOMI**, Alexandru Ioan Cuza University of Iasi,  
Romania

**Valentin CRACIUN**, National Institute for Laser, Plasma and  
Radiation Physics, Magurele, Romania

**Romulus TETEAN**, Babes Bolyai University, Cluj-Napoca,  
Romania

**Isabelle BERBEZIER**, Institute for Materials, Microelectronic  
and Nanosciences of Provence, France

**Marijana PECAREVIC**, University of Dubrovnik, Croatia

### Co-organizers:



## ICPAM-14, PAMS-4 Committees

### *Secretariate & IT & Communication*

Laura LACKO, Secretariate Manager

Dragos DUTU, Event planner

Madalin IONEL, Production Manager, Streambox

Marijana LUJO, University of Dubrovnik, Croatia

Marijana MILATIC, University of Dubrovnik, Croatia

Tihi BILAS, University of Dubrovnik, Croatia

Davorka TURCINOVIC, University of Dubrovnik, Croatia

Mislav CIMIC, University of Dubrovnik, Croatia

Cristina PACHIU, National Institute for R&D in  
Microtechnologies, Bucharest, Romania

Razvan HIRIAN, Babes-Bolyai University, Cluj-Napoca

Radu UDREA, Apel Laser, Bucharest

Stefan IRIMICIUC, National Institute for Laser, Plasma &  
Radiation Physics, Magurele, Romania

Roman ATANASOV, Faculty of Physics Babes-Bolyai University,  
Cluj-Napoca, Romania

Izabela BALASZ, Faculty of Physics Babes-Bolyai University, Cluj-  
Napoca, Romania

### *Organizing Committee*

Sanja TOMSIC, University of Dubrovnik, Croatia

Josip MIKUS, University of Dubrovnik, Croatia

Daniel TIMPU, Petru Poni Institute of Macromolecular  
Chemistry, Iași, Romania

Ioan DUMITRU, Alexandru Ioan Cuza University of Iasi, Romania

Liviu LEONTIE, Alexandru Ioan Cuza University of Iași, Romania

Mirela SUCHEA, National Institute of R&D for Microelectronics, Bucharest, Romania; Hellenic Mediterranean University, Heraklion, Greece

Shizutoshi ANDO, Tokyo University of Science, Tokio, Japan

Luc FAVRE, Institute for Materials, Microelectronic and Nanosciences of Provence Marseille, France

Violeta DEDIU, National Institute of R&D for Microelectronics, Bucharest, Romania

Aurelian ROTARU, Stefan cel Mare University of Suceava, Romania

Emmanuel KOUDOUMAS, Hellenic Mediterranean University, Heraklion, Greece

#### *Advisory Committee*

Kruno BONACIC, University of Dubrovnik, Croatia

Cristian SILVESTRU, Babes-Bolyai University, Cluj-Napoca, member of Romanian Academy

Bogdan C. SIMIONESCU, Petru Poni Institute of Macromolecular Chemistry, Iasi, member of Romanian Academy

Raluca MULLER, National Institute for R&D in Microtechnologies, Bucharest, Romania

Munizer PURICA, National Institute for R&D in Microtechnologies, Bucharest, Romania

Emil BURZO, Babes-Bolyai University, Cluj-Napoca, member of Romanian Academy

Nikolaos KATSARAKIS, Hellenic Mediterranean University, Heraklion, Greece

Jean-Noel AQUA, Institut des NanoSciences de Paris, France

Yoshimasa KAWATA, Shizuoka University, Hamamatsu, Japan



Norbert KUCERKA, Joint Institute for Nuclear Research,  
Russian Federation

Cristian FOCSA, University of Lille, France

## Conference topics and topics chairpersons

**T1:** Thin Films and Nanostructures for Modern Electronics

Daniel MORARU, Research Institute of Electronics, Shizuoka University

**T2:** Fundamentals of Plasma and Laser-Material Interactions and Processing

Ionut TOPALA, Alexandru Ioan Cuza University of Iasi, Romania

**T3:** Materials for Energy and Environment

Silviu COLIS, University of Strasbourg, France

**T4:** Magnetic Materials, Spintronics and Related Devices

Coriolan TIUSAN, Babes-Bolyai, Cluj-Napoca, Romania

Aurelian ROTARU, Stefan cel Mare University, Suceava, Romania

**T5:** Nanostructures and Low Dimensional Systems

Mathieu Abel, Institute for Materials, Microelectronic and Nanosciences of Provence, Marseille, France

**T6:** Emerging Electronic Memory Materials and Devices

Shashi PAUL, De Montfort University, Leicester, United Kingdom

**T7:** Polymer Materials and Composites

Valeria HARABAGIU, Petru Poni Institute of Macromolecular Chemistry, Romania

**T8:** Biomaterials and Healthcare Applications

Daniela UHRIKOVA, Comenius University, Bratislava

**T9:** Functional Materials. Processing and Characterization

Abdullah YILDIZ, Ankara Yıldırım Beyazıt University, Turkey

**T10:** New Developments in Sensing Materials and Sensor Devices

**Jan LANCOK**, Institute of Physics of the Czech Academy of Sciences, Czech Republic

**T11:** Trends in Condensed Matter Theory

**Liviu CHIONCEL**, Augsburg University, Germany

**T12:** Self-assembly and Patterning

**Joerg K. N. LINDNER**, Paderborn University, Germany

**T13:** Advanced photonic materials and devices

**Dana CRISTEA**, National Institute for Research and Development in Microtechnologies, Bucharest

**T14:** Waste materials and bioeconomy

**Branko GLAMUZINA**, University of Dubrovnik, Croatia

**Simona PINZARU**, Babes-Bolyai University Cluj-Napoca

**T15:** Materials in conservation-restoration of cultural heritage monuments and objects

**Josko BOGDANOVIC**, University of Dubrovnik, Croatia

## Sponsors

10



**NANO**TEAM



## Partners



**NANO**  
EXPRESS

**Thursday, September 08, 2022**

**Akademis Academia**

**Foyer**

16:00 Venue & Registration

18:00 Welcome Cocktail & "Microscopic Art in Science"

19:30 Dinner

08:00	<b>Registration</b>
08:20	<b>Opening</b> HALL 1-University of Dubrovnik
09:00	<b>Plenary Session</b> HALL 1
10:10	<b>Coffee break</b>
11:40	<b>Plenary Session</b> HALL 1
12:45	<b>Lunch</b>
15:00	<b>Invited and Oral Sessions</b> HALL 1, HALL 2
17:20	<b>Coffee break</b>
17:50	<b>Invited and Oral Sessions</b> HALL 1, HALL 2
19:30	<b>Dinner</b>

### **PL-online: Doping and interface effects on polarization of ferroelectric HfO<sub>2</sub>**

F. Sanchez

*Institut de Ciència de Materials de Barcelona (ICMAB-CSIC), Campus UAB,  
08193 Bellaterra, Spain*

Ferroelectric HfO<sub>2</sub> is a promising material for new memory devices, but the microstructure of the films needs to be better controlled and some properties such as endurance need to be improved. Research of ferroelectric HfO<sub>2</sub> has been focused mainly on polycrystalline films. Epitaxial films, of great interest to understand properties and prototyping devices, are now being investigated. In this talk I will show the impact of i) the epitaxial interface [1-3] and ii) doping (oxygen vacancies and cations) on the stabilization of the ferroelectric phase [3-5].

[1] T. Song, H. Tan, S. Estandia, J. Gazquez, M. Gich, N. Dix, I. Fina, F. Sanchez, **2022**, 4, 2337

[2] T. Song, S. Estandia, N. Dix, J. Gazquez, M. Gich, I. Fina, F. Sanchez, J. Mater. Chem. C **2022**, 10, 8407

[3] I. Fina and F. Sanchez, ACS Appl. Electron. Mater. **2021**, 3, 1530

[4] T. Song, H. Tan, R. Bachelet, G. Saint-Girons, I. Fina, F. Sanchez, ACS Appl. Electron. Mater. **2021**, 3, 4809

[5] T. Song, R. Solanas, M. Qian, I. Fina, F. Sanchez, J. Mater. Chem. C **2022**, 10, 1084

## **PL: High-resolution (S)TEM studies on self-organized nanostructures and materials**

14

J. K. N. Lindner

*Dept. of Physics and Center for Optoelectronics and Photonics Paderborn (CeOPP), Paderborn University, 33098 Paderborn, Germany*

Bottom-up techniques in nanopatterning of solid surfaces bare the inherent advantage in comparison to top-down methods such as light optical or electron beam lithography that they allow to fabricate myriads of periodically arranged nanoobjects in a highly parallel way and therefore allow to fabricate nanopatterns on large areas in short times and with little effort. Out of the different bottom-up techniques that have emerged in the last two decades, nanosphere lithography and block-copolymer lithography will be considered in detail in this presentation. The aim is to show what the state-of-the-art is with these techniques, which applications are possible and how these techniques can be combined to fabricate hierarchical nanostructures. Since the minimum feature size of nanostructures that can be obtained has reached the sub-ten nanometer range, it also has become ever more important to be able to characterize nanoobjects at ultimate spatial resolution, morphologically and chemically. For this, low-voltage analytical (scanning) transmission electron microscopy (S)TEM is employed, and examples will be given where in polymeric materials almost molecular resolution, in inorganic materials even sub-atomic resolution is achieved.

**PL: Scanning electron microscopy for nano-scale fabrication**

A. Dinescu<sup>1</sup>, M. Dragoman<sup>1</sup>, A. Muller<sup>1</sup>, Daniela Dragoman<sup>2</sup>

<sup>1</sup>IMT Bucharest, Romania

<sup>2</sup>Faculty of Physics, University of Bucharest, Romania

Many advances in fabrication processes at micro and nanoscale in the past two decades were possible due to scanning electron microscopy, which is now an indispensable tool for analyzing and fabricating new nanostructures and nanomaterials.

The development of very efficient in-lens detectors for SEM and the capability to use low energy electron probes are the gateway to the revelation of new features and new properties of nanomaterials that have been hidden by the use of high accelerating voltages and large interaction of volume, in the high-resolution SEM.

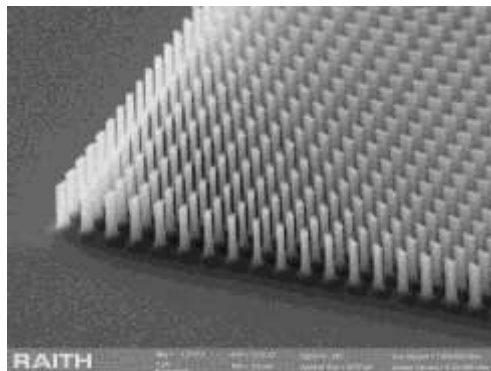


Fig. 1. DOE fabricated on silicon by electron beam lithography and cryogenic DRIE.



Electron beams have been used for lithography for decades and pattern generators can be fitted to all modern SEMs, converting them in very powerful nanolithographic tools, without degrading or limiting their imaging capabilities. The SEM became a very versatile tool for micro and nanofabrication, the same equipment used for fabrication being used to view the resulting nanostructures.

To illustrate the patterning capabilities of electron microscopy, the second part of the talk will be focused on fabrication of a few nanoelectronic devices, like field effect transistors on graphene [1,2] and on SOI wafers for quantum computing or diffractive optical elements (Fig.1).

[1] M. Dragoman, A. Dinescu, D. Dragoman, *Nanotechnology*, **2014**, 25(41), 415201.

[2] M. Dragoman, A. Dinescu, D. Dragoman, *IEEE Trans. Nanotechnol.*, **2018**, 17(2), 362-367.

### **PL: Versatile Plasmonic and Fluorescence-Based Nanoprobes for Optical Bioimaging and Light-Activated Therapy**

Simion Astilean<sup>1,2</sup>

*<sup>1</sup>Department of Bimolecular Physics, Faculty of Physics, Babes-Bolyai University, M Kogalniceanu Str 1, 40084, Cluj-Napoca, Romania*

*<sup>2</sup>Nanobiophotonics and Laser Microspectroscopy Center, Interdisciplinary Research Institute in Bio-Nano-Sciences, T. Laurian Str. 42, 400271, Babes-Bolyai University, Cluj-Napoca, Romania*

Optical nanoprobes are designed for monitoring biological events at the cellular levels via optical and spectroscopic signals in order to perform early detection, accurate diagnosis, and image-guided treatment of diseases. Due to several

advantages such as unique optical signature, easy surface functionalization and favorable pharmacokinetic feature, plasmonic and fluorescent nanoplatforms have been extensively investigated in recent years as new versatile optical nanoprobcs. In this presentation, we give an overview on our current approaches in fabrication plasmonic-based nanoplatforms and their implementation in a large variety of applications from cell imaging, drug delivery and light-activated nanotherapeutics. Since several years, our group has successfully synthetized a large variety of gold or silver nanoparticles with well-defined optical properties, providing the right size (2-100 nm), shape (sphere, rod, prism, star-like shape...), required biocompatibility and specific functionality to be translated into in vitro and in vivo studies. For instance, several classes of biocompatible "optically hot" biopolymer (chitosan, poly(ethylene) glycol, pluronic, gelatin...)-coated plasmonic nanoparticles were implemented as versatile nanoprobcs for spectroscopic investigation of cells by intracellular imaging via surface-enhanced Raman scattering (SERS), localized surface plasmon resonant scattering (LSPR-S) and steady-state and fluorescent lifetime imaging (FLIM). Scanning confocal Raman microscopy combined with dark-field and confocal fluorescence microscopy were used to record relevant intracellular information as nanoparticle localization, chemical interaction and pH mapping. In recent years, our research group has developed several "proofs of concept" for light-activated nanotherapies against cancer by integration into a single plasmonic nanoplatform of plasmon-induced photothermal therapy (PTT), plasmon-enhanced photodynamic therapy (PE-PDT) and delivery of chemotherapeutic drugs (doxorubicin, cisplatin) [1,2]. Currently, we focus on the

development of new organic and hybrid fluorescent nanoprobe with potential to serve as near-infrared (NIR) contrast agents for real-time image-guided surgery of ovarian cancer [3].

Aknowledgments. This work was supported by a grant of Ministry of Research and Innovation, CNCS-UEFISCDI, project number PN-III-P4-ID-PCCF-2016-0142, within PNCDI III.

[1]. M. Potara, T. Nagy Simon, A. M. Craciun, S. Suarasan, E. Licarete, F. I. Lucaci, S. Astilean, *ACS Appl. Mater. Interfaces* **2017**, 9, 32565–32576.

[2]. S. Suarasan, A-M Craciun, E. Licarete, M. Focsan, K. Magyari, S. Astilean, *ACS Appl. Mater. Interfaces*, **2019**, 11, 7812–7822.

[3]. R. Borlan, M. Focsan, et al. *Biomater. Sci.* **2021**, 9, 6183-6202

### **PL: Sustainable bio-based materials for non-conventional energy production and environment protection**

V. Harabagiu<sup>1</sup>, P. Samoila<sup>1</sup>, C. Cojocaru<sup>1</sup>, A.C. Enache<sup>1</sup>, S.F. Cosmulescu<sup>2</sup>, G. Predeanu<sup>3</sup>

<sup>1</sup>*Laboratory of Inorganic Polymers, “Petru Poni” Institute of Macromolecular Chemistry, Romanian Academy, 700487 Iasi, Romania*

<sup>2</sup>*S.C. COSFEL ACTUAL S.R.L., 010705 Bucharest, Romania*

<sup>3</sup>*Research Center for Environmental Protection and Ecotechnologies, University Politehnica of Bucharest, 011061 Bucharest, Romania*

Energy and environment related issues are, between others, acute challenges in the complex context of actual socio-economic development and of capital importance for the future of the human society. The vanishing fossil energy resources should be replaced, while friendly/sustainable technologies and materials for environment protection have to be imagined and developed.

In this respect, our research team revisited the properties of some regenerable polymeric materials of vegetal and animal origin and proposed simple approaches to yield polyelectrolyte membranes for fuel cells and sorbents for oil spills or for heavy metal cations from contaminated waters [1-4]. Details on the preparation methods and the properties of the resulted materials will be given.

Further, the project “Innovative and integrated recovery of biopolymer waste through intelligent microwave-assisted synthesis processes to obtain carbon materials for niche applications” (acronym, 4WASTEUPGRADE) aims:

- to build an innovative and integrated pilot line for preparation of activated carbons (ACs) through a microwave-assisted process;
- capitalizing some biopolymer/lignocellulosic wastes that are not currently exploited, such as: fruit seeds and shells;
- to demonstrate the feasibility of ACs on the designed pilot line and the performances of the as obtained ACs in wastewater treatment by adsorption and catalytic processes.

Acknowledgements. The support of European Regional Development Fund, Competitiveness Operational Programme 2014–2020; POC/163/1/3 – Project 4WASTEUPGRADE (Contract no. 386/390062/04.10.2021, MySMIS code: 120696) is gratefully acknowledged.

[1] A.C. Humelnicu, P. Samoila, M. Asandulesa, C. Cojocaru, A. Bele, A.T. Marinoiu, A. Sacca, V. Harabagiu, *Polymers* **2020**, 12(5) Art. no. 1125.

[2] P. Samoila, I. Grecu, M. Asandulesa, C. Cojocaru, V. Harabagiu, *React. Funct. Polym.* **2021**, 165, 104967.

[3] B.-C. Condurache, C. Cojocaru, P. Samoila, M. Ignat, V. Harabagiu, *Int J. Env. Sci. Technol.* **2022**, 19(1), 367-378.

[4] R. Rotaru, M.E. Fortună, C. Cojocaru, P. Samoilă, L. Pricop, V. Harabagiu, *Env. Eng. Manag. J.* **2019**, 18(6), 1193-1200.

## Invited Lectures (HALL 3)

### PAMS-L: Pulsed laser deposition

F. Sanchez

*Institut de Ciència de Materials de Barcelona (ICMAB-CSIC), Campus UAB, 08193 Bellaterra, Spain*

Pulsed laser deposition (PLD) is the most commonly used technique to grow thin films of complex oxides. PLD is considered simple, but understanding of the laser ablation mechanisms is necessary to take advantage of their benefits and avoid film off-stoichiometry. In this lecture, after a brief overview of the main thin film deposition techniques, I will first describe the laser ablation process and the properties of the generated plasma. Next, the main limitations and advantages of PLD will be discussed.

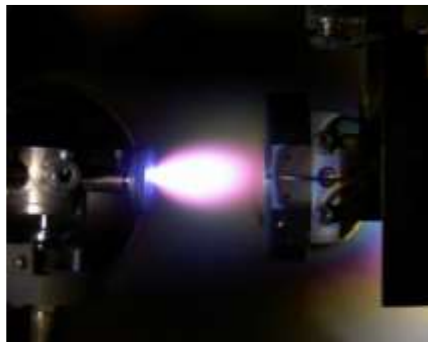


Fig. 1. Picture of a PLD plasma produced when an excimer laser beam ablates an oxide target (at the left of the image) under an oxygen atmosphere. The substrate heater can be seen at the right of the image.

Finally, the possibilities of in-situ control of epitaxial growth mechanisms when using in-situ reflection high-energy electron diffraction (RHEED) in PLD will be detailed.

In this lecture, after a brief overview of the main thin film deposition techniques, I will first describe the laser ablation process and the properties of the generated plasma. Next, the main limitations and advantages of PLD will be discussed. Finally, the possibilities of in-situ control of epitaxial growth mechanisms when using in-situ reflection high-energy electron diffraction (RHEED) in PLD will be detailed.

### **PAMS-L: Electron-beam technologies for micro and nano fabrication**

A. Dinescu<sup>1</sup>, M. Dragoman<sup>1</sup>, A. Muller<sup>1</sup>, Daniela Dragoman<sup>2</sup>

<sup>1</sup>*IMT Bucharest, Romania*

<sup>2</sup>*Faculty of Physics, University of Bucharest, Romania*

Since many years the electron beam proved to be a very versatile tool for a large variety of industrial applications: melting, evaporation, surface treatment, curing, surface treatment, machining, additive manufacturing, etc. In the field of micro and nano fabrication, the electron-beam technology provided the basis for three important techniques: microscopy (SEM and TEM), electron beam evaporation and electron beam lithography.

In this talk we will emphasize the role of the e-beam technology in micro and nanofabrication, for imaging, patterning and thin film deposition. The main topics are:

- Low voltage scanning electron microscopy for true surface imaging
- Electron beam nanolithography
- Fabrication of electrical contacts at micro and nanoscale by electron beam evaporation

The presentation will be illustrated with examples of various devices, such as: high frequency SAW filters, resonators, wireless temperature sensors and pressure sensors on GaN and AlN (1,2), graphene field effect transistors and other graphene devices (3,4), silicon FETs for quantum computing (fig.1), diffractive optical elements and other structures for nanophotonics etc.

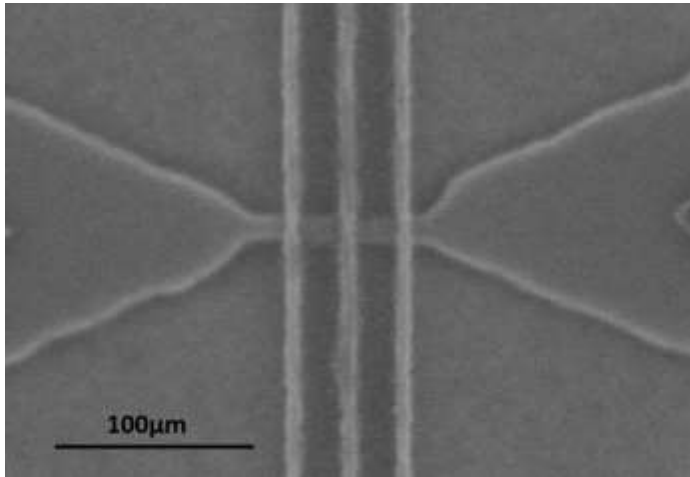


Fig. 1. Silicon qubit fabricated on SOI wafer

[1] A. Muller et al. IEEE Sensor J. **2017**, 17(22), 8052477, 7383-7393

[2] A. Muller et al., Electron Device Lett, **2015**, ,36(12),7305747, 1299-1302

[3] M. Dragoman, A. Dinescu, D. Dragoman, Phys. E: Low-Dimens. Syst. Nanostructures., **2018**, 97, 296–301

[4] M. Dragoman, A. Dinescu, D. Dragoman, IEEE Trans. Nanotechnol., 2018, 17 (2), 362-367.

## **PAMS-IL: Surface plasmons in metallic nanoparticles: from fundamentals to applications**

23

S. Astilean

*Department of Bimolecular Physics, Faculty of Physics, Babes-Bolyai University, M Kogalniceanu Str 1, 400084, Cluj-Napoca, Romania*

The course is focused on optical phenomena related to the electromagnetic response of metallic nanostructures. This subject has led to the development of an emerging and fast-growing research field called plasmonics which builds a bridge between micro- and nanoscale by confining light on sub-wavelength volumes. In the first part, we recall the classic physics of localized surface plasmon resonances (LSPR) by first considering the interaction of spherical metallic nanoparticles with an electromagnetic wave, in particular with light wave, in order to arrive at the resonance condition. Subsequently, we discuss plasmon resonances in nanoparticles of a variety of different shapes and sizes and the effects of interactions between particles in ensembles as well how metallic nanoparticles interact with their surroundings. The second part of the course is devoted to the progress in the fabrication of plasmonic nanoobjects in the last decade. Finally, we discuss several certain promises of plasmonics in nanotechnology, optoelectronics, photovoltaics and nanomedicine, in particular new possibilities to treat cancer and fabricate ultrasensitive molecular detectors.



### **T4-I: Soft magnetic composite powders and compacts obtained by mechanosynthesis and spark plasma sintering**

I. Chicinas<sup>1</sup>, T.F. Marinca<sup>1</sup>, F. Popa<sup>1</sup>, B.V. Neamtu<sup>1</sup>, L. Cotojman<sup>1</sup>, O. Isnard<sup>2</sup>

<sup>1</sup>Department of Materials Science and Engineering, Technical University of Cluj-Napoca, Cluj-Napoca, Romania

<sup>2</sup> Institut Néel, CNRS / Université Grenoble-Alpes, BP166, 38042 Grenoble, Cédex 9, France

High magnetic properties (magnetic flux density and magnetic permeability) and high electrical resistivity are required in many AC applications for magnetic cores, in order to reduce core losses. Usually, magnetic alloys based on Fe powder are coated with a thin dielectric, organic or inorganic layer [1]. To avoid the decrease in the magnetic properties of the material by the dielectric layer, we use a magnetic dielectric layer which consists of a layer of soft magnetic ferrite particles with the nanometric size, in order to electrically isolate the metal particles from each other [2].

The nanocrystalline Permalloy/Supermalloy powders were obtained by mechanical alloying in high planetary ball mill Fritsch Pulverisette 6. The milling time was up to 12 h and the mean crystallite size was 18-20 nm. In Fe-Ni@Me<sub>1</sub>Me<sub>2</sub>Fe<sub>2</sub>O<sub>4</sub> composite powders, the core is a large metal particle (Fe or nickel-iron alloy) and the shell is a pseudo-continuous layer of nanometric soft magnetic ferrite particles (NiFe<sub>2</sub>O<sub>4</sub>, Ni<sub>0.5</sub>Zn<sub>0.5</sub>Fe<sub>2</sub>O<sub>4</sub>, Mn<sub>0.5</sub>Zn<sub>0.5</sub>Fe<sub>2</sub>O<sub>4</sub>, Ni<sub>0.5</sub>Cu<sub>0.5</sub>Fe<sub>2</sub>O<sub>4</sub>). Composite particles with a pseudo-core-shell structure were prepared using acetone as the surfactant by mixing metal particles with

very small particles of ferrite and subsequent annealing to argon.

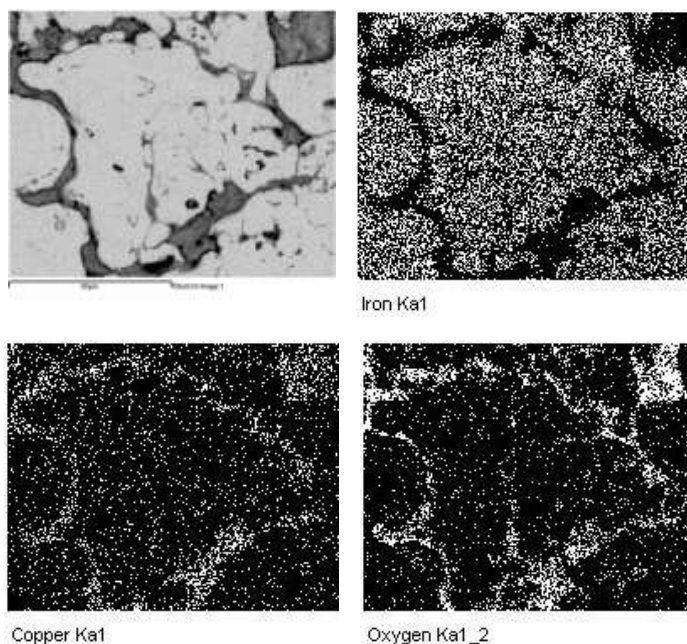


Figure 1 : SEM image on a section of SMC core and maps of distribution of Fe, Cu and O (EDX analysis)

The pseudo core-shell powders thus obtained were compacted by spark plasma sintering ( $400^{\circ}\text{C}$  -  $900^{\circ}\text{C}$ , 30 MPa, 0 - 10 minutes).

The powders and sintered compacts were studied by: X-ray diffraction, in-situ high-temperature X-ray diffraction, scanning electron microscopy, energy dispersive X-ray spectrometry, magnetic hysteresis measurements ( $M(H)$  and  $B(H)$ ) and electrical resistivity. In Fig. 1 can be observed that the alloy particles are surrounded by a pseudo-continuous layer of ferrite. A relative permeability of 75 at  $B = 0.7\text{ T}$  and 10 kHz was

obtained for Fe/CuFe<sub>2</sub>O<sub>4</sub> core. The electrical resistivity of SPS-ed composite cores is 3 to 4 orders of magnitude higher than the electrical resistivity of Fe-Si alloys.

[1] Robert W. Ward, David E. Gay, Composite iron material, US Patent No. 5,211,896/May 18, **1993**

[2] T.F. Marinca, B.V. Neamțu, F. Popa, V.F. Tarța, P. Pascuta, A.F. Takacs, I. Chicinaș, , Appl. Surf. Sci. **2013**, 285P, 2– 9.

#### **T4-I: The influence of Ni<sup>2+</sup> and Co<sup>2+</sup> ions doping on the magnetic properties of the MnFe<sub>2</sub>O<sub>4</sub>/SiO<sub>2</sub> nanocomposites**

T. Dippong<sup>1</sup>, R. Tetean<sup>2</sup>, I. G. Deac<sup>2</sup>

<sup>1</sup> *Department of Chemistry and Biology, Technical University of Cluj-Napoca, North University Center of Baia-Mare, Romania*

<sup>2</sup> *Facultatea de Fizica, Universitatea Babes-Bolyai, Cluj-Napoca, Romania*

We report on the influence of Ni<sup>2+</sup> and Co<sup>2+</sup> ions doping on the magnetic properties of the MnFe<sub>2</sub>O<sub>4</sub>/SiO<sub>2</sub> nanocomposites, obtained by various inovative routes. Saturation magnetization ( $M_S$ ), remanent magnetization ( $M_R$ ), squareness ( $S$ ), coercivity ( $H_C$ ), magnetic moment per formula unit ( $n_B$ ) and anisotropy constant ( $K$ ) were determined since they are key parameters for a magnetic material to be used in various applications. X-ray diffraction (XRD) indicated the presence of nanocrystalline mixed cubic spinel ferrites in the presence of several secondary phases. The crystallite sizes varie with the increase of the annealing temperature and with Ni and Co content. The shape of the hysteresis loops revealed the dependence of magnetic behavior on the structural properties. The saturation magnetization and coercivity increase with the degree of crystallinity, crystallite size and annealing temperature for the both Ni and Co containing systems. The coercive field behaves

differently for different heat treatment temperatures, increasing for 800 °C and decreasing for 1200 °C with increasing Mn content.

The Ni-rich nanocomposites show superparamagnetic-like behavior, while the Mn-rich nanocomposites have paramagnetic behavior. For the Ni containing samples, the main magnetic parameters  $M_s$ ,  $M_R$ ,  $n_B$  and  $K$  increase, while  $H_c$  decreases with increasing Ni content. NCs annealed at 1200 °C have increased  $M_s$  (16.0-45.8 emu/g),  $M_R$  (4.5-16.8 emu/g), and  $K$  (2.876-5.430 erg/dm<sup>3</sup>). The  $H_c$  (265-175 Oe), decreases with increasing Ni content at 1200 °C [1]. The different behavior of these samples from the un-coated Mn(Ni;Co)Fe<sub>2</sub>O<sub>4</sub> particles came from the SiO<sub>2</sub> matrix and from the preparation routes [2]. For the Co doping samples, for 800 °C heat treatment temperature,  $M_s$  increase from 19.4 emu/g to 38.2 emu/g and  $K$  from 0.365 to  $1.32 \cdot 10^{-3}$  erg/cm<sup>-1</sup> while for 1200 °C  $M_s$  decreases from 32.6 emu/g to 18.3 emu/g. When Mn is replaced by Co the behavior is ferromagnetic-like for both low and high Co ions concentration. The magnetic properties were discussed in the frame of the collinear two-sublattices Néel's theory and of the non-collinear Yafet-Kittel model considering the presence of hematite and some other parasitic phases [1,2].

[1] T. Dippong, I.G. Deac, O. Cadar, E.A. Levei, *Nanomaterials* **2021**, 11, 3455.

[2] T. Dippong, M.D. Lazar, I.G. Deac, P. Palade, I. Petean, G. Borodi, O. Cadar, *J. Alloys Compd.* **2022**, 895, 162715.

## T4-I: Smart electronic devices based on molecular spin crossover compounds

A. Diaconu<sup>1</sup>, R. Cimpan<sup>1</sup>, G.-V. Ciobanu<sup>1</sup>, L. Salmon<sup>2</sup>, G. Molnar<sup>2</sup>, A. Bousseksou<sup>2</sup>, I. Seguy<sup>3</sup>, A. Rotaru<sup>1</sup>

<sup>1</sup>FIESC & Research Center MANSiD, USV, Suceava, Romania

<sup>2</sup>LCC, CNRS & Université de Toulouse (UPS, INP), Toulouse 31013, France

<sup>3</sup>LAAS, CNRS & Université de Toulouse INSA, UPS F-31077 Toulouse, France

Bistable molecular complexes that can exist in two interchangeable states can act as switches under external stimuli. In this context, molecular spin crossover (SCO) compounds present a special interest due to their response to various external stimuli that might lead to a wide range of potential applications [1].

This research highlights the spin transition properties of spin crossover complexes in various forms such as powder, thin films and polymeric composites. We focused on the spin crossover complex with the chemical formula  $[\text{Fe}(\text{Htrz})_2(\text{Trz})]\text{BF}_4$ . This complex shows a spin transition above room temperature, with a large hysteresis, which can be monitored by various detection techniques such as: magnetometry, dielectric spectroscopy, optical reflectivity etc. [2]. One important particularity of this system entails the spin state dependence of the electrical conductivity which opens new opportunities to use these materials in electronic and spintronic devices.

Thin films showing spin transition properties have been obtained by thermal evaporation. The SCO thin films have been integrated into both magnetic and non-magnetic metallic electrodes. The structures obtained with magnetic electrodes show a magnetoresistive effect.

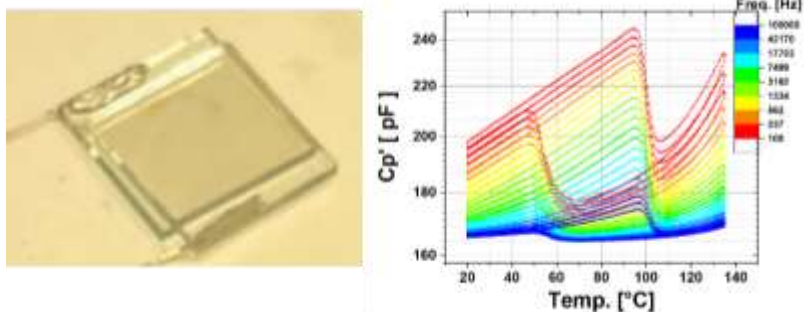


Fig. 1. (Left) SCO-PVP composite between two ITO electrodes and (Right) Temperature dependence of the capacitance.

The composites containing  $[\text{Fe}(\text{Htrz})_2(\text{Trz})]\text{BF}_4$  nanoparticles incorporated in PVP (Polyvinylpyrrolidone) matrix have been synthesized and studied by various techniques such as FE-SEM, EDX, AFM, dielectric spectroscopy, magnetometry, Raman, FTIR. The obtained composites are optically transparents preserving the spin transition properties.

Acknowledgments. This work was funded by UEFISCDI, project number PN-III-P1-1.1-TE-2019-2194 (Contract No: TE 123/2020).

- [1] A. Enriquez-Cabrera, et al., Coord. Chem. Rev., **2020**, 419, 213396
- [2] A. Diaconu, et al., J. Phys. Chem. Lett., **2017**, 8, 3147-3151.
- [3] C. Lefter, et al., Adv. Mater., **2016**, 28, 7508-7514.

#### **T4-I: A revision of Kittel's theory for ferromagnetic domains**

C. M. Teodorescu

*National Institute of Materials Physics, Atomistilor 405A, Măgurele – Ilfov, Romania*

Kittel's model for ferromagnetic domains [1,2] starts with a infinite sample extent over two directions and with and a finite

thickness  $d$ , though much larger than the typical domain size  $l$ , the domains being also infinite over the other in-plane direction. The surface magnetostatic energy density scales with  $M_0^2 l$  ( $\pm M_0$  being the magnetization of the domains) and the energy corresponding to  $180^\circ$  domain walls scales with  $w_{wall} d/l$ , where  $w_{wall}$  is the wall energy per unit area of the wall and it comprises the uniaxial magnetic anisotropy constant  $K_v$ , the exchange interaction between neighboring atoms  $J$  and the interatomic distance  $a$ ,  $w_{wall} \propto (JK_v/a)^{1/2}$ . By minimizing the total energy, one derives Kittel's scaling law of the domain size vs. the sample thickness  $l \propto d^{1/2}$ . Here we re-visit Kittel's theory of ferromagnetic domains, because in particular in Ref. [1], Kittel computes the average value of the square of the intensity of the magnetic field,  $\langle \int H^2 dz \rangle$ , while in Ref. [2] the scalar product between the magnetization and the intensity of the magnetic field  $\langle - \int \mathbf{H} \cdot \mathbf{M} dz \rangle$  is computed. One needs to take into account the dipolar interaction energy, responsible for the shape anisotropy.

Some values derived by Kittel must be corrected, but the most important fact is that the magnetostatic volume density energy has to be written as [3]:  $w = (\mathbf{B} \cdot \mathbf{H})/2 = (\mu_0 H^2)/2 + (\mu_0 \mathbf{M} \cdot \mathbf{H})/2$ . This means that one has to consider the energy from Ref. [1] with the energy from Ref. [2] with minus sign, thus in the approximation  $l \ll d$  the total magnetostatic energy yields zero value! This finding requires a more detailed derivation of the magnetostatic energy. This can be easily achieved if one considers all solutions for the intensity of the magnetic field inside and outside the sample. An important parameter with dimensions of distance comprises the magnetic anisotropy energy, the exchange integral, the spin of one atom  $S$  and the interatomic distance  $a$   $d_0 = \pi^3 (2JK_v a^{11})^{1/2} / (32S\mu_0\mu_B^2)$ , where it

was supposed that  $M_0 \approx 2S\mu_B a^{-3}$ , i. e. one spin  $S$  carries a magnetic moment  $2S\mu_B$  ( $\mu_B$  is the Bohr magneton), the gyromagnetic factor is 2 and this magnetic moment corresponds to a volume  $a^3$  of the sample. This parameter has the value of about 0.8 nm for  $a \approx 2.5 \text{ \AA}$ ,  $J \approx 10 \text{ meV}$ ,  $K_v \approx 2 \text{ } \mu\text{eV/atom}$ ,  $S \approx 1$ . For  $d \lesssim d_0$ , the minimization of the energy yields the validity of Kittel's scaling law, whereas for  $d \gtrsim d_0$  the dependence  $l(d)$  is almost linear. The same is obtained when the dipole-dipole interactions are included. On the other hand, experimental data on samples with perpendicular magnetocrystalline anisotropy [4] reported the validity of Kittel's scaling law up to sample thicknesses of hundreds of nanometers or even some micrometers. This means that the  $d_0$  parameter is in the same range, which implies that the magnetic anisotropy energy is of some meV/atom. This is in line with theoretical previsions, where the magnetic anisotropy energy is in the range of the spin-orbit interaction [5].

In this case, the Stoner-Wohlfarth model fails to describe the hysteresis cycle of most solids. The coercive field should be in the range of  $2K_v/M_0$ , yielding tens of Tesla. The Curie-Weiss mean field theory also fails to explain the coercive field in ferromagnets, its order of magnitude being of  $J\eta S/\mu_B$ , hundreds of Tesla for usual systems.

Kittel's model was adapted in the case of successive ferromagnetic domains with alternating sizes. Hysteresis cycles are derived in several hypotheses, by considering or not the dipolar interaction, or assuming or not the domain average size dependence on the applied field. Some models are able to predict non-rectangular hysteresis cycles with shapes quite similar to experimental ones [4,6], but the smallest coercive field is in the range of  $\mu_0 M_0/4$  ( $\mu_0$  is the vacuum permeability)



which is still too elevated with respect to experimental values (it yields some Tesla). Therefore none of the three basic models (Curie-Weiss mean field theory, Stoner-Wohlfarth theory of magnetization rotation in small magnetic nanoparticles, domain wall migration theory) is able to predict the small values observed in the coercive fields of most ferromagnetic materials. Band ferromagnetism could offer an explanation for the smallness of coercive fields [7].

The actual theory is discussed also for the case of ferroelectrics.

- [1] C. Kittel, Phys. Rev. **1946**, 70, 965–971.
- [2] C. Kittel, Rev. Mod. Phys. **1949**, 21, 541–583.
- [3] J.D. Jackson, Classical Electrodynamics, Third Edition, Wiley, Hoboken, **1999**.
- [4] O. de Abril, M. del Carmen Sánchez, C. Aroca, J. Appl. Phys. **2006**, 100, 063904.
- [5] G. van der Laan, J. Phys. Cond. Matt. **1998**, 10, 3239–3253.
- [6] L.-C. Garnier, M. Marangolo, M. Eddrief, D. Bisero, S. Fin, F. Casoli, M.G. Pini, A. Rettori, S. Tacchi, J. Phys.: Materials **2020**, 3, 024001.
- [7] C.M. Teodorescu, Res. Phys. **2021**, 25, 104241.

#### **T4-O-online: Spin current transport in multifunctional Pt/FeV<sub>2</sub>O<sub>4</sub> heterostructures**

A. Pena Corredor<sup>1</sup>, A. Anadon<sup>2</sup>, S. Petit-Watelot<sup>2</sup>, J. C. Rojas-Sanchez<sup>2</sup>, N. Viart<sup>1</sup>, D. Preziosi<sup>1</sup>, C. Lefevre<sup>1</sup>

<sup>1</sup>*Institute of Physics and Chemistry of Materials of Strasbourg (University of Strasbourg). Strasbourg, France*

<sup>2</sup>*Jean-Lamour Institute (University of Lorraine). Nancy, France.*

Iron vanadate, FeV<sub>2</sub>O<sub>4</sub> (FVO), is a strongly correlated oxide which displays low-temperature ferrimagnetism [1],

ferroelectricity [2] and multiferroism [3]. The material presents a strong spin-orbit coupling and both  $\text{Fe}^{2+}$  and  $\text{V}^{3+}$  cations are Jahn-Teller active. As a result, FVO adopts different crystal structures with varying temperatures, which are associated to different orbital orderings [4]. We have shown the possibility to grow epitaxial FVO films using a low Ar pressure [5], [6]. FVO films onto  $\text{SrTiO}_3$  (STO) single crystals present a perpendicular magnetic anisotropy, providing a promising platform for spintronics studies.

In the present work, we have grown Pt/FVO//STO heterostructures via pulsed laser deposition and engineered Hall bar geometries (Fig. 1a) via optical lithography. Angle-dependent magnetotransport measurements in both Spin Magnetoresistance (SMR) and Anisotropy Magnetoresistance (AMR) configurations have been carried out at several magnetic field and temperature values. The amplitude of the magnetotransport signals within temperature varies as FVO changes its structure and orbital ordering, showing thus a strong interaction between Pt and the FVO underneath. SMR was detected at all temperatures, even above the magnetic transition, and was found significantly larger ( $>1\%$ ) than that of better-known Pt/YIG heterostructures ( $\approx 0.1\%$ ) [7], other spinel-based systems ( $\text{Pt}/\text{Fe}_3\text{O}_4$ ,  $\approx 0.2\%$ ) [8] or other multifunctional oxides ( $\text{Pt}/\text{Ga}_{0.6}\text{Fe}_{1.4}\text{O}_3$ ,  $\approx 0.04$ ) [9]. Additionally, our SMR and AMR measurements show an unusual unidirectional-like (Fig. 1b) behaviour – difference between  $0^\circ$  and  $180^\circ$  – whose underneath microscopic mechanism might be linked to the presence of a non-zero spin-orbit coupling in FVO. The observed giant SMR signal in high-quality Pt/FVO heterostructures opens the door to spinel iron vanadates as

promising material platform for the next generation of oxide-based spintronics.

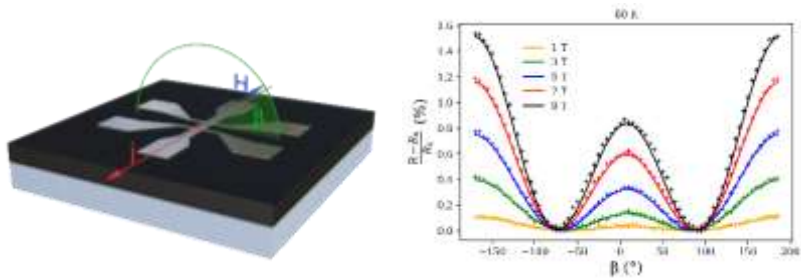


Fig. 1. (1a - left) Hall Bar lithographed on Pt/FVO/STO. (1b - right) angle scan for the characterisation of the Spin Magnetoresistance.

- [1] G. J. MacDougall, et al. Phys. Rev. B, **2012**, 86, 6, 060414.
- [2] K.-H. Zhao, et al. Chinese Phys. Lett., **2015**, 32, 8, 087503.
- [3] M. V. Eremin et al. Phys. Rev. B, **2019**, 100, 14, 140404.
- [4] W. Xie et al. J of Appl. Phys., **2019**, 26, 24, 244904.
- [5] F. Roulland et al. Materials Chemistry and Physics, **2022**, 276, 125360.
- [6] A. Pena Corredor et al. J Appl Crystallogr, 2022, 55, 3, 526-532.
- [7] M. Althammer et al., Phys. Rev. B, **2013**, 87, 22, 224401.
- [8] Z. Ding et al. Phys. Rev. B, 2014, 90, 13, 134424.
- [9] S. Homkar et al. ACS Appl. Electron. Mater., 2021, 3, 10, 4433-4440.

### T8-I: New biocomposites from waste materials

S. Cinta Pinzaru<sup>1,2</sup>, G. Lazar<sup>1,2</sup>, F. Nekvapil<sup>1,2</sup>, R. Hirian<sup>1</sup>, T. Tamas<sup>3</sup>, L. Barbu-Tudoran<sup>4,5</sup>, M. Suci<sup>4,5</sup>, M. Aluas<sup>1</sup>, I. Bajama<sup>1,2</sup>, D. A. Dumitru<sup>1,2</sup>, S. Tomsic<sup>6</sup>, B. Glamuzina<sup>6</sup>

<sup>1</sup>*Ioan Ursu Institute, Babes Bolyai University, Kogalniceanu 1, RO-400084 Cluj-Napoca, Romania*

<sup>2</sup>*RDI Institute in Applied Natural Science, Babes-Bolyai University, Fântânele 30, 400327, Cluj-Napoca, Romania*

<sup>3</sup>*Department of Geology, Babeş-Bolyai University, 1 Kogălniceanu, 400084 Cluj-Napoca, Romania*

<sup>4</sup>*Electron Microscopy Centre, Babeş-Bolyai University, Clinicilor 5-7, 400006 Cluj-Napoca, Romania*

<sup>5</sup>*Advanced Research and Technology Center for Alternative Energy, National Institute for Research and Development of Isotopic and Molecular Technologies, Donat 67-103, 400293 Cluj-Napoca, Romania*

<sup>6</sup>*Applied Ecology Department, University of Dubrovnik, Cira CariCa 4, 20 000, Dubrovnik, Croatia*

Our latest research results and outlook will be summarized to reveal amazing facets and properties of several biomaterials of aquatic, biogenic, origin. Their processing and reuse as added-value products such as new composites, new biostimulans, innovative drug carriers [1,2] will be highlighted (Fig. 1). The potential of such abundant materials for blue bioeconomy will be discussed. Formulations with improved biocompatibility and antioxidant character relying on organic-inorganic composite will be illustrated for new drug carriers or innovative biostimulants for slow release. Along the processing steps to obtain, refine, load porous materials with certain solutions and tableting or pelleting, the composite materials are investigated

using non-destructive Raman spectroscopy-based methods in conjunction with imaging and complementary techniques, such as XRD, SEM-EDX and others.

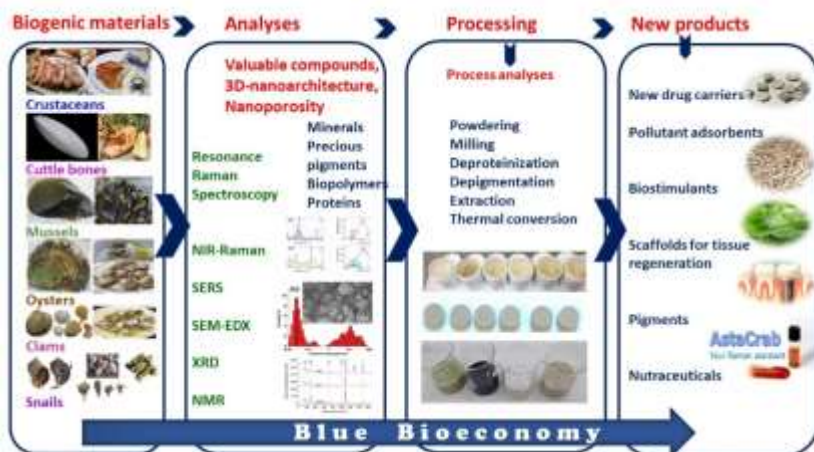


Fig. 1. Graphical sketch of knowledge-based transforming waste biogenic materials into added-value products following the blue bioeconomy principle.

We further show how the translational research could turn biogenic wasted materials in added-value by-products such as smart materials for solutions loading and slow delivery, selective absorbents, smart bio-fertilizers or photonic materials. The crucial role of the high-quality scientific data generation and their management, from handling to results dissemination, education and communication following the FAIR data principle and general pillars of open science could contribute in building synergies across sectors as an innovation speeder of Blue Growth.

Acknowledgements. This work was supported by a grant of the Romanian Ministry of Education and Research, CCCDI-UEFISCDI, project nr. PN-III-P2-2.1-PED-2019-4777, acronym *BluBioSustain*.

[1] F. Nekvapil, S. C. Pinzaru, et al. *Sci. Rep.*, **2020**, 10, 3019.

[2] G. Lazar, S. C. Pinzaru et al., *ACS Omega*, **2021**, 6, 42, 27781–27790.

### **T8-I: Silicone microstructuring strategy for studying microorganisms and cells-topography interaction: attachment and growth**

S. Stroescu (Nistorescu)<sup>1,2</sup>, A. M. Negrescu<sup>3</sup>, L. Rusen<sup>1</sup>, A. Bonciu<sup>1</sup>, G. Gradisteanu<sup>4</sup>, N. Dumitrescu<sup>1</sup>, A. Cimpean<sup>3</sup>, V. Dinca<sup>1</sup>

<sup>1</sup>*INFLPR, 409 Atomistilor street, Magurele, RO-077125, Romania*

<sup>2</sup>*University of Bucharest, Faculty of Biology, Splaiul Independentei 91-95, Bucharest, R-050095, Romania*

<sup>3</sup>*Department of Biochemistry and Molecular Biology, Faculty of Biology, University of Bucharest, 91-95 Splaiul Independenței, 050095 Bucharest, Romania.*

<sup>4</sup>*ICUB, Bucharest, Romania*

Nowadays, it is known that macrophages and bacterial adhesion have been implicated with both breast implant acceptance and complications, from capsular contracture to breast implant-associated anaplastic large cell lymphoma. Therefore, understanding the relationship between implant surface texture and cellular and microbial adhesion represents still a challenge. In the present work, we obtained and characterized 7 types of PDMS microreplicated surfaces and the macrophages and microbial attachment onto the different types of microtopographies of silicone were examined.

The surfaces were tested in contact with *Staphylococcus aureus* ATCC 25923 bacterial strain by visualizing the biofilm formation up to 25 days using electron microscopy. The growth of bacteria was compared using various surface textures, from smooth to linear topographies. The results of bacterial attachment on the surfaces showed that the microbial adhesion to the textured substrates is deficient and decreased in time, also numerous cellular remains are found on parallel continuous and interrupted linear patterns, which confirms the anti-biofilm effect of the PDMS microreplicated. Furthermore, RAW 264.7 cells were exposed for 24 and 72 h to PDMS microtopographies to investigate the cell viability, morphology, proliferation and cell adhesion that provide mechanical support, determine cell shape, and allow movement of the cell surface, thereby enabling cells to migrate. Morphological observations revealed good biocompatibility with the PDMS samples. Our preliminary results show that the *in vitro* assays revealed different macrophages adherence, from cells alignment to stretching depending on the pattern disposal onto the substrates. As perspective, further molecular analysis are necessary to assess their adherence nature related to the pattern disposal onto the surface.

## **T8-O: Synthesis of magnetic nanoparticles coated with three methacrylate-type polymers obtained by SI-ATRP functionalized with methotrexate for antineoplastic activity on HeLa cells**

R. Ghiarasim, S-A. Ibanescu, C.-D. Varganici, N. Simionescu, M. Pinteala

*Centre of Advanced Research in Bionanoconjugates and Biopolymers, "Petru Poni" Institute of Macromolecular Chemistry, 41 A Grigore Ghica Voda Alley, 700487 Iasi, Romania*

In recent decades, nanomedicine has seen a rapid evolution in terms of the development of new biofunctionalized nanostructures for applications in cancer therapy. Knowing that the majority of tumor cells overexpress folic acid receptors on their cell surface and its antagonists such as methotrexate<sup>1-3</sup>, in this work three nanocarriers involving methotrexate were synthesized. Thus, three methacrylate type polymers (biocompatible) were grown through surface-initiated atom transfer radical polymerization (SI-ATRP) such as poly(2-hydroxyethyl methacrylate) (PHEMA) which contains a single unit of ethylene glycol per polymeric repetitive structural unit, poly(poly(ethylene glycol)methacrylate (PPEGMA6) with 6 units of ethylene glycol and poly(poly(ethylene glycol)methacrylate) (PPEGMA10) with 10 units of ethylene glycol, from the surface of the nanoparticles magnetic (biocompatible), and then methotrexate was covalently bound to the hydroxyl groups on the side chains of the three polymers. The methotrexate drug has been used due to its double action, one to target folate receptor  $\beta$ , which leads to the internalization of the nanoparticles and their subsequent subjection to an acidic pH leads to the release of methotrexate inside the cell, and the



second due to the fact that this compound locks dihydrofolate reductase which contributes to cell division and thus cell division is stopped. The biocompatibility of these nanocarriers was determined by testing them on the human gingival fibroblast (HGF) cell line, and the antineoplastic activity of free methotrexate compared to that bound to polymers was highlighted by tests on the HeLa cell line.

Acknowledgments. This work was supported by a grant of the Romanian Ministry of Research and Innovation, CNCS – UEFISCDI, project number PN-III-P1-1.1-TE-2019-0922, within PNCDI III.

[1] N. Nakashima-Matsushita, et al., *Arthritis Rheum*, 1999 42(8), 1609-1616.

[2] P. T. Wong, S. K. Choi. *Int J Mol Sci.* **2015**, 16(1), 1772–1790.

[3] A. Cheung, et al., *Oncotarget*, 2016, 7 (32), 52553.

### **T8-O: Multi-shell gold nanoparticles functionalized with methotrexate for targeted therapy of breast cancer**

D-I. Bostiog, N. Simionescu, M. Pinteala

*Centre of Advanced Research in Bionanoconjugates and Biopolymers, “Petru Poni” Institute of Macromolecular Chemistry, 700487, Iasi, Romania*

Breast cancer is one of the most common types of cancer worldwide and it's psycho-social and clinical impacts are extremely high. Methotrexate (MTX) is a folic acid antagonist routinely used in cancer treatment, including breast cancer. However, when taken for a longer period, side effects of MTX such as stomatitis, mucosal ulcers, bone marrow suppression, loss of appetite, and drug-induced hepatic fibrosis and cirrhosis are observed [1]. Moreover, MTX has poor water solubility and

low permeability, suggesting the administration of higher doses, which in turn decreases its bioavailability [2].

In order to overcome these problems, new strategies should be used, combating the side effects and effectively using MTX drug for a longer period of time. In this context, targeted therapies have been on the rise in recent years and functionalized gold nanoparticles could provide new tools for personalized medicine.

The aim of this study was to develop multi-shell gold nanoparticles functionalized with MTX with potential applications in breast cancer treatment. In the first step of the synthesis, the ability of small concentrated and stable phosphine-coated gold nanoparticles to be functionalized was investigated by using tailored oligomers of poly(ethylene glycol) for covalent attachment to the surfaces of the gold nanoparticles. Subsequently, short-branched poly(ethylene-imine) moieties were coupled as the second shell, followed by methotrexate covalent binding.

The functionalized gold nanoparticles were characterized from physico-chemical point of view in order to establish the degree of functionalization at each step of the preparation. The physico-chemical characterization showed the development of stable gold nanoparticles by the emergence of surface plasmon bands at 524 nm. Dynamic light scattering measurements revealed that the hydrodynamic diameter of nanoparticles started from 50 nm for phosphine coated gold nanoparticles up to 400 nm for nanoparticles containing methotrexate.

Lastly, the cytotoxicity of the nanosystem was determined *in vitro* on normal fibroblasts and MCF-7 breast cancer cell line using the Alamar Blue assay. The functionalized nanosystems with very low MTX concentration (1,7 µg/mL) showed a cytotoxic

trend in MCF-7 breast cancer cell line, but not in normal fibroblasts, compared to free MTX.

In conclusion, multi-shell gold nanoparticles functionalized with MTX developed in this study represent potential therapeutic tools for breast cancer.

Acknowledgements. This work was supported by a grant of the Romanian Ministry of Education and Research, CNCS - UEFISCDI, project number PN-III-P4-ID-PCE-2020-1523, within PNCDI III.

[1] N. K. Garg et al., Colloids Surf. B **2016**, 146.

[2] V. Yang et al., RSC Med. Chem. **2020**, 11.

### **T8-O: Triangular gold nanoparticles as efficient NIR photothermal agents in biological phantoms and melanoma cells**

S. Suarasan<sup>1</sup>, A. Campu<sup>1</sup>, A. Vulpoi<sup>2</sup>, M. Banciu<sup>3</sup>, S. Astilean<sup>1,4</sup>

<sup>1</sup>*Nanobiophotonics and Laser Microspectroscopy Center, Interdisciplinary Research Institute in Bio-Nano-Sciences, Babes-Bolyai University, Cluj-Napoca, Romania*

<sup>2</sup>*Nanostructured Materials and Bio-Nano-Interfaces Center, Interdisciplinary Research Institute in Bio-Nano-Sciences, Babes-Bolyai University, Cluj-Napoca, Romania*

<sup>3</sup>*Department of Molecular Biology and Biotechnology, Center of Systems Biology, Biodiversity and Bioresources, Faculty of Biology and Geology, Babes-Bolyai University, Cluj-Napoca, Romania*

<sup>4</sup>*Department of Biomolecular Physics, Faculty of Physics, Babes-Bolyai University, M Kogalniceanu Str. 1, 400084 Cluj-Napoca, Romania*

Efficient photothermal agents are extremely important for photothermal therapy (PTT). Gold nanoparticles (AuNPs) based PTT agents under laser irradiation absorb photon energy and convert it into heat to induce hyperthermia, which induces

cellular death. Their properties influence the photothermal conversion efficiency [1].

Here, we evaluate the light-to-heat conversion features of gold nanotriangular nanoparticles (AuNTs) with three different localized surface plasmon resonances (LSPR) in- and out- of irradiating laser resonance of 785 nm. After identical NIR irradiation conditions, the AuNTs with LSPR response in resonance with the 785 nm laser exhibit the highest photothermal conversion efficacy of 80% correlated with a temperature increase of 22 °C. The PTT performance of irradiated AuNTs was further assessed inside skin-like biological phantoms that mimic the melanoma AuNTs treated tissue and surrounding healthy tissue (Figure 1).

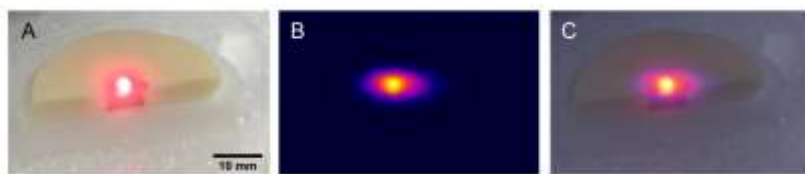


Fig. 1. A. Cross-section picture of a skin phantom with two different regions that mimic the normal and tumoral tissue treated with AuNTs, under NIR laser irradiation B. Thermal contrast image of the skin phantom after 5 min laser irradiation C. merged A and B images

Finally, the efficiency of these photothermal agents on melanoma cells PTT was validated by fluorescence staining and MTT assay performed on B16.F10 cells.

Therefore, in terms of PTT therapy, this study brings us a step forward to the understanding of the PTT effect on skin-like biological phantoms and melanoma cells, which could facilitate the AuNTs translation into clinical studies.

## **T8-O-online: Computational and experimental study of cysteamine capped magnetite nanoparticles (MNP@cys) stability in aqueous suspension**

A. Les<sup>1</sup>, D.-E. Creanga<sup>1</sup>, I. Motrescu<sup>2</sup>

<sup>1</sup>*Alexandru Ioan Cuza University, Iasi, Romania*

<sup>2</sup>*University of Life Sciences, Iasi, Romania*

Magnetite nanoparticles (MNP) functionalization represents a major challenge when designing nanomaterials for medical purposes.

We focused on the interaction of magnetite nanoparticles synthesized by chemical co-precipitation (MNP) with cysteamine based on this molecule's usefulness in biomedicine.

Cysteamine is an amino thiol compound known as radioprotector and recognized in treating cystinosis being also recommended for the treatment of Huntington's disease, Parkinson's disease, nonalcoholic fatty liver disease, malaria and cancer [1]. In the presence of transition metals – e.g. iron in our study, two phenomena occur: cysteamine oxidation and hydrogen peroxide generation [2] while magnetite could be involved in further degrading the hydrogen peroxide to hydroxyl radicals which recommend MNP@cys as an efficient and heterogeneous catalyst [3].

Computational calculations (Spartan '18 software) with DFT algorithms revealed the good kinetic stability for the chosen MNP capping agent, sustained by the similar HOMO-LUMO gap of the cysteamine molecule in gas and water, respectively. The promising reactivity of cysteamine molecule was emphasized by the increased value of the dipole moment when surrounded by water molecules.

The studies carried out by XRD (Shimadzu LabX XRD-6000 Diffractometer with a Cu K $\alpha$  radiation,  $\lambda = 1.54059 \text{ \AA}$ ) and SEM

(Quanta 450, FEI, ThermoScientific) showed good crystallinity and granularity of the cysteamine coated MNPs in water suspension. Raman spectroscopy (Renishaw, inVia device) was applied to analyze the binding of cysteamine to the synthesized MNP, the Raman peaks of MNP@cys being shifted (Fig. 1) in comparison to MNP and cysteamine spectrum [4].

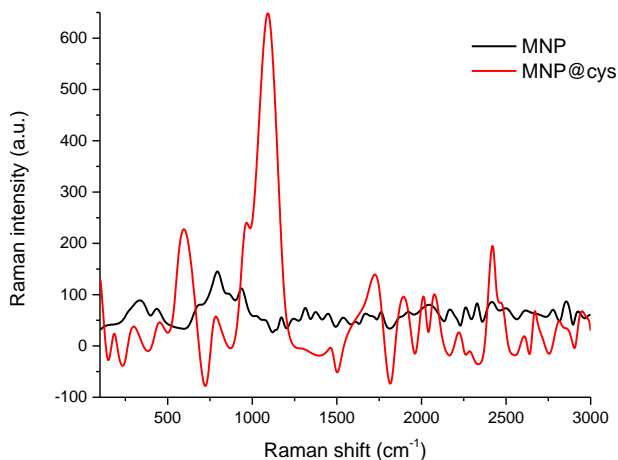


Fig. 1. Smoothed Raman spectra (processed in Origin) for MNP and MNP@cys; vibration bands for MNP@cys are shifted in comparison with the bands of pure cysteamine, available in literature.

Also, UV-vis absorption spectroscopy (Shimadzu, PharmaSpec device) analysis was done to reveal the formation of hydrogen peroxide in solution. Energy-dispersive X-ray spectroscopy (EDS) images of the MNP@cys showed they are better dispersed than pristine, uncoated MNP, that confirm the cysteamine binding and balancing the interparticle attraction forces. Further studies are planned to test the bio-toxicity of MNP@cys nanostructures in the environment where they are released finally following the use in drug delivery purpose.

- [1] M. Besouw et al., Drug Discov Today, **2013**, 18(15-16), 785-92.
- [2] C. Atallah et al., J. Pharm. Anal., **2020**, 10, 499-516.
- [3] R. Maleki et al., 2017, Appl. Organomet. Chem., **2017**, 31(11) e3795
- [4] X. Jiang et al., ACS Appl. Mater. Interfaces 2013. 5 (15) 6902–6908.

- |       |                         |                                 |
|-------|-------------------------|---------------------------------|
| 08:00 | <b>Plenary Session</b>  | HALL 1- University of Dubrovnik |
| 10:20 | <b>Coffee Break</b>     |                                 |
| 10:50 | <b>Plenary Session</b>  | HALL 1                          |
| 12:25 | <b>Lunch</b>            |                                 |
| 15:00 | <b>Plenary Session</b>  | HALL 2                          |
| 17:20 | <b>Coffee Break</b>     |                                 |
| 17:50 | <b>Invited Lectures</b> | HALL 3                          |
| 19:30 | <b>Dinner</b>           |                                 |



### PL-online: A new look at metal oxides

T. Yamamoto

*Materials Design Center, Kochi University of Technology, Kochi, Japan*

Metal oxides are a group of materials that fulfill a wide variety of application properties or encourage evolution or development of near-future application. The applications, for example, include as follows: (1) power electronics such as high  $\text{Ga}_2\text{O}_3$ -based high-electron-mobility transistors (HEMTs) [1] and Field-effect transistors (FETs) [2] and optoelectronics such as vacuum ultraviolet (VUV) light emitter [3] and deep ultraviolet (DUV) light emitting diodes (LEDs) [4]; (2) transparent conductive electrodes for use in touch screen, LCD-TV, organic LED [5] and photovoltaic solar cells [6]; (3) Radiation resistant materials for space industry [7,8]; (4) biological and medical applications such as antibacterial agents [9,10].

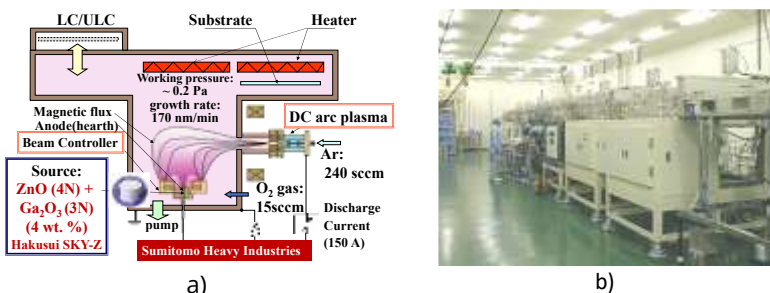


Fig. 1. a) A schematic diagram of reactive plasma deposition with dc arc discharge (RPD) for use of research. b) A photograph of RPD for the mass production line.

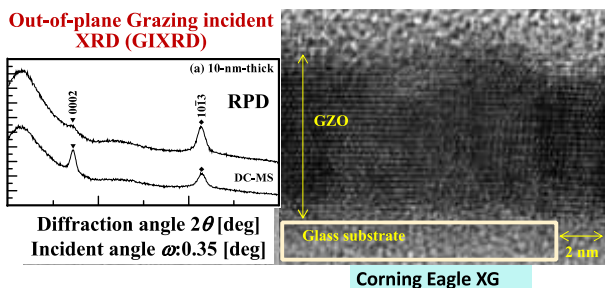


Fig. 2 (left): Out-of-plane grazing incident XRD profile of 10-nm-thick GZO films deposited by RPD and DC-magnetron sputtering as a reference. (right): cross-sectional TEM image of the above films.

I will discuss the features of metal oxides to give answers to the question below: Why metal oxides suitable for the applications? In our group, we have been developing reactive plasma deposition with dc-arc discharge (see Fig. 1) which enables with the deposition of ZnO- and  $\text{In}_2\text{O}_3$ -based highly transparent conductive films causing the low damage to glass or polymer substrates [6,8,10]. I will make key points of materials design to meet the requirements of the applications. In addition, I will introduce the characteristics of Ga-doped ZnO (GZO) films (Fig. 2) showing the radiation resistant [8] and exhibit the specific antibacterial function [10].

- [1] R. Singh et al., Mater. Sci. Semicond. **2020**, 119, 105216-1– 16.
- [2] M. Higashiwaki et al., Appl. Phys. Lett. **2013**, 103, 123511-1 – 4.
- [3] T. Onuma et al., Appl. Phys. Lett. **2021**, 119, 132105-1 – 5.
- [4] Y-J Lu Z-F Shi, C-X Shan, D-Z. Shen, Chin. Phys. B, **2017**, 26, 047703.
- [5] H. Linxiang, C. T. Sie, Mater. Sci. Eng. R Rep. **2016**, 109, 1–101.
- [6] E. Kobayashi, Y. Watabe, T. Yamamoto, Y. Yamada, Sol. Energy Mater. Sol. Cells, **2016**, 149, 75–80.
- [7] K. E. Sickafus et al., Sci. **2000**, 289, 748–751.

- [8] C. Barone, V. Craciun, T. Yamamoto et al., Phys. Status Solid B **2021**, 2100469-1 – 5.
- [9] S. V. Gudkov, et al., Front. Phys. **2021**, 9, 641481-1 –12
- [10] T. Yamamoto, H. Makino, K. Shinomori, J. Jpn. Coat. Tech. Assoc. in Japanese, **2022**, 57, 44–53.

## **PL-online: Silicon Nano-Electro-Mechanical Resonators for Sensing and Information Processing**

Y. Tsuchiya

*Smart Electronic Materials and Systems (SEMS) Group, School of Electronics and Computer Science, University of Southampton, Southampton, UK*

Silicon Nano-Electro-Mechanical Systems (NEMS) have been attracting considerable attention in development of modern electronics due to their exceptional features with mechanically movable objects and their friendliness with the state-of-the-art Si nanofabrication technology [1].

Among various NEMS devices developed in recent decades, Nano-Electro-Mechanical (NEM) resonators have been investigated for ultra-sensitive mass detection [2] down to the single atom level [3]. Figure 1 (a) shows a schematic of a doubly-clamped NEM resonator and an SEM image of a suspended nanobeam, fabricated on Silicon-on-Insulator (SOI) in a CMOS-compatible manner [4,5]. A fundamental-mode resonance at 332 MHz, the highest of its kind has been shown in Fig. 1 (b) for an 800-nm-long beam [5]. Zeptogram ( $\text{zg} = 10^{-21}\text{g}$ ) level mass responsivity estimated numerically for those nanobeams [6] suggests their suitability for weighing nanoparticles.

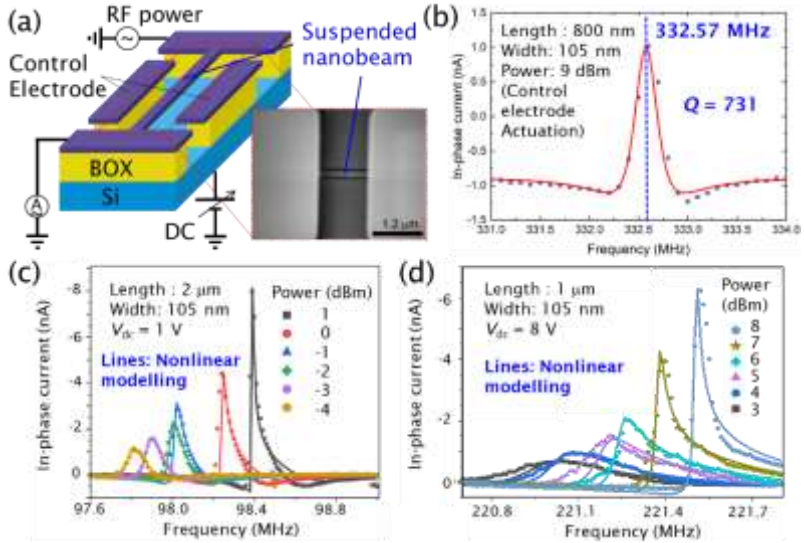


Fig. 1. (a) A schematic diagram of a Si NEM resonator with an SEM image of a suspended Si nanobeam [5]. (b) NEM resonance at 332 MHz observed for an 800-nm-long beam [5]. Nonlinear resonance characteristics of Si NEM resonators with the beam length of (c) 2 microns and (d) 1 micron are shown, respectively. The lines in (c) and (d) are drawn based on numerical solutions of a nonlinear Duffing oscillator model [8].

Integratable Si NEM resonators can be applied for coupled-oscillator-based information processing systems [7], where nonlinear characteristics of individual resonators play a key role in their neuromorphic operation. Figure 1 (c) and (d) show that the line shapes of the NEM resonances are changed from symmetric to asymmetric, and that the resonance peak positions are shifted higher with increasing the RF power for 2- and 1-micron-long beams, respectively. A series of resonance data taken for the devices with varied beam lengths have been analysed with the Duffing equation and found well consistent between each other [8]. The analysis provides a solid basis of nonlinear NEM resonator modelling, which will be pivotal in

developing large-scale integrated coupled NEM oscillator arrays in future.

- [1] Y. Tsuchiya, H. Mizuta "NEMS Devices," in Nanoscale Silicon Devices, S. Oda & D. K. Ferry (Eds.), **2016**, CRC Press.
- [2] K. L. Ekinci, M. L. Roukes, Rev. Sci Inst. **2005**, 76, 061101.
- [3] J. Chaste et al., Nature Nanotech. **2012**, 7, 301.
- [4] F. Arab Hassani, Tsuchiya et al., Sensors **2013**, 13, 9364.
- [5] Y. Tsuchiya et al., IEEE MEMS **2018**, p515
- [6] F. Arab Hassani, Tsuchiya et al., Microelec. Eng. **2011**, 88, 2879.
- [7] G. Csaba, W. Porod, Appl. Phys. Rev. **2020**, 7, 011302.
- [8] F. Ben, Y. Tsuchiya et al., IEEE MEMS **2021**, p515.

### **PL-online: Ultra-short laser pulses as material synthesis and lithography tool**

S. Juodkazis, J. Maksimovic, D. Smith, S-H. Ng

*Optical Sciences Centre, Swinburne University of Technology, Melbourne, Australia*

High average power > 10W and high repetition rate ~1 MHz of ultra-short sub-1 ps lasers have become a widely available, affordable and reliable tool for material processing. We showed that average power of ultra-short lasers is increasing exponentially and follows the Moore's law from 2000 [1]. Review of current developments in industrial applications of ultra-short lasers will be presented with focus on laser ablation, patterning, nanoscale alloying, and nano-texturing over large areas with cross sections in tens-of-centimeters.

Current strength of fs-laser processing is in the fields of micro-machining: cutting, drilling, inscribing refractive index patterns and waveguides. Flexibility of material processing for the additive and subtractive modes of micro-fabrication are

demonstrated in variety of applications where different materials have to be modified, welded, joined, and alloyed. Complexity of approaches where fs-laser microfabrication is combined with other material processing steps including electron and ion beam modifications, plasma etching and sputtering, thermal post-processing further strengthens versatility of fs-laser micro-fabrication. We review recent trends in this field.

[1] M. Han, D. Smith, S.H. Ng, V. Anand, T. Katkus, S. Juodkazis, Ultra-Short-Pulse Lasers—Materials—Applications, **2021**, Eng. Proc., 11, 44.

### **PL-online: Single-charge tunneling functionalities in co-doped silicon nanostructures for dopant-based electronics**

D. Moraru

*Research Institute of Electronics, Shizuoka University, Japan*

Silicon nano-electronics is rapidly advancing towards the end of the Moore's Law, as gate lengths of just a few nanometers have been already reported as feasible for transistors. In the nanostructures that act as channels in transistors or depletion layers in pn diodes, the role of dopants (impurities) becomes critical, since the transport properties will now depend only on a limited number of such dopants and/or on the random distribution of dopants.

Here, we will focus on systems of co-doped nano-structures, in which both phosphorus (P) donors and boron (B) acceptors are introduced intentionally, in order to enhance the functionalities by the specific interplay between donors and acceptors. We will report the possibility of single-charge band-to-band tunneling (BTBT) in highly-doped pn diodes, resulting from the likely

formation of quantum dots due to the random dopant distribution in nanoscale depletion layers of so-called tunnel (Esaki) diodes [1-3]. We will also report signatures of single-electron tunneling (SET) in nanoscale silicon-on-insulator field-effect transistors (SOI-FETs) doped heavily with P-donors [4], but also counter-doped with B-acceptors.

These reports build up on the established field of dopant-based electronics [5-10], in which SET or BTBT via individual dopant-states and/or few-donor clusters reveals basic transport mechanisms for future electronics.

**Acknowledgments.** This work was partially supported by Grant-in-Aid for Scientific Research (19K04529, 22K04216) from MEXT, Japan, and a Cooperative Research Project of the Research Institute of Electronics, Shizuoka University.

- [1] G. Prabhudesai, et al., D. Moraru, Appl. Phys. Lett. **2019**, 114, 243502.
- [2] A. Udhiarto et al., D. Moraru, Jpn. J. Appl. Phys. **2021**, 60, 024011.
- [3] M. Tabe et al., D. Moraru, Appl. Phys. Lett. **2016**, 108, 093502.
- [4] T. T. Jupalli et al., D. Moraru, Appl. Phys. Express 15, 065003 (2022).
- [5] D. Moraru et al., Nanoscale Res. Lett. **2011**, 6, 479-1-9.
- [6] A. Samanta, D. Moraru, T. Mizuno, M. Tabe, Sci. Rep. 2015, 5, 17377.
- [7] D. Moraru, et al., Nanoscale Res. Lett., **2015**, 10, 377.
- [8] D. Moraru, A. Samanta, L. T. Anh, T. Mizuno, H. Mizuta, M. Tabe, Sci. Rep., **2014**, 4, 6219.
- [9] A. Samanta, D. Moraru et al., Appl. Phys. Lett. 2017, 110, 093107.
- [10] A. Afiff et al., D. Moraru, Appl. Phys. Express, 2019, 12, 085004.

### **PL: Electric Transport and Photoresponse in 2D Materials-based Field-Effect Transistors**

A. Di Bartolomeo<sup>1,2</sup>, E. Faella<sup>1,2</sup>, F. Giubileo<sup>2</sup>, A. Kumar<sup>1</sup>, K. Intonti<sup>1</sup>, A. Pelella<sup>1,2</sup>, L. Viscardi<sup>1</sup>

<sup>1</sup>*Department of Physics, University of Salerno, Fisciano, Italy*

<sup>2</sup>*CNR-SPIN, uo Salerno, Fisciano, Italy*

Two-dimensional materials hold great promise for electronics and optoelectronics applications. Their atomic thickness enables highly scaled field-effect transistors with reduced short-channel effects and relatively high carrier mobility. The intrinsic electrical transport properties of 2D materials are commonly investigated using back-gated field-effect transistors, due to the low density of process-induced defects and the easy fabrication.

In this presentation, the electrical and optical properties of several 2D materials are discussed. The focus is on the wide family of transition-metal dichalcogenides (TMDs), such as MoS<sub>2</sub>, WSe<sub>2</sub>, ReSe<sub>2</sub>, PtSe<sub>2</sub>, PdSe<sub>2</sub> (Fig.1) [1-3], as well as on black phosphorus (BP) and GeAs [4]. Electrical transport, modulation of the conductivity by a back-gate, effect of electron irradiation, role of surface adsorbates and photoresponse are investigated in nanosheets obtained by either mechanical exfoliation or chemical vapor deposition on SiO<sub>2</sub>/Si substrates.

The formation of low-resistance contacts and the control of process-induced defects or interface states are issues to consider in the electrical characterization of 2D materials. It is shown that the contact resistance can be tuned by electron irradiation that reduces the Schottky barrier and improves the



2D material/metal contacts [5-7]. It is demonstrated that adsorbates can change the polarity of the majority charge-carriers and enhance the hysteresis in the transfer characteristics of TMD-based field-effect transistors [8].

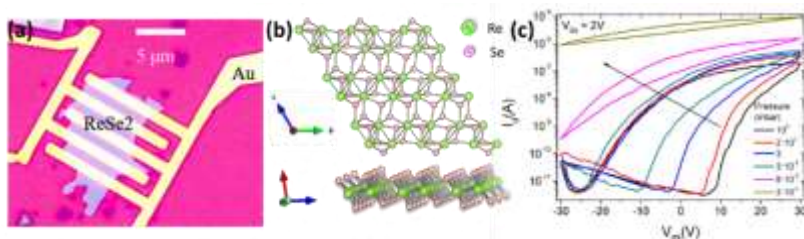


Fig. 1. (a) Optical image of a few-layer ReSe<sub>2</sub> field-effect transistor. (b) ReSe<sub>2</sub> atomic structure (the green and pink dots represent Re and Se atoms, respectively). (c) Transfer characteristics of ReSe<sub>2</sub> transistor for decreasing air pressure (room to 10<sup>-4</sup> mbar).

It shown that excitation from intrinsic or extrinsic trap states enables slow optical response and persistent photoconductivity [2]. It is highlighted how positive and negative photoconductivity can coexist in the same device, the dominance of one type over the other being controlled by the adsorbed oxygen.

The strong dependence of the channel conductance on the environmental gas, air pressure, light and electrical stress make 2D materials-based devices suitable for memory, gas and light sensing applications.

Finally, the tunable conductivity and the sharp-edge geometry facilitate the extraction of electrons (field emission) from 2D materials upon application of an electric field [9-10]. It is shown that several 2D materials are effective field emitters and that their emission current can be modulated by a back-gate.

- [1] E. Faella, K. Intonti, L. Viscardi, F. Giubileo, A. Kumar, H. T. Lam, K. Anastasiou, M. F. Craciun, S. Russo, A. Di Bartolomeo, *Nanomaterials* **2022**, 12, 1886.
- [2] A. Grillo, E. Faella, A. Pelella, F. Giubileo, L. Ansari, F. Gity, P.K. Hurley, N. McEvoy, A. Di Bartolomeo, *Adv. Funct. Mater.* **2021**, 31, 2105722.
- [3] A. Pelella, A. Grillo, F. Urban, F. Giubileo, M. Passacantando, E. Pollmann, S. Sleziona, M. Schleberger, A. Di Bartolomeo, *Adv. Electron. Mater.* **2021**, 7, 2000838.
- [4] A. Grillo, A. Pelella, E. Faella, F. Giubileo, S. Sleziona, O. Kharsah, M. Schleberger, A. Di Bartolomeo *2D Materials* **2022**, 9, 015028.
- [5] A. Di Bartolomeo, F. Urban, A. Pelella, A. Grillo, M. Passacantando, X. Liu, F. Giubileo, *Nanotechnology* **2020**, 31, 375204.
- [6] A. Pelella, O. Kharsah, A. Grillo, F. Urban, M. Passacantando, F. Giubileo, L. Lemmo, S. Sleziona, E. Pollmann, L. Madau, M. Schleberger, A. Di Bartolomeo, *ACS App. Mater. Interfaces*, **2020**, 12, 40532.
- [7] A. Grillo, A. Di Bartolomeo, *Adv. Electron. Mater.* **2021**, 7, 2000979.
- [8] F. Urban et al., A. Di Bartolomeo, *2D Materials* **2019**, 6, 045049.
- [9] A. Grillo, M. Passacantando, Z. Alla, A. Pelella, A. Di Bartolomeo *Small*, **2020**, 16, 202002880.
- [10] A. Di Bartolomeo, A. Pelella, F. Urban, A. Grillo, L. Lemmo, M. Passacantando, X. Liu, F. Giubileo *Adv. Electron. Mater.*, **2020**, 6, 2000094.

## **PL: Emergence of transition metal oxynitrides as next-generation (photo)electrocatalysts**

58

D. Kumar

*Department of Mechanical Engineering, North Carolina A & T State University*

The importance of research in the field of non-conventional energy generation and storage cannot be overemphasized in order to be less dependent on limited resources in nature. Our research has established the effectiveness of pulsed laser deposition method for the synthesis of an emerging class of transition metal oxynitride (TMON) material systems in epitaxial 2D, 1D, and 0D (e.g., quantum dot) geometries. The material systems cover a wide range of composition and exhibits the physicochemical properties needed in electrocatalysis, photocatalytic activity in visible light, extended-life electrochemical energy storage, and photodetector responsivity. The attraction of TMONs over more widely studied transition metal oxides (TMOs) is rooted in the polarizability, electronegativity, and anion charge of nitrogen versus that of oxygen, which induces an enormous change in the physical and chemical properties of the resulting compounds. The computational approach combining molecular dynamics (MD) simulation and Density Functional Theory (DFT) calculation has resulted in an expedited materials design with optimized chemical and electronic structures. A controlled modification in the electronic band structure of the TMON systems by aptly changing the oxygen content and/or by manipulating its size has been used to produce semiconducting TMONs films with tunable conductivity and bandgaps. These features of the TMONs can be used in the fabrication of multijunction solar

cells, electrocatalysts, photoelectrocatalysts, photodetectors, plasmonic, and metamaterial devices.

## **PL: New Insights into Visible Light Active Photocatalysts**

S. C. Pillai

*Nanotechnology and Bio-Engineering Research Group, Atlantic Technological University, ATU Sligo, Ash Lane, Sligo, Ireland*

Nanomaterials exhibit photocatalytic/ hydrophilic activities under the ordinary light (typically >400 nm) is favored for various functional applications. As part of a research program to develop functional surface coatings, our investigations were aimed at developing various photocatalysts for anti-microbial applications. Titanium dioxide in its anatase form thermally stable up to the sintering temperature of the building material substrates (e.g., bathroom tiles) is ideal for various manufacturing applications. High temperatures anatase phase stability is one of the necessities for making such coatings on industrial scale. The preparation of novel photo-catalytic materials by modifying the bandgap using various dopants such as F, S, N and C will be discussed.

- [1] P. Ganguly, S. Kumar, M. Muscetta, N. T. Padmanabhan, L. Clarizia, A. Akande, S. Hinder, S. Mathew, H. John, A. Breen, S. C. Pillai. *Appl. Catal. B: Environ.*, **2021**, 1282, 119612.
- [3] C. Byrne, G. Subramanian, S. C. Pillai. *J. Environ. Chem. Eng.* **2018**, 6, 3531-3555.

### **PL: Reorganization of Lipid Membranes Triggered by Amyloid-beta peptide**

O. Ivankov<sup>1</sup>, T. Murugova<sup>1</sup>, S. Kurakin<sup>1,2</sup>, E. Ermakova<sup>1</sup>, E. Dushanov<sup>1,3</sup>, D. Badreeva<sup>1</sup>, Kh. Kholmurodov<sup>1,3</sup>, A. Kuklin<sup>1,4</sup>, N. Kucerca<sup>1,5</sup>

<sup>1</sup>*Joint Institute for Nuclear Research, Dubna, Russia*

<sup>2</sup>*Kazan Federal University, Kazan, Russia*

<sup>3</sup>*Dubna State University, Dubna, Russia*

<sup>4</sup>*Moscow Institute of Physics and Technology, Dolgoprudny, Russia*

<sup>5</sup>*Comenius University in Bratislava, Bratislava, Slovakia*

Alzheimer's disease (AD) is a conformational disease caused by the formation of senile plaques, consisting primarily of amyloid-beta (A $\beta$ ) peptides. The A $\beta$  peptide is considered a key factor in AD ever since the discovery of the disease. The understanding of its damaging influence has however shifted recently from large fibrils observed in the inter-cellular environment to the small oligomers interacting with a cell membrane. By means of small angle neutron scattering (SANS), we have observed for the first time a spontaneous reformation of extruded unilamellar vesicles (EULVs) to discoidal bicelle-like structures (BLSs) and small unilamellar vesicles (SULVs). These changes in the membrane self-organization happen during the thermodynamic phase transitions of lipids and only in the presence of the peptide. We interpret the dramatic changes in the membrane's overall shape with parallel changes in its thickness as the A $\beta$  triggered membrane damage and a consequent reorganization of its structure. The suggested process is consistent with an action of separate peptides or

small size peptide oligomers rather than the result of large A $\beta$  fibrils.

Acknowledgements. This work has been supported by the Russian Science Foundation under grant 19-72-20186.

## **PL: Exogenous pulmonary surfactant as a drug delivery vehicle**

D. Uhríková<sup>1</sup>, L. Hubčík<sup>1</sup>, N. Kralović<sup>1</sup>, N. Kucerka<sup>1</sup>, A. Calkovská<sup>2</sup>

<sup>1</sup>*Department of Physical Chemistry of Drugs, Faculty of Pharmacy, Comenius University Bratislava, Bratislava, Slovakia*

<sup>2</sup>*Department of Physiology, Jessenius Faculty of Medicine in Martin, Comenius University Bratislava, Martin, Slovakia*

Pulmonary surfactant (PS) lines the interior of the lung alveoli and acts to lower the surface tension at air-liquid interface (Fig. 1a). PS is composed of lipids (~90 wt%) and specific surfactant associated proteins (~10 wt%). The absence of PS due to prematurity, or its damage, is treated by exogenous PS in neonatal medicine, and promising results are obtained also in ventilated Covid-19 patients. Curosurf® (Cur), an extract of porcine lung tissue, is one such clinically used replacement surfactant. It is composed of at least 50 different phospholipids and a small amount of the essential proteins SP-B and SP-C (~2 wt%). The hydrophobic protein SP-B generates oligo- and multi-lamellar organization of Cur. Combining techniques of small angle X-ray and neutron scattering (SAXS and SANS) we determined structural parameters of Cur bilayers, the repeat distance,  $d$ , and the thickness of lipid bilayer  $d_L$  (Fig. 1a).

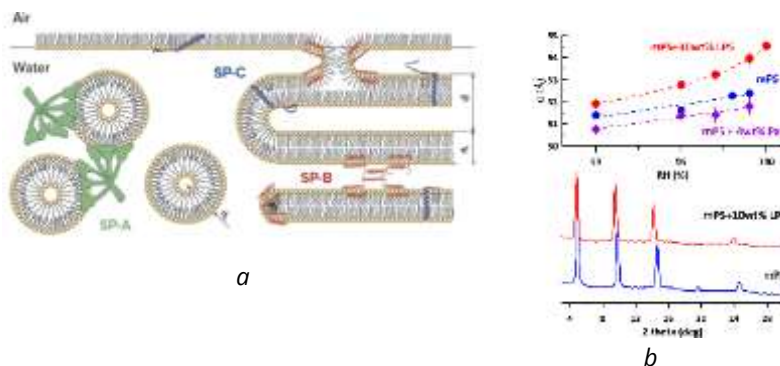


Fig. 1. a) Illustration of pulmonary surfactant structure; b) SAND patterns of aligned lipid bilayers and extracted repeat distances ( $d_L$ ) of exogenous PS in the presence of LPS and PxB, respectively.

Bacterial endotoxin, lipopolysaccharide (LPS), is the major component of the outer membrane of Gram-negative bacteria. At pulmonary infection, LPS interferes with PS and disturbs its structure and function [1]. Polymyxin B (PxB) is an antimicrobial peptide primarily used to treat infections by resistant Gram-negative bacteria. In addition, PxB improves the surface properties of exogenous PS and combined therapy (PxB-Cur) was found as benefiting at treatment of animal models [2]. We investigated structural changes of Cur and its model lipid system free of proteins (mPS) in the presence of LPS and PxB combining techniques of SAXS, SANS and small angle neutron diffraction (SAND). Differential scanning calorimetry was used to characterize the temperature ( $T_m \sim 30^\circ\text{C}$ ) of gel to liquid-crystalline phase transition of lipid mixtures (Cur and mPS). We found that PxB affects  $d_L$  and induces a fusion of unilamellar vesicles of exogenous PS. SAND on the stacks of aligned mPS bilayers deposited on a silicon wafer and hydrated in vapors (at four different RH %) of 8 %  $\text{D}_2\text{O}$  (representative diffraction

patterns Fig. 1b) allowed to unravel the effect of both LPS and PxB on the PS bilayer thickness,  $d_L$ , in this complex system. Our structural findings accurately reflect the situation with a native lung surfactant as confirmed by recent *in vivo* study [2] and support the idea of PxB/PS combined therapy in neonatal medicine.

Acknowledgements. SAXS experiments were performed at BL11-NCD beamline at Alba Synchrotron with the collaboration of Alba staff. SANS experiments were performed at PAXY instrument of LLB CEA Saclay; SAND at D16 spectrometer of ILL, Grenoble. Experiments were supported by projects APVV-17-0250, JINR 04-4-1121-2021/2025 and VEGA 1/0223/20.

[1] M. Kolomaznik et al., *Int. J. Mol. Sci.* **2018**, 19, 1964

[2] A. Calkovska et al., *Sci Reports* **2021**, 11, 22

### **PL: Magnetic Nanoparticles for Solving Diagnostics - Therapeutic problems with COVID-19**

A. Zelenakova<sup>1</sup>, V. Zelenak<sup>2</sup>, P. Hrubovcak<sup>1</sup>, J. Szucsova<sup>1</sup>, E. Benova<sup>2</sup>, Lubos Nagy<sup>1</sup>, M. Barutiak<sup>1</sup>, J. Kosuth<sup>3</sup>, Z. Sulinova<sup>4</sup>, S. Vilcek<sup>4</sup>

<sup>1</sup>*Department of Condensed Matter Physics, Pavol Jozef Šafárik University, Košice, Slovakia*

<sup>2</sup>*Department of Inorganic Chemistry, Pavol Jozef Šafárik University, Košice, Slovakia*

<sup>3</sup>*Institute of Biology and Ecology, P. J. Safarik University, Kosice, Slovakia*

<sup>4</sup>*Department of Epizootiology and Parasitology, University of Veterinary Medicine and Pharmacy, Komenského 73, 040 01 Kosice, Slovakia*

Last two years have shown us our limits in the fight with global pandemic. The spread of COVID19 disease revealed our vulnerability and inefficiency when dealing with a kind of serious virus in general. Despite of a large effort of scientific community, many crucial questions regarding corona virus



disease are still remaining unaddressed. The most important is concern a fast and plausible diagnostics and effective treatment. In response to these challenges, we have developed nanocomposite systems based on  $\text{Fe}_3\text{O}_4$  magnetic nanoparticles (NPs) for COVID19 diagnostics and therapeutic applications. Series of nanoparticle systems with magnetic core and amorphous silica ( $\text{SiO}_2$ ) shell have been prepared and their surface has been modified by specific organic ligands (Fig.1). Owing to the ligands, the prepared NPs are capable of bonding either virus RNA or anti-virus drug. By the action of applied magnetic field, the NPs may be concentrated in a certain point (diagnostics) or delivered into the affected tissue (treatment). Feasible magnetic performance of the prepared nanoparticle systems is therefore crucial for their application.

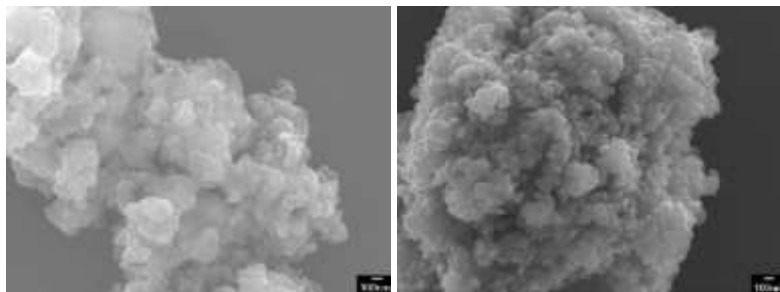


Fig.1. Structure of magnetic beads modified by organic ligands for RT-PCR diagnostics.

We have conducted series of magnetic measurements in order to distinguish between magnetic behavior of the pure nanoparticle system and systems with various coatings. We demonstrate the application of the fundamental models that have been modified in order to fit the experimental zero-field cooling magnetization data. We discuss the influence of the nanoparticle shell parameters (morphology, thickness, ligands) on the overall magnetic performance of the systems. With the

aid of magnetic data modeling along with the strong experimental support provided by other methods (electron microscopy, X-ray diffraction) we can conclude on nanoparticle structural and magnetic characteristics and the presence/absence of interparticle interactions. Accurate determination of nanoparticle system properties is essential for its further tuning towards the desired application.

Acknowledgments. This work was supported by the Operational Programme Integrated Infrastructure, project “NANOVIR”, ITMS:313011AUW7, co-funded by ERDF and APVV-20-0512.

### **PL: The challenge of protecting cultural heritage assets: the HERACLES project vision and experience**

G. Padeletti

*CNR-ISMN Rome 1 – Research Area, Italy*

Europe’s significant cultural diversity together with exceptional ancient architectures and artefact collections attracts millions of tourists every year. These global assets are of incalculable value and have to be preserved for future generations. The effects of floods, extreme windstorms or rains on these assets are clearly identifiable but it should be worth to note that all these effects are seriously amplified on ancient and fragile assets where advanced techniques, commonly used for modern buildings and structures, cannot be applied to preserve their originality. In order to address all of the above challenges the European project HERACLES proposed a holistic, multidisciplinary, and multi-sectorial approach with the aim to provide an operative system and eco-solutions to innovate and to promote a strategy and vision for the future of CH resilience. In this framework, HERACLES proposes a novel systematic

approach to ensure the sustainable management and protection of the different CH typologies with respect to the CC impacts. The approach benefits from a multidisciplinary methodology that bridges the gap between the two different worlds: the CH stakeholders and the scientific/technological experts, which are both involved in the project

### Invited Lectures (HALL 3)

#### **PAMS-IL: 2D Materials for electronic and optoelectronic applications**

A. Di Bartolomeo<sup>1,2</sup>, E. Faella<sup>1,2</sup>, F. Giubileo<sup>2</sup>, A. Kumar<sup>1</sup>, K. Intonti<sup>1</sup>, A. Pelella<sup>1,2</sup>, L. Viscardi<sup>1</sup>

<sup>1</sup>*Department of Physics, University of Salerno, Fisciano, Italy*

<sup>2</sup>*CNR-SPIN, uo Salerno, Fisciano, Italy*

Two-dimensional materials hold great promise for electronics and optoelectronics applications. Their atomic thickness enables highly scaled field-effect transistors with reduced short-channel effects and relatively high carrier mobility. The intrinsic electrical transport properties of 2D materials are commonly investigated using back-gated field-effect transistors, due to the low density of process-induced defects and the easy fabrication.

In this lecture, the electrical and optical properties of several 2D materials are discussed. The focus is on the wide family of transition-metal dichalcogenides (TMDs), such as MoS<sub>2</sub>, WSe<sub>2</sub>, ReSe<sub>2</sub>, PtSe<sub>2</sub>, PdSe<sub>2</sub> [1-3], as well as on black phosphorus (BP) and GeAs [4]. Electrical transport, modulation of the conductivity by a back-gate, effect of electron irradiation, role of surface adsorbates and photoresponse are investigated in

nanosheets obtained by either mechanical exfoliation or chemical vapor deposition on  $\text{SiO}_2/\text{Si}$  substrates (Fig.1).

The formation of low-resistance contacts and the control of process-induced defects or interface states are issues to consider in the electrical characterization of 2D materials. It is shown that the contact resistance can be tuned by electron irradiation that reduces the Schottky barrier and improves the 2D material/metal contacts [5-7]. It is demonstrated that adsorbates can change the polarity of the majority charge-carriers and enhance the hysteresis in the transfer characteristics of TMD-based field-effect transistors [8]. It is shown that excitation from intrinsic or extrinsic trap states enables slow optical response and persistent photoconductivity [2]. It is highlighted how positive and negative photoconductivity can coexist in the same device, the dominance of one type over the other being controlled by the adsorbed oxygen.

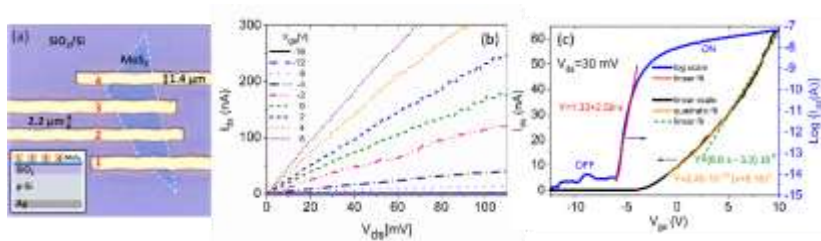


Fig. 1. Monolayer  $\text{MoS}_2$  back-gate transistor: (a) Optical top view and schematic device cross-section, (b) output characteristics and (c) transfer characteristics.

The strong dependence of the channel conductance on the environmental gas, air pressure, light and electrical stress make

2D materials-based devices suitable for memory, gas and light sensing applications.

Finally, the tunable conductivity and the sharp-edge geometry facilitate the extraction of electrons (field emission) from 2D materials upon application of an electric field [9-10]. It is shown that several 2D materials are effective field emitters and that their emission current can be modulated by a back-gate.

[1] E. Faella, K. Intonti, L. Viscardi, F. Giubileo, A. Kumar, H. T. Lam, K. Anastasiou, M. F. Craciun, S. Russo, A. Di Bartolomeo, *Nanomaterials* **2022**, 12, 1886.

[2] A. Grillo, E. Faella, A. Pelella, F. Giubileo, L. Ansari, F. Gity, P.K. Hurley, N. McEvoy, A. Di Bartolomeo, *Adv. Funct. Mater.* **2021**, 31, 2105722.

[3] A. Pelella, A. Grillo, F. Urban, F. Giubileo, M. Passacantando, E. Pollmann, S. Sleziona, M. Schleberger, and A. Di Bartolomeo *Adv. Electron. Mater.* **2021**, 7, 2000838.

[4] A. Grillo, A. Pelella, E. Faella, F. Giubileo, S. Sleziona, O. Kharsah, M. Schleberger, A. Di Bartolomeo, *2D Materials* **2022**, 9, 015028.

[5] A. Di Bartolomeo, F. Urban, A. Pelella, A. Grillo, M. Passacantando, X. Liu, F. Giubileo, *Nanotechnology* **2020**, 31, 375204.

[6] A. Pelella, O. Kharsah, A. Grillo, F. Urban, M. Passacantando, F. Giubileo, L. Iemmo, S. Sleziona, E. Pollmann, L. Madau, M. Schleberger, A. Di Bartolomeo, *ACS Appl. Mater. Interfaces* **2020**, 12, 40532.

[7] A. Grillo, A. Di Bartolomeo *Adv. Electron. Mater.* **2021**, 7, 2000979.

[8] F. Urban et al., *2D Materials* **2019**, 6, 045049.

[9] A. Grillo, M. Passacantando, Z. Alla, A. Pelella, and A. Di Bartolomeo, *Small* **2020**, 16, 202002880.

[10] A. Di Bartolomeo, A. Pelella, F. Urban, A. Grillo, L. Iemmo, M. Passacantando, X. Liu, F. Giubileo, *Adv. Electron. Mater.* **2020**, 6, 2000094.

## **PAMS-IL-online: Growth of Silicon Nano-structures at low Temperature and their application in Energy related Devices**

S. Paul

*Emerging Technologies Research Centre, De Montfort University, Leicester, UK*

Silicon is widely used in electronic industries in a number of forms, for example: amorphous silicon is used in liquid-crystal display units; polysilicon is used in Flash memory structures & photovoltaic solar cells and single crystals are used in C-MOS technologies. Among various forms of silicon embodiments, silicon nanostructures (for example silicon nanowires). However, before silicon nanostructures become integrated into a commercial product (for example in consumer plastic electronics or batteries), there are still major challenges to conquer. These include optimizing growth conditions, low-temperature growth of silicon nanostructures. For the growth of nanostructures, widely employed chemical vapour deposition (CVD) techniques is in practice. However, the growth temperatures relevant to this technique exceed 600°C, which results in very high thermal budgets and process is not compatible cheap and flexible substrates. Using a combination of pre-growth preparation steps and plasma enhanced chemical vapour deposition (PECVD), (, have been shown to result in the growth of silicon structures (micro and nano sized) 300°C. Using this process, we are able to grow silicon structures

on plastic/glass substrates and have demonstrated their use in lithium-ion batteries and photovoltaic solar cells

### **Sunday, September 11, 2022**

9:30      **Excursion I: Three Island Cruise**

19:30      Dinner break

### **Monday, September 12, 2022**

7:30      **Excursion II: Montenegro Highlights**

19:30      Dinner break

## Tuesday, September 13, 2022

- 08:00 **Invited Lectures**  
HALL 3 - University of Dubrovnik
- 10:10 **Coffee break**
- 11:40 **Plenary and Invited Session**  
HALL 1
- 12:40 **Lunch**
- 15:00 **Invited Lectures**  
HALL 3
- 18:30 **Excursion III**  
**Sunset and dinner on KARAKA boat**



**PAMS-IL-online: Carrier scattering mechanism of polycrystalline transparent conductive ZnO films and how to tailor their carrier transport**

T. Yamamoto<sup>1</sup>, T. Terasako<sup>2</sup>, H. Makino<sup>1</sup>

<sup>1</sup>Research Institute, Kochi University of Technology, Kochi, Japan,

<sup>2</sup>Graduate School of Science & Engineering, Ehime University, Ehime, Japan,

Highly transparent and conductive oxide (TCO) films such as *n*-type In<sub>2</sub>O<sub>3</sub>- and ZnO-based films have captivated potential interest as transparent conducting electrodes in optoelectronic devices (e.g., photovoltaic solar cells and all types of flat display panel, see Fig.1[1]).

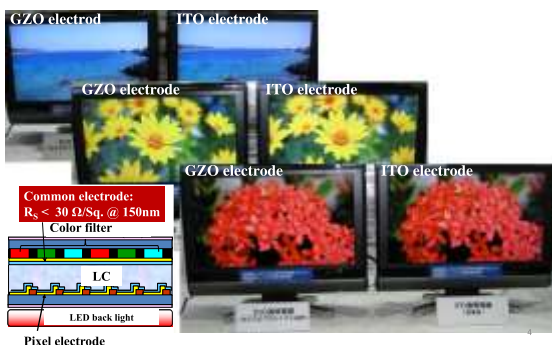


Fig. 1. Display of LCD TV mounted with a Ga-doped ZnO or Sn-doped In<sub>2</sub>O<sub>3</sub> transparent electrode prepared on an RGB color filter. [1]

Note that tailoring and controlling of the trade-off properties such as optical transparency and electrical conductivity is essential to achieve TCO films which meet the requirements depending on applications. In this talk, we focus on

electrical properties, and discuss carrier electron scattering mechanisms to clarify the dominant factors that limit the carrier transport in TCO films.

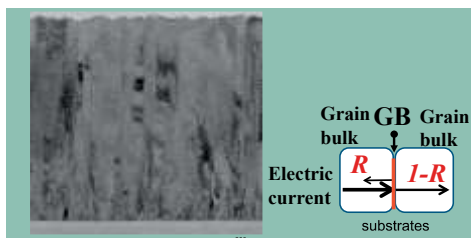


Fig. 2. Cross-sectional TEM image (left part) of Ga-doped ZnO films deposited on glass substrates. Lateral grain/grain interface effect model (right part):  $R$ , grain boundary (GB) resistance coefficient.

Polycrystalline Ga-doped ZnO (GZO) films deposited on glass substrates or polymer substrates [2] shows typically columnar structure with preferential (0001) crystallographic grain orientation. We reported that lateral grain sizes vary from 20 to 40 nm and mean free paths of the carriers are of less than 10 nm. This implies that grain boundary scattering will affect the carrier transport (see Fig. 2). In such a case, we must investigate Hall mobility limited by the piezoelectric, acoustic phonon, longitudinal phonon, ionized impurity and grain boundary scattering mechanism.[3] We will elucidate mechanisms to govern the carrier transport, that strongly depend on carrier concentration and also temperature, on the basis of the analysis of the experimental data combined with theoretical approach in GZO films. Those study will serve for selecting and developing suitable TCO films according to specific application.

[1] N. Yamamoto, H. Makino, S. Osone, A. Ujihara, T. Ito, H. Hokari, T. Maruyama, T. Yamamoto, Thin Solid Films **2012**, 520, 4131–4138.

[2] T. Yamamoto, T. Yamada, A. Miyake, H. Makino, N. Yamamoto, J. SID, **2008**, 16/7, 713–719.

[3] T. Terasako, H. Song, H. Makino, S. Shirakata. T. Yamamoto, Thin Solid Films **2013**, 528, 19–25.

## **PAMS-IL: Raman spectroscopy techniques for materials science**

S. Cinta Pinzaru

*Faculty of Physics, Babes-Bolyai University, Cluj-Napoca*

Raman spectroscopy techniques and applications are increasingly expanding in the materials science field [1]. Two key issues, Raman signal enhancement and spatial resolution are crucial in successful applications for surface analysis of materials of choice. Significant progress in materials science, particularly nanomaterials, allowed to design novel strategies for plasmon-enhanced Raman spectroscopy, exploited in SERS, TERS and many other linear or non-linear techniques, as recently reviewed [1]. Additionally, not any Raman spectroscopy technique suits well for any material characterization. Surface analysis versus bulk material will be also discussed with several examples. How to select proper technique and optimal conditions for targeted analysis will be emphasized for several inorganic materials, hybrid composites, biomaterials [2] and others. To avoid failure and deception while working in the Raman lab, some basic notions related to the techniques, spatial resolution, confocal configuration, wavelength excitation, resonance Raman conditions when apply, as well as the Raman acquisition conditions are necessary in choosing the optimal experimental setup for certain type of material characterization.

[1] Ding, S.-Y., Yi, J., Li, J.-F., Ren, B., Wu, D.-Y., Panneerselvam, R., & Tian, Z.-Q. Nature Rev. Mater., 2016, 1(6) 21.

[2] L. Ogresta, F. Nekvapil, T. Tămaş, L. Barbu-Tudoran, M. Suci, R. Hirian, M. Aluăş, G. Lazar, E. Levei, B. Glamuzina, S. Cinta Pinzaru, ACS Omega 2021, 6, 42, 27773-27780.

## **PAMS-IL: Epitaxial growth of group IV 2D materials beyond graphene.**

P. Castrucci

*Department of Physics, University of Roma Tor Vergata, Roma, Italy*

The number of the theoretically predicted and the experimentally obtained two-dimensional (2D) materials has been increasing more and more over the last years. Among them, silicene, germanene, and stanene attracted a particular attention for the challenge to obtain them in absence of their layered bulk counterparts, for their closeness to graphene and its properties and for their high compatibility with current Si technology. They have been reported to be synthesized on a number of metallic substrates, though the interaction between metals and these 2D materials, strongly modifies their predicted intrinsic electronic properties and makes their future applications not straightforward. More recently a promising route to obtain free-standing silicene, germanene and stanene has been identified in their growth on inert substrates, even if unexpected intercalation processes have been detected to occur because of the presence of surface defects. In this lecture, a review of these works, current scientific debates and discussion of the major scientific and technological challenges will be provided.

**PL: Advanced magnetic nanodevices as therapeutic agent**

G.F. Goya<sup>1,2,3</sup>, C. Marquina<sup>1,2,3</sup>, J. A. Fuentes-Garcia<sup>1,2,3</sup>, M. R. Ibarra<sup>1,2,3</sup>

<sup>1</sup>*Instituto de Nanociencia y Materiales de Aragón (INMA), CSIC-Universidad de Zaragoza, Zaragoza 50009, Spain*

<sup>2</sup>*Laboratory of Advanced Microscopies, University of Zaragoza, Zaragoza 50420, Spain*

<sup>3</sup>*Departamento de Física de la Materia Condensada, Universidad de Zaragoza, Zaragoza 50009, Spain*

Magnetic based nanodevices are considered as promising nanovectors for tumor treatment at the clinic and also for therapeutic drug release [1]. The knowledge of the mechanisms triggering the cell death using magnetic nanodevices as targeting vectors is relevant for the design of these nanovectors for therapeutic purposes. For that objective several nanodevices as core-shell magnetic nanoparticles [2] and magnetic nanofibers [3] have been synthesized and tested in vitro using several cell lines (Fig.1).

Our first approach is based on the influence of the nanovector physical properties and its response to an applied electromagnetic field [1]. The drastic effect induced by magnetic hyperthermia is a key issue for the use of magnetic functional nanodevices in focused therapies. Our results in in vitro models demonstrate that a complex interplay of physical effects makes this technique a very promising alternative or adjuvant therapy for tumor treatment, first, due to the nanovector biocompatibility, (verified at cell level and in vivo), and second, because it is a localized treatment avoiding the

side effects provoked by the currently used therapies. Consequently, the optimization of the functional nanomaterials is very relevant for their application.

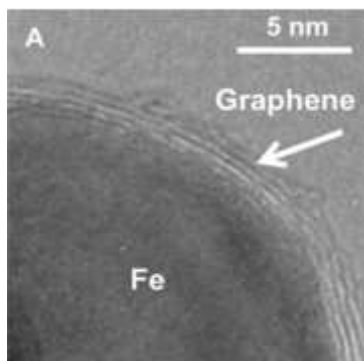


Fig. 1. Core&shell magnetic nanoparticles encapsulated in graphene cages

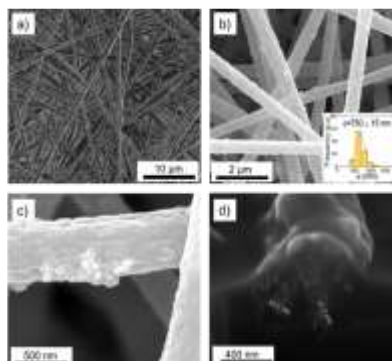


Fig. 2. SEM images of magnetic fibers: a) BES image; b) SE image and fiber diameter histogram (inset) c), close-up showing magnetic nanoparticles in the surface d), cross section of single magnetic fiber

Other field of relevance among the applications of magnetic nanoparticles is the targeted drug release. In this field the use of our core@shell nanoparticles becomes relevant, due to their biocompatibility and their outstanding adsorption/desorption properties [4].

- [1] H G.F: Goya, V. Grazu and M.R. Ibarra, Curr. Nanosci. **2008**, 4, 1-16.
- [2] B. Sanz, M.P. Calatayud, E. De Biasi, E. Lima Jr., M. Vasquez Mansilla, R.D. Zysler, M.R. Ibarra, G.F. Goya. Scie. Rep. **2016**. 6, 38733.
- [3] J.A. Fuentes-Garcia, B. Sanz, R. Mallada, M.R. Ibarra, G. F. Goya, submitted.

[4] B. Zhong, A. Mateu-Roldan, M. L. Fanarraga, W. Han, D. Munoz-Guerra, J. Gonzalez, L. T. Weng, M. R. Ibarra, C. Marquina, K.L. Yeung, Chem. Eng. J., **2022**, 435 134466.

## **PL: Superconducting spintronics with spin-orbit coupling and symmetry filtering**

F. G. Aliev<sup>1,2</sup>, C. Gonzalez-Ruano<sup>1</sup>, D. Caso<sup>1</sup>, P. Tuero<sup>1</sup>, L. G. Johnsen<sup>3</sup>, C. Tiusan<sup>4,5</sup>, M. Hehn<sup>5</sup>, I. Zutic<sup>6</sup>, J. Fabian<sup>7</sup>, J. Linder<sup>3</sup>

<sup>1</sup>Departamento Física de la Materia Condensada C-III, Universidad Autonoma de Madrid, Madrid 28049, Spain.

<sup>2</sup>Instituto Nicolas Cabrera (INC) and Condensed Matter Physics Institute (IFIMAC), Madrid 28049, Spain.

<sup>3</sup>Department of Physics, Center for Quantum Spintronics, Norwegian University of Science and Technology, 7491 Trondheim, Norway.

<sup>4</sup>Department of Solid State Physics and Advanced Technologies, Faculty of Physics, Babes-Bolyai University, Cluj-Napoca 400114, Romania.

<sup>5</sup>Institut Jean Lamour, Nancy Universite, 54506 Vandoeuvre-les-Nancy Cedex, France.

<sup>6</sup>Department of Physics, University at Buffalo, State University of New York, Buffalo, New York 14260, USA.

<sup>7</sup>Institute for Theoretical Physics, University of Regensburg, 93040 Regensburg, Germany.

Generation and control over long-range triplet (LRT) Cooper pairs is a key milestone for applications in superconducting spintronics. Here we overview fully epitaxial ferromagnet-superconductor hybrids with interfacial spin orbit coupling as a new platform for superconducting spintronics compatible with commercial spintronics [1-4].

We have studied all-epitaxial V/MgO/Fe junctions with competing in-plane and out-of-plane (OOP) magnetic anisotropies, and spin-orbit coupling (SOC) at the MgO interface. First, we experimentally demonstrated a thousand-

fold increase in tunnelling anisotropic magnetoresistance below the vanadium critical temperature ( $T_c$ ), which supports LRT formation depending on the magnetic configuration of the Fe layer [1]. Then we observed the predicted converse effect: the transformation of the in-plane and out-of-plane magneto crystalline anisotropies of the Fe layer driven by the superconductivity of vanadium through the SOC-bearing MgO interface [2] (Fig.1). The effective perpendicular magnetic anisotropy (PMA) is also enhanced, inducing a partial OOP magnetization reorientation without any applied field, and a reduction of the field required to induce a complete OOP transition [3].

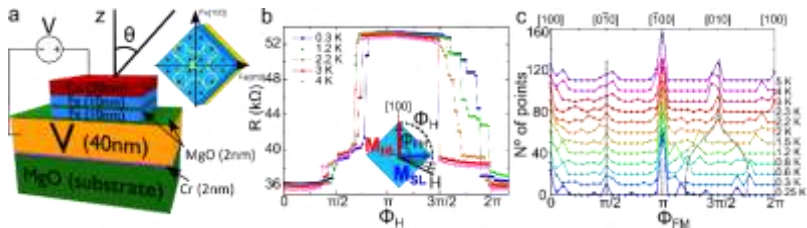


Fig. 1. Studied samples: a) sketch of the layer structure and in-plane magnetocrystalline anisotropy profile b) resistance during in-plane rotations of the magnetic field for several temperatures, from above to below  $T_c$ ; c) calibrated angle between the two ferromagnetic layers during the rotations, showing the new stable configurations at  $45^\circ$  below  $T_c$ .

We modelled our results in terms of an additional contribution to the free energy of the ferromagnet arising from the controlled generation of triplet Cooper pairs, which depends on the relative angle between the exchange field of the ferromagnet and the spin-orbit field. Finally, we discovered that V/MgO/Fe/MgO/Fe/Co junctions show record high tunnelling magnetoresistance in the normal state (at room temperature), making them also applicable for high bias conventional



spintronics [4]. Our findings offer the ability to tune magnetic anisotropies using superconductivity - a key step in designing future cryogenic magnetic memories.

[1] I. Martinez et al., Phys. Rev. Appl. **2020** 13, 014030.

[2] C. Gonzalez-Ruano et al., Phys. Rev. B, **2020** 102, 020405(R).

[3] C. Gonzalez-Ruano et al., Scientific Reports 11, **2021** 19041.

[4] C. Gonzalez-Ruano et al., Adv. Elect. Materials, **2021** 8, 2100805.

#### **T4-I: Magnetic skyrmions for neuromorphic and qubit applications**

C. Tiusan<sup>1</sup>, R. One<sup>2</sup>, S. Mican<sup>3</sup>, A. G. Cimpoesu<sup>4</sup>

<sup>1</sup>*Department of Solid-State Physics and Advanced Technologies  
Faculty of Physics, Babeş-Bolyai University Cluj-Napoca, Romania*

<sup>2</sup>*Doctoral School of Physics, Faculty of Physics, Babeş-Bolyai University Cluj-Napoca, Romania*

<sup>3</sup>*Department of Solid-State Physics and Advanced Technologies  
Faculty of Physics, Babeş-Bolyai University Cluj-Napoca, Romania*

<sup>4</sup>*Faculty of Physics, Babeş-Bolyai University Cluj-Napoca, Romania*

One of the most recent magnetic paradigms in the information technologies is based on the use of magnetic skyrmions. These solitons are vortex-like swirling topological defects in the magnetization texture [1] with diameters in the nanometer-range suitable for classical, neuromorphic or quantum spintronics applications.

In this paper we illustrate our results of multiple scale modelling, from ab-initio to micromagnetic simulations. They were performed to identify the phase diagrams of materials parameters allowing either to stabilize skyrmionics ground states or to write them from initially saturated state using the spin-transfer torque of a pulsed perpendicular current in

nanometer-size disks based on magnetic materials with electric field tuneable perpendicular magnetic anisotropy and Dzyaloshinskii–Moriya interactions (DMI) (Fig.1). Moreover, the temperature dependence of skyrmion stability has been analysed to point out the main/critical material properties allowing to get stable skyrmions beyond cryogenic conditions, towards the room-temperature goal.

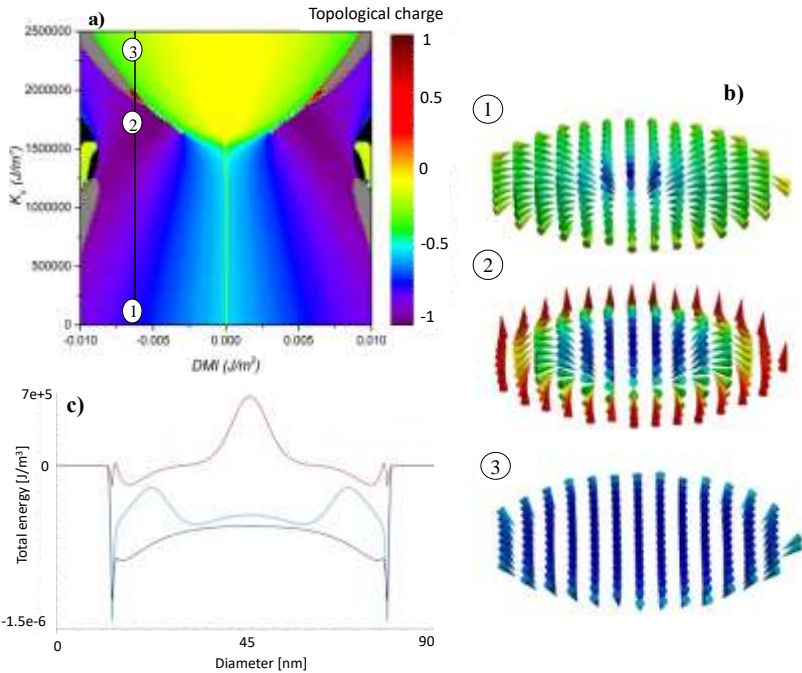


Fig. 1. a) Calculated phase diagram: PMA-DMI-Topological charge illustrating skyrmionics the regime (topological charge  $Q = -1$ ,  $Q = \frac{1}{4\pi} \int d^2x \vec{m} \cdot \left( \frac{d\vec{m}}{dx} \times \frac{d\vec{m}}{dy} \right)$ ). b) vortex, skyrmionics and perpendicular saturation configuration and corresponding total energy (c).

Following these material issues, we illustrate and briefly discuss some current advances in the underlying Physics and potential

applications of skyrmions as classical bits in racetrack memories [2], as artificial neurons in neuromorphic architectures and devices [3] and helicity qubits [4].

[1] A. Fert et al, Nature Reviews Materials, **2017**, 2, 17031.

[2] Tomasello et al, Sci Rep **2014**, 4, 6784 .

[3] Sai Li *et al* , Nanotechnology **2017**, 28 31LT01

[4] [C. Psaroudaki et al, Phys. Rev. Lett. **2021**,127, 067201.

#### **T4-I: Intercalation enhanced superconducting response in hyper-expanded hybrid iron chalcogenides**

A. Deltsidis,<sup>1,2</sup> L. Simonelli,<sup>3</sup> G. Vailakis,<sup>1,2</sup> I. Capel Berdiell,<sup>1</sup> G. Kopidakis,<sup>1,2</sup> E.S. Bozin,<sup>4</sup> and A. Lappas<sup>1</sup>

<sup>1</sup>*Institute of Electronic Structure and Laser, Foundation for Research and Technology - Hellas, 71110 Heraklion, Greece*

<sup>2</sup>*Department of Materials Science and Technology, University of Crete, 70013 Heraklion, Greece*

<sup>3</sup>*ALBA Synchrotron Light Source, 08290 Cerdanyola del Vallés, Spain*

<sup>4</sup>*Condensed Matter Physics and Materials Science Department, Brookhaven National Laboratory, 11973 New York, USA*

2D iron chalcogenides offer a rich playground where structural and electronic correlations can be tuned by intercalation chemistry [1]. Electron donor molecules co-intercalated with alkalis in the  $\beta$ -FeSe (Fig. 1b) impact the electronic structure of the parent phase as the intercalation increases the interlayer separation and leads to a five-fold rise of the superconducting critical temperature ( $T_c \sim 44$  K). We have developed low-T solvothermal routes that afford the high- $T_c$   $\text{Li}_x(\text{C}_5\text{H}_5\text{N})_y\text{Fe}_{2-z}\text{Se}_2$  system (Fig. 1a) in order to understand the parametrization of  $T_c$  with structure-property aspects probed by high-resolution synchrotron X-ray based tools. Total scattering experiments, combined with quantitative pair distribution function (PDF) analysis uncovers that high- $T_c$  in these materials relates to the

tetragonal  $\text{ThCr}_2\text{Si}_2$ -type average structure. However, in-situ PDF study of the  $[\text{Li-C}_5\text{H}_5\text{N-FeSe}]$  reaction pathway over time, uncovers local distortions, involving the  $\text{FeSe}_4$  edge-sharing units that swell as a consequence of the electron donating  $[\text{Li-C}_5\text{H}_5\text{N}]$  moieties being accommodated in the interlayer space [2].

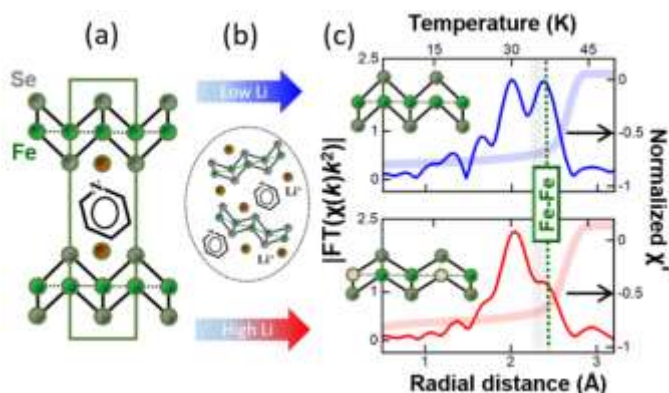


Fig. 1. 2D hybrid iron-selenides, with large interlayer separation (a), are investigated by high-resolution synchrotron X-ray tools to find that increasing Fe-vacancy concentration with Li-level (b), retains a robust superconducting response,  $T_c \sim 44$  K (c).

Motivated by such findings, element-specific (Fe & Se K-edge) X-ray absorption (XAS) and emission (XES) spectroscopies ( $T = 20$ – $300$  K) were utilised to find that (a)  $\text{FeSe}_4$  units carry a slightly reduced local Fe magnetic moment, while (b) doping-mediated local lattice modifications, delved by conventional  $T_c$ -optimization measures (cf. anion height and  $\text{FeSe}_4$  tetrahedra regularity), become less relevant when layers are spaced far away [3]. EXAFS analysis, recognizes that such distortions are compensated by a softer Fe-network that relates to Fe-site vacancies, while DFT calculations corroborate that Fe-site deficiency of isolated  $\text{Fe}_{2-z}\text{Se}_2$  ( $z$ , vacant sites) planes occurs at

low energy cost, giving rise to stretched Fe-sheets, in accord with the experiments. The work provides insights on the interplay of electron donating spacers and the iron-selenide layer's tolerance to defect chemistry, offering a tool to favorably tune the Fermi surface properties and engineer robust superconducting states at elevated temperature.

- [1] H.K. Vivanco and E.E. Rodriguez, J. Solid State Chem. **2016**, 242, 3-21.
- [2] I. Capel Berdiell, E. Pesko, E. Lator, A. Deltsidis, A. Krztoń-Maziopa, A.M.M. Abeykoon, E.S. Bozin, A. Lappas, Inorg. Chem. **2022**, 61, 4350-4360.
- [3] A. Deltsidis, L. Simonelli, G. Vailakis, I. Capel Berdiell, G. Kopidakis, A. Krztoń-Maziopa, E.S. Bozin, A. Lappas, Inorg. Chem. **2022**, 61, 12797-12808.

### Invited Lectures (HALL 3)

#### **PAMS-IL: X-ray absorption and photoelectron spectroscopies**

C. M. Teodorescu

*National Institute of Materials Physics, Atomîştilor 405A, 077125 Măgurele-Ilfov, Romania*

This lecture will present the main aspects of X-ray absorption and photoelectron spectroscopy. After a simplified theoretical view, one will concentrate on the dependence of the X-ray absorption cross section on the final state of the electron undergoing X-ray induced transitions. Therefore, X-ray absorption spectroscopy will be discussed as a tool to investigate the available one-electron free states, including orbitals with different symmetries in molecules or ionic solids, or conduction states modified by the presence of the core hole

in metals [1]. Then, for energies above the absorption edge, the modification of the free electron's wavefunction by the environment of the absorbing atom will be shown to induce oscillations of the absorption cross section as function of the photon energy, giving rise to near-edge X-ray absorption spectroscopy (NEXAFS), X-ray absorption near-edge structure (XANES) or extended X-ray absorption fine structure (EXAFS) [2]. One will show how these data are analyzed and how atomic structures can be obtained, even for disordered solids or liquids where X-ray diffraction cannot provide detailed structural information. Finally, for absorption of circularly-polarized photons on magnetic solids, the technique of X-ray magnetic circular dichroism (XMCD) will be presented, together with the sum rules allowing one to derive separately orbital and spin moments for each kind of atom from the sample [3].

The second part of the lecture will deal with photoelectron spectroscopy. Firstly, the X-ray photoelectron spectroscopy (XPS) or electronic structure for chemical analysis (ESCA) method will be presented, emphasizing the main abilities of this technique: it allows one to derive chemical composition and the nature of the compounds formed (i. e. ionization states, hybridization) with surface sensitivity [4]. Then, other XPS-based techniques will be introduced, such as ion sputtering assisted depth profiling, XPS with angular resolution which is affected by diffraction phenomena [5] of the outgoing photoelectrons on the environment (X-ray photoelectron diffraction, similar to XANES and EXAFS), then we will concentrate on the spectroscopy of electrons excited from the valence band, allowing one to derive the occupied density of states or, when performed with angular resolution, to derive the electronic structure of single crystals, i. e. the dispersion law

[4,6]. This technique can also be performed with spin resolution, allowing one to characterize completely the electronic states in magnetic materials [7]. Novel developments in the field of photoelectron spectroscopies will be briefly reviewed, such as the ability of this technique to investigate band bending at surfaces or interfaces [8], and to characterize free ferroelectric surfaces by this technique. Another developments concerns X-ray spectroscopies with spatial resolution, such as nano-XAFS [9] or ESCA spectro-microscopy [10]. Finally, a short review will be provided regarding the instrumentation needed for such investigations, in particular surface and interface methods, ultrahigh vacuum requirements, and synchrotron radiation X-ray sources available nowadays.

**Acknowledgements.** This work was funded by the Romanian Ministry of Research, Innovation and Digitalization through the UEFISCDI Project PN-III-P4-ID-PCCF-2016-0047 (Contract No. 16/2018).

- [1] J. Stöhr, NEXAFS Spectroscopy, Springer, Berlin, **1996**.
- [2] B. K. Teo, EXAFS: Basic principles and data analysis, Springer, Berlin, **1986**.
- [3] C. M. Teodorescu, F. Chevrier, R. Brochier, V. Ilakovac, O. Heckmann, L. Lechevalier, K. Hricovini, Eur. Phys. J. B **2002**, 28, 305–313.
- [4] S. Hüfner, Photoelectron spectroscopy: Principles and applications, Third Edition, Springer, Berlin, **2003**.
- [5] M. Izquierdo, M. E. Dávila, J. Avila, H. Ascolani, C. M. Teodorescu, M. G. Martin, N. Franco, J. Chrost, A. Arranz, M. C. Asensio, Phys. Rev. Lett. **2005**, 94, 187601.
- [6] A. Damascelli, Z. Hussain, Z. X. Shen, Rev. Mod. Phys. **2003**, 75, 473–541.

- [7] S. LaShell, B. A. McDougall, E. Jensen, Phys. Rev. Lett. **1996**, 77, 3419–3422.
- [8] N. G. Apostol, C. M. Teodorescu, in Surface Science Characterization Techniques for Nanomaterials, C. Kumar (Ed.), Springer, Berlin, **2015**, pp. 405–461.
- [9] M. Janousch, A. M. Flank, P. Lagarde, G. Cauchon, S. Bac, J. M. Dubuisson, T. Schmidt, R. Wetter, G. Grolimund, A. M. Scheidegger, AIP Conf. Proc. **2004**, 705, 312–315.
- [10] D. G. Popescu, M. A. Huşanu, L. Trupină, L. Hrib, L. Pintilie, A. Barinov, S. Lizzit, P. Lacovig, C. M. Teodorescu, Phys. Chem. Chem. Phys. **2015**, 17, 509–520.

## **PAMS-IL: Synthesis and properties of low-dimensional electronic and magnetic materials**

D. Kumar

Department of Mechanical Engineering, North Carolina Agricultural and Technical State University, Greensboro North Carolina, USA

This talk will focus on the synthesis of advanced top-down and bottom-up methods of the synthesis of low-dimension materials electronic and magnetic materials. The research interests in LD materials are motivated by the opportunity to realize properties that lie between that of individual atoms and the three-dimensional (3D) bulk materials. The energy levels of the LD materials are different from bulk, which provides a unique handle to fine-tune the electronic states. The emphasis will be given to the synthesis of 1D nanostructures that is quite challenging as it requires constraining the growth of materials in two directions to a few nanometers and allowing a faster growth in the third direction. The second part of the presentation will focus on the



novel electronic and magnetic properties in these materials that is realized at their quantum mechanical length scales.

## **PAMS-IL-online: Plasma Processes for Advanced Materials-Related Applications**

I. Topala

*Iasi Plasma Advanced Research Center (IPARC), Faculty of Physics, 'Alexandru Ioan Cuza' University of Iasi, Iasi, Romania*

Plasmas are being used for long time for treatment and deposition of advanced materials. Compared to the materials deposited using other methods (e.g. mechanochemical synthesis, condensation, physical vapour deposition, plasma deposition, combustion and pyrolysis, pulsed laser deposition, atomic layer deposition), the physical and chemical properties of plasma deposited materials, as well as the microscopic aspects are remarkably different, making them suitable for a various applications: quantum processes, optics, electricity and magnetism, energy conversion and storage, life sciences, protection, tribology.

A large family of industrial and laboratory plasma sources are available nowadays, employing technological solutions from low pressure to atmospheric pressure, very different pulsing regimes and working gases. Indeed, plasma deposition represents nowadays top technological solution for many applications. The performance of plasma deposited materials in real applications are intrinsically linked with the control of plasma processes as well with the advanced knowledge and real-time diagnosis of plasma parameters (Fig. 1).

## Wednesday, September 14, 2022

08:00	<b>Poster Session PAMS-5</b> Near HALL 1-University of Dubrovnik
10:00	<b>Poster Sessions II and Coffee break</b>
12:00	<b>Lunch</b>
15:00	<b>Invited Lectures</b> HALL 3
17:00	<b>Coffee break</b>
17:30	<b>Invited Lectures</b> HALL 3
20:00	<b>Gala Dinner</b>

## Poster Session (near HALL 1)

### PAMS-P: Synthesis of cobalt and manganese ferrite nanoparticles uncoated and coated with silver as contrast agents in magnetic resonance imaging

V. Sabie<sup>1</sup>, R. S. Danila<sup>2</sup>, I. Radu<sup>2</sup>, A. Pui<sup>2</sup>, I. Dumitru<sup>1</sup>, F. Iacomi<sup>1</sup>

<sup>1</sup> Faculty of Physics, Alexandru Ioan Cuza University, Iasi, Romania

<sup>2</sup> Faculty of Chemistry, Alexandru Ioan Cuza University, Iasi, Romania

$\text{Co}_n\text{Zn}_n\text{Fe}_2\text{O}_4$  and  $\text{Mn}_n\text{Zn}_n\text{Fe}_2\text{O}_4$  nanoparticles were obtained by chemical co-precipitation method, by mixing certain contents of cobalt, manganese, zinc and iron chlorides in distilled water. Some of the nanoparticles were covered with silver, using silver nitrate and carboxymethylcellulose as surfactant. The water colloidal suspensions obtained were investigated as contrast agents in magnetic resonance imaging (MRI).[1]

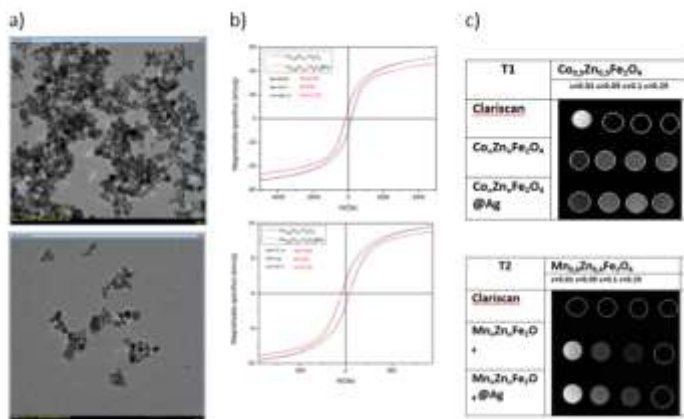


Figure 1.  $\text{Co}_n\text{Zn}_n\text{Fe}_2\text{O}_4/\text{Ag}$  and  $\text{Mn}_n\text{Zn}_n\text{Fe}_2\text{O}_4/\text{Ag}$  nanoparticles and colloids characterization: a) TEM; b) VSM; c) MRI.

[1] D. D. Andharea, S. R. Patadea, J. S. Kounsalyea, K. M. Jadhava, Phys. B: Condens. Matter. 2020, 583, 15, 412051.

### **PAMS-P: Study of the efficiency of solar cells in polluted environments: advanced analysis techniques in vivo and in the laboratory, through COMSOL type simulations**

A. Cocean<sup>1</sup>, S. Garofalide<sup>1</sup>, V. Pelin, G. Cocean<sup>1,2</sup>, C. Postolachi<sup>1</sup>, I. Motrescu<sup>3</sup>, L. Leontie<sup>1</sup>, I. Cocean<sup>1</sup>, S. Gurlui<sup>1</sup>

<sup>1</sup>*Alexandru Ioan Cuza University of Iasi, Faculty of Physics, Atmosphere Optics, Spectroscopy and Laser Laboratory (LOASL), 11 Carol I Bld. 700506 Iasi, Romania*

<sup>2</sup>*Rehabilitation Hospital Borsa, 1 Floare de Colt Street, 435200 Borsa, Romania*

<sup>3</sup>*Sciences Department & Research Institute for Agriculture and Environment, Iasi University of Life Sciences, 3 Sadoveanu Alley, 700490 Iasi, Romania*

The solar panel transforms sunlight into energy, depending on the amount of sunlight absorbed. It can be affected by deposits of pollutant particles on the surface, due to solar radiation lower absorption. The purpose of the study is to develop a simulation model that allows the optimization of the placement of solar panels in relation to the location parameters (air currents, distance from dust sources (road), as well as adhesion depending on the size of the particles. In order to predict the amount of particles deposited on a surface, such as the solar panel, a simulation was performed using COMSOL Multiphysics. Particle Tracing for Fluid Flow module based on Newton's second law was used in order to predict the motion of particles [1]. A virtual wind tunnel ending with the outlet was built up in a 3-D geometry where the surface is razed on a level to simulate the solar panel mount using a constant air flow in a time dependent mode. The deposition is virtually performed on

a ledge in the wind tunnel. The number of deposited particles is evaluated using the particle counting function. Parametric sweep on particles size, wind velocity, number of particles released and their density is applied to cover a large variety of possible situations. The ledge influenced the number of particles deposited presumably due to air currents. The height from which the particles are launched is also very important concerning distance where they tend to deposit. Optimization was studied using geometry variation (Figure 1 (a)). The numerical study, by simulation in COMSOL, using the finite element method, is part of the work program that also involves the experimental study in situ and spectroscopic analysis. For this reason, the parameters used in the simulation are characteristics of the area where the experimental, in situ study is intended to be continued, namely the solar panels located in the courtyard of the Golia Monastery in Iasi, Romania (Figure 1 (b)).

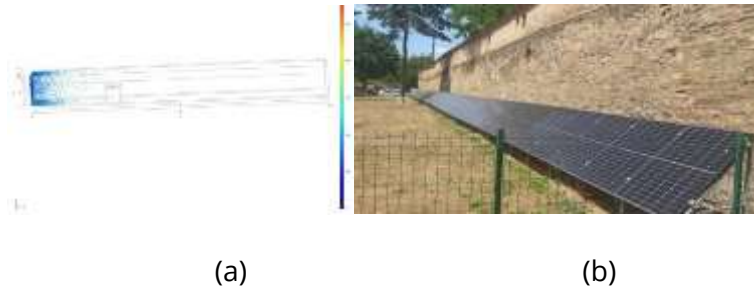


Figure 1. Optimization of solar panel disposal (a). The placement of solar panels in the courtyard of the Golia Monastery in Iasi, Romania (b).

Aknowledgements. This work was supported by a grant of the Ministry of Research, Innovation and Digitization, CNCS - UEFISCDI, project number PN-III-P1-1.1-PD-2021-0208, PD 53, within PNCDI III; Ministry of Research, Innovation and Digitization, project FAIR\_09/24.11.2020, the Executive Agency for Higher Education, Research, Development and Innovation, UEFISCDI, ROBIM, project number PN-III-P4-ID-PCE2020-0332, and Operational Program Competitiveness 2014–2020, Axis 1, under POC/448/1/1 research infrastructure projects for public R&D institutions/Section F 2018, through the Research Center with Integrated Techniques for Atmospheric Aerosol Investigation in Romania (RECENT AIR) project, under grant agreement MySMIS No. 127324.

1]A. Cocean, I. Cocean, S. Gurlui, F. Iacomi, U.P.B. Sci. Bull., Series A, 2017, 79(2) 1-12, ISSN 1223-7027.

### **PAMS-P: Synthesis, characterization and spectroscopic properties of Eu-doped SrTiO<sub>3</sub> ceramics sintered from sol-gel derived powders**

C. Tihon<sup>1</sup>, C. Stanciu<sup>1</sup>, G. Stanciu<sup>1</sup>, M. Cernea<sup>2</sup>

<sup>1</sup>*National Institute for Laser, Plasma and Radiation Physics, Laboratory of Solid-State Quantum Electronics, Atomistilor Street 409, Magurele 077125, Ilfov, ROMANIA*

<sup>2</sup>*National Institute of Materials Physics, Atomistilor 405 A Magurele Ilfov, ROMANIA*

In recent years, oxide materials doped with rare-earth (REs) have attracted significant attention because they can be excited with infrared and ultraviolet light to produce red, green, and blue emissions [1–3]. Luminescent oxides are phosphors that

possess higher physical and chemical stability than traditional luminescent materials based on sulfur and phosphorus. They are also interesting because they can be synthesized with low-cost methods, and most of them are not toxic [4].

The present work focuses on the synthesis and spectroscopic characterization of Eu-doped  $\text{SrTiO}_3$  ceramics, obtained by the sol-gel method, from stoichiometric quantities of high purity alkoxides. As a result of the thermal treatment, solid ceramic samples were obtained. To establish the phase composition, the crystallinity of the precursors, and purity of the final powders and related ceramics, X-ray diffraction (XRD) measurements were performed. A HITACHI S2600N scanning electron microscope (SEM) coupled with energy-dispersive X-ray spectroscopy (EDX) analyzed the ceramic samples microstructure and chemical composition. The grain size of the ceramics was determined as the mean intercept length by taking into account measurements on  $\sim 60$  grains and was 80nm.

The luminescence properties of the perovskites are improved by increasing the europium concentration. The narrow bands in the luminescent spectrum of  $\text{Eu}^{3+}$  are sensitive to the crystallographic site symmetry occupied by  $\text{Eu}^{3+}$  ions. The electric dipole transition,  $^5\text{D}_0 \rightarrow ^7\text{F}_2$ , is allowed when  $\text{Eu}^{3+}$  is located at a noncentrosymmetric crystallographic site, while the  $^5\text{D}_0 \rightarrow ^7\text{F}_1$  magnetic dipole transition comes from Eu ions in sites with inversion symmetry. Usually, the luminescence intensity ratio of  $^5\text{D}_0 \rightarrow ^7\text{F}_2$  to  $^5\text{D}_0 \rightarrow ^7\text{F}_1$ , also called the asymmetry ratio, is considered a probe to detect the inversion symmetry around  $\text{Eu}^{3+}$  ions in the host [5].

This work was supported by a grant of the Ministry of Research, Innovation and Digitization, CNCS – UEFISCDI, project number

PN-III-P1-1.1-TE-2021-1624 within PNCDI III and project 16N/08.02.2019 Program NUCLEU-LAPLAS VI.

- [1] Q. Liu et al., Spectrochim. Acta A Mol., **2012**, 87, 190–193, 2012.
- [2] Z. Xia et al., J. Mater. Chem. C, **2013**, 1, 37, 5917–5924.
- [3] X. Zhao et al., Optics Express, 2013, 21, 25, 31660–31667.
- [4] V. Sivakumar et al., J. Electrochem. Soc., **2005**, 152, 10, H168–H171.
- [5] F. Gu et al., J. Cryst. Growth, **2006**, 289, 1, 400–404.

**PAMS-P: Copolymers-based micelles obtained by solid-phase synthesis with controlled disassembly property triggered by pH variation for drug delivery applications**

R. Ghiasim<sup>1</sup>, C. E. Tiron<sup>2</sup>, A. Tiron<sup>2</sup>, M.-G. Dimofte<sup>2</sup>, M. Pinteala<sup>1</sup>

<sup>1</sup>*Centre of Advanced Research in Bionanoconjugates and Biopolymers, “Petru Poni” Institute of Macromolecular Chemistry, 41A Grigore Ghica Voda Alley, 700487 Iasi, Romania*

<sup>2</sup>*TRANSCEND Centre, Regional Institute of Oncology, 2-4 General Henri Mathias Berthelot Street, 700483 Iasi, Romania*

Diblock copolymers of polyhistidine are known for their self-assembly into micelles and their pH-dependent disassembly due to the amphiphilic character of the copolymer and the unsaturated imidazole groups that undergo a hydrophobic-to-hydrophilic transition in an acidic pH. This property has been largely utilized for the design of drug delivery systems that target a tumor environment possessing a slightly lower extracellular pH (6.8–7.2). The main purpose of this study was to investigate the possibility of designed poly (ethylene glycol)-polyhistidine sequences synthesized using solid-phase peptide synthesis (SPPS), to self-assemble into micelles, to assess the ability of the corresponding micelles to be loaded with



doxorubicin (DOX), and to investigate the drug release profile at pH values similar to a malignant extracellular environment. The designed and assembled free and DOX-loaded micelles were characterized from a physico-chemical point of view, their cytotoxicity was evaluated on a human breast cancer cell line (MDA-MB-231), while the cellular areas where micelles disassembled and released DOX were assessed using immunofluorescence. We concluded that the utilization of SPPS for the synthesis of the polyhistidine diblock copolymers yielded sequences that behaved similarly to the copolymeric sequences synthesized using ring-opening polymerization, while the advantages of SPPS may offer facile tuning of the histidine site or the attachment of a large variety of functional molecules<sup>1</sup>.

Acknowledgements. The research leading to these results has received funding from the EEA Grants 2014-2021, under Project contract no. 37/2021.

[1] R. Ghiarasim, et al. *Nanomaterials* **2022**, 12, 11, 1798.

### **PAMS-P: Structure of bicelle-like lipid objects formed in the presence of amyloid beta peptides and calcium ions**

S. Kurakin<sup>1,2</sup>, O. Ivankov<sup>1</sup>, S. Efimov<sup>2</sup>, T. Mukhametzyanov<sup>3</sup>, N. Kucerka<sup>1,4</sup>

<sup>1</sup>*Frank Laboratory of Neutron Physics, Joint Institute for Nuclear Research, Dubna, Russia*

<sup>2</sup>*Institute of Physics, Kazan Federal University, Kazan, Russia*

<sup>3</sup>*Butlerov Chemical Institute, Kazan Federal University, Kazan, Russia*

<sup>4</sup>*Faculty of Pharmacy, Comenius University Bratislava, Bratislava, Slovakia*

Alzheimer's disease (AD), an incurable neurodegenerative disease, is one of the most dangerous illnesses in the present time and future in particular. It is known that the amyloid beta ( $A\beta$ ) peptide plays a key role in this disease, one of the transmembrane fragments of which ( $A\beta_{25-35}$ ) demonstrates extremely destructive toxic properties. Importantly, the toxic properties of this fragment are manifested in the lipid membrane of cells.

Recently the membrane breakage has been documented when studying the interactions between  $A\beta_{25-35}$  and model biological membranes mimicking the pre-AD conditions [1]. Namely, it was found that the  $A\beta_{25-35}$  peptide incorporated in the lipid bilayer consisted of fully saturated DPPC or DMPC lipids is able to cause a dramatic reorganization between initially extruded unilamellar vesicles (ULVs) and bicelle-like structures (BLSs) when transitioning through lipid thermodynamic phases. All the morphological changes in the system are triggered by the membrane-peptide interactions at the molecular level of a lipid bilayer, whereas they occur at the superstructure level. At the same time, while the membrane elastic properties are determined mainly by its thermodynamic phase, the lateral structure and fluidity of lipid bilayers has been suggested recently to be modulated by surrounding divalent ions through the formation of lipid-ion-lipid bridges and separated lipid-ion pairs [2-4].

In this work, we closely characterize the structure of BLSs in the presence of peptide for two-component systems DPPC(DMPC)+ $A\beta_{25-35}$  in water. Using small angle neutron scattering (SANS),  $^{31}\text{P}$  and  $^2\text{H}$  nuclear magnetic resonance spectroscopy (NMR), circular dichroism (CD), and dynamic light scattering (DLS), we estimate the size and structural features of

the BLSs, the secondary structure and supposed localization of the A $\beta$ <sub>25-35</sub> peptide. Experimental results suggest that the peptide forms an irregular secondary structure and apparently it is situated near the rim of BLSs to restrain the shape. At the same time, lipids are additionally located on the rim of BLSs mixing with peptides and covering the hydrophobic part of the bilayer. Intriguingly, the addition of calcium ions to the lipid-peptide systems prevents the “ULVs-BLSs” morphological transformations. Namely, NMR and SANS results have shown that already at 50 mM of calcium cations added to the lipid-peptide dispersion, the system is in the ULVs state and the transformation to BLSs is obstructed. This effect might be explained in terms of rigidification of the DMPC and DPPC lipid bilayers, when lipid-ion-lipid bridges condense the lipid packing in the ULV bilayer [3-4].

Acknowledgement. SK, OI, and NK have been supported by the Russian Science Foundation under grant 19-72-20186 with an additional support for SK (JINR AYSS-2022 grant 22-402-02).

### **PAMS-P: Cluster-assembled nanostructured films of Ni and Sn grown by cluster beam deposition technique**

J.E. Martinez Medina<sup>1,2\*</sup> D. Arl<sup>1</sup>, J. Polesel<sup>1</sup>, A.M. Philippe<sup>1</sup>, P. Grysan<sup>1</sup>, J. Guillot<sup>1</sup>, C. Vergne<sup>1</sup> and E. Barborini<sup>1</sup>

<sup>1</sup>*Materials Research and Technology department, Luxembourg Institute of Science and Technology, Belvaux, Luxembourg*

<sup>2</sup>*Department of Physics and Materials Science, University of Luxembourg, Esch-Sur-Alzette, Luxembourg*

Cluster Beam Deposition (CBD) is a very effective bottom-up technique for the synthesis of highly porous nanostructured films assembled by atomic clusters that preserve their individuality during film growth [1].

By controlling the process parameters, we can be able to tune the morphological features of cluster-assembled nanostructured films (eg, cluster size distribution, thickness, surface morphology, and porosity).

In this work is presented the achievement in production of isolated atomic clusters and the fabrication of nanostructured cluster-assembled films of Ni and Sn in a CBD prototype equipped with a Pulsed Microplasma Cluster Source (PMCS). The intraparticle structure, morphology and elemental composition features are characterized by TEM, AFM and XPS, respectively. The combination of these characterization techniques suggests that room-temperature oxidation mechanism of Sn clusters can be ascribable to Mott-Cabrera model, while for Ni clusters it is in line with the Kirkendall effect [2, 3].

[1] F. Borghi, et al., Phys. Rev. Applied **2018**, 9, 044016.

[2] E. Sutter, et al., Part. Part. Syst. Charact. **2014**, 31, 879-885.

[3] B. D. Anderson and J. B Tracy, Nanoscale **2014**, 6, 12195-12216.

### **PAMS-P: Characterizations of vacuum sintered europium doped $\text{SrTiO}_3$ ceramics using sol-gel synthesized nanopowders**

C. Stanciu<sup>1</sup>, C. Tihon<sup>1</sup>, G. Stanciu<sup>1</sup>, S. Hau<sup>1</sup>, M. Cernea<sup>2</sup>

<sup>1</sup>National Institute for Laser, Plasma and Radiation Physics, Laboratory of Solid-State Quantum Electronics, Atomistilor Street 409, Magurele 077125, Ilfov, Romania

<sup>2</sup>National Institute of Materials Physics, Atomistilor 405 A Magurele Ilfov, Romania

Perovskites-containing  $\text{Eu}^{3+}$  ions are promising for optoelectronic devices, LEDs, and lasers due to their excellent photoluminescence properties. The human eye sees optical radiation in the europium emission as red light, making these

materials particularly important. Properties of  $\text{SrTiO}_3$  depend not only on the chemical composition but also on the structure and morphology. A decrease in the grain size of  $\text{SrTiO}_3$  at the nanoscale leads to distinctive properties compared to the bulk material.

Different formulae describe europium-doped strontium titanate nanopowders: (i)  $\text{Sr}_{1-3x/2}\text{Eu}_x\text{TiO}_3$  and (ii)  $\text{Sr}_{1-x}\text{Eu}_x\text{Ti}_{1-x/4}\text{O}_3$ , where  $0 \leq x \leq 0.07$ , were prepared by the alkoxide variant of the sol-gel method.

After annealing at  $1000^\circ\text{C}$  for 3 hours, the non-stoichiometric powders with built-in Ti vacancies ( $\text{Sr}_{1-x}\text{Eu}_x\text{Ti}_{1-x/4}\text{O}_3$ ) show single-phase compositions for all the samples stoichiometric powders described by the formula  $\text{Sr}_{1-3x/2}\text{Eu}_x\text{TiO}_3$  show small amounts of secondary phases ( $\text{TiO}_2$  and  $\text{Sr}_3\text{Ti}_2\text{O}_7$ ). A slight decrease in the average particle size and a higher aggregation tendency were observed with the increase of the dopant concentration.

The pellets were vacuum sintered at  $1400^\circ\text{C}$ / 4 hours.

SEM investigations of the ceramics vacuum sintered at  $1400^\circ\text{C}$  for 4 hours indicate significant changes in the microstructural features due to dopant content and stoichiometry.

Fewer pores were observed on Eu doped  $\text{SrTiO}_3$  ceramics vacuum sintered surface, indicating a dense microstructure. The average grain sizes of Eu doped  $\text{SrTiO}_3$  ceramics are between  $0.50\ \mu\text{m}$  -  $1.08\ \mu\text{m}$  for  $x = 0, 0.1\%, 0.2\%, 0.3\%, 0.4\%, 0.5\%, 0.6\%$  and  $0.7\%$ .

A noticeable decrease in the average grain size was observed as the  $\text{Eu}^{3+}$  content increased, irrespective of the presence or absence of Ti vacancies in the nominal formula. On the other hand, more homogeneous and denser microstructures were observed for the ceramics with built-in titanium vacancies than in the case of the ceramics with strontium compensating defects, no matter the  $\text{Eu}^{3+}$  concentration.

The luminescence properties of the perovskites are improved by increasing the europium concentration.

This work was supported by a grant of the Ministry of Research, Innovation and Digitization, CNCS – UEFISCDI, project number PN-III-P1-1.1-TE-2021-1624 within PNCDI III and project 16N/08.02.2019 Program NUCLEU-LAPLAS VI.

### **PAMS-P: Studies on the Si codoped channel of a junctionless transistor**

D. Moraru<sup>1</sup>, H. Mimura<sup>1</sup> L. Hutusoru (Toderică)<sup>2</sup>, M. Dobromir<sup>3</sup> F. Iacomi<sup>2</sup>

<sup>1</sup> *Research Institute of Electronics, Shizuoka University, Hamamatsu, Japan*

<sup>2</sup>*Research Department, Faculty of Physics, Alexandru Ioan Cuza University of Iasi, Romania*

<sup>3</sup>*Faculty of Physics, Alexandru Ioan Cuza University of Iasi, Romania*

Junctionless transistors require high doping ( $>10^{19}$  atoms  $\text{cm}^{-3}$ ) to ensure a high current drive and to minimize contact resistance [1]. In this study we investigate of the dopants, P and B, in the transistor nano-channel, the I-V characteristics at low temperatures and as a function of temperature, and the influence of channel size on transport mechanism.

XPS investigations showed the presence of P and B in the junctionless transistor nano-channel.

It was observed that at low temperature and  $V_g=0$  the Coulomb gap and resistance anomaly are manifested (Fig.1).

Low temperature I-V measurements evidenced the dependence of resistance on channel width. A nonlinear decay of resistance maximum value with the increase in the channel width and temperature was established. The resistance peak width increased with the temperature.

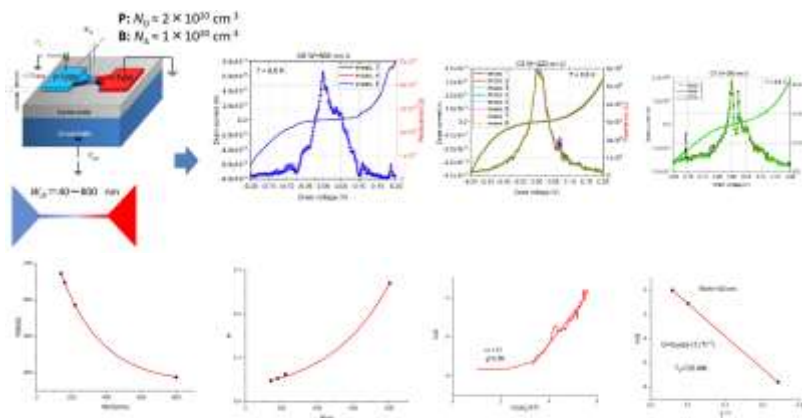


Fig.1. Effect of channel size on I-V characteristics and on Coulomb gap and resistance anomaly.

[1] D. Moraru et al, *Nanoscale Res. Lett.* **2015**, 10, 372.

## **PAMS-P: Studies on the structure and properties of some blue pigment/polydimethylsiloxane composite layers.**

A. Hrib<sup>1</sup>, G. G. Nedelcu<sup>1</sup>, M. Cazacu<sup>2</sup>, D. Timpu<sup>2</sup>, F. Iacomi

<sup>1</sup>*Faculty of Physics, Alexandru Ioan Cuza University of Iasi, Romania*

<sup>2</sup>*Petru Poni Institute of Macromolecular Chemistry, Iasi, Romania*

<sup>3</sup>*National Institute for Research and Development in Microtechnologies-IMT Bucharest, Romania*

Organic and inorganic pigments are an important group of additives that not only give color to the materials to which they are added but can also improve their applicative properties. Composites layers of cobalt blue/PDMS and ultramarine/PDMS were prepared using the mechanical mixture method, by varying the pigment content in the range 1% - 50%. Structural, optical, and dielectric properties of composite structures were investigated through X-ray diffraction, optical spectroscopy, and impedance spectroscopy.

**PAMS-P: Preparation and characterization of iron oxide thin films prepared by the metal organic deposition process**

R. Honda<sup>1</sup>, F. Iacomi<sup>2</sup>, S. Ando<sup>1</sup>

<sup>1</sup>*Department of Electrical Engineering, Faculty of Engineering, Tokyo University of science, 6-3-1 Nijuku, Katsushika, Tokyo 125-8585, Japan*

<sup>2</sup>*Faculty of Physics, "Alexandru Ioan Cuza" University of Iasi 11 Carol I Blvd., 700506 Iasi, Romania*

Currently, Silicon (Si)-based solar cells have a market share of more than 90% and are expanding in this market. On the other hand, compound semiconductor solar cells, such as Cu(In,Ga)Se<sub>2</sub> (CIGS) and CdTe/CdS, are typical examples. However, there are problems such as the presence of indium (In), a rare metal, and selenium (Se), an environmental pollutant, in the materials. Therefore, there is a need for solar cell materials that are inexpensive and excellent for the global environment. Iron oxide ( $\alpha$ -Fe<sub>2</sub>O<sub>3</sub>) is a low-cost material which is abundantly contained in the earth as a mineral (hematite), and an environmentally friendly material because of its non-toxicity.

In this study, we tried to prepare  $\alpha$ -Fe<sub>2</sub>O<sub>3</sub> thin films with good crystallinity by the metal organic deposition method using the metal-naphthenate and aimed to establish conditions for preparation.

The raw material used was iron naphthenate. In the first, the Fe naphthenate solutions were spin-coated on quartz substrates to obtain precursor films with smooth surface. Next, the spin-



coated films were heat-treated (Pyrolysis process) at 500°C for 10 min using an IR lamp in air. This process was repeated 4 times (process A). An annealing process was carried out at 800°C for 30 min in air in order to crystallize  $\alpha$ -Fe<sub>2</sub>O<sub>3</sub> thin films (Process B).

XRD patterns of so obtained thin films evidenced the diffraction peaks of  $\alpha$ -Fe<sub>2</sub>O<sub>3</sub> (Fig.1).

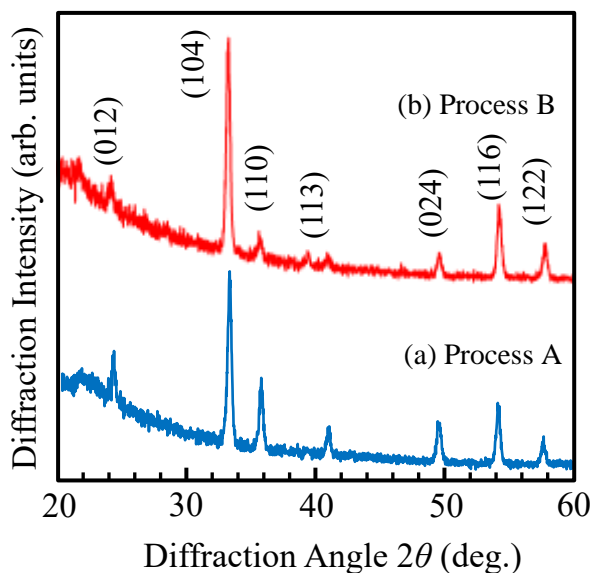


Fig.1. XRD patterns of  $\alpha$ -Fe<sub>2</sub>O<sub>3</sub> thin films prepared by: a) process A; b) process B.

## **PAMS-P: Preparation and characterization of CuInSe<sub>2</sub> thin films by an electro-deposition method**

Y. Inoue, S. Ando

*Department of Electrical Engineering, Faculty of Engineering, Tokyo University of Science, 6-3-1 Nijuku, Katsushika, Tokyo 125-8585, Japan*

Currently, silicon-based solar cells are occupying approximately 95% in the solar cell market. Copper indium gallium diselenide (Cu(In,Ga)Se<sub>2</sub> - CIGS) has attracted attention due to its high absorption coefficient and the high conversion efficiency of thin film solar cells. These thin-film solar cells already have reached the conversion efficiency in excess of 20%, and also have excellent radiation and cosmic ray resistance, making them suitable for space solar cells. Wet process for the preparation of thin films is a non-vacuum process and high raw material usage efficiency. Electro-deposition method is a low-cost one, being performed at room temperature, in a short time, with a simple apparatus.

In this study, we obtained CIS thin films by electrodeposition and established the optimal fabrication conditions. Annealing (heat treatment) was also applied to improve the crystallinity.

To prepare CIS thin films by electrodeposition, copper chloride (CuCl<sub>2</sub>), indium chloride (InCl<sub>3</sub>), and selenium dioxide (SeO<sub>2</sub>) were used as raw materials. A growth substrate (ITO/Soda lime glass) was used for the cathode and a Pt plate for the anode. The raw materials of Cu, In and Se were weighted to 1:12:2 molar ratios and dissolved in pure water to prepare an electrolyte with a total volume of

200 ml. CIS thin films were obtained by applying the constant potential pulses between the electrodes for 10 min using a pulse generator. Heat treatment was carried out at 400°C for 10 min in N<sub>2</sub> atmosphere.

Figure 1 shows the surface morphologies of (a) before annealing and (b) after annealing of CIS thin films fabricated under optimum conditions (redox potential -0.8 V,  $pH = 1.6$ ). This research enabled us to fabricate CIS thin films by the electrodeposition method. Annealing at 400°C was found to improve the crystallinity of the CIS thin films.

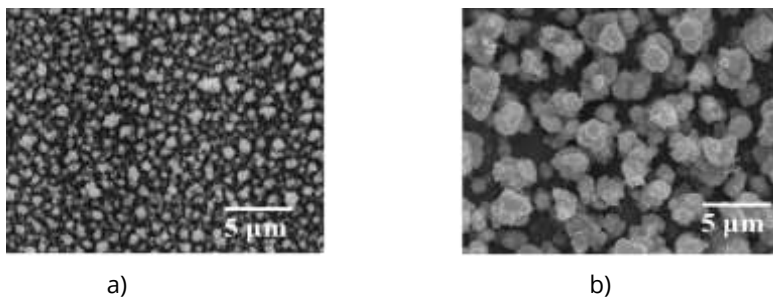


Fig.1. Surface morphologies of CIS thin films: a) before annealing and (b) after annealed (Conditions: Redox potential

### **Preparation and Characterization of SnS Thin films by the Electro-deposition Method for application to Solar Cell**

S. Takizawa, S. Ando

*Department of Electrical Engineering, Faculty of Engineering, Tokyo University of Science, 6-3-1 Nijjuku, Katsushika, Tokyo 125-8585, Japan.*

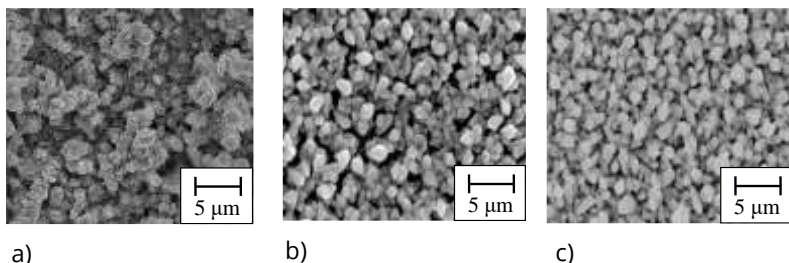
In recent years, demand for solar cells that use sunlight as an energy source has been increasing as a measure against energy conservation and global warming, and research and development of next-generation solar cells for lower cost and higher efficiency has been actively conducted. One of the materials of solar cell for the next-generation is tin sulfide (SnS), which is inexpensive because it is composed of the elements sulfur (S) and tin (Sn) and has a large absorption coefficient of the order of  $10^5 \text{ cm}^{-1}$ . Therefore, this material applied for solar cell is expected to reduce cost and increased conversion efficiency. Furthermore, the electro-deposition method is expected to reduce the cost of thin film solar cells because large area production of thin film is possible, and the cells can be prepared at normal pressure and temperature.

In this study, we investigated the establishment of conditions for the fabrication of SnS thin film by electrodeposition in order to realize SnS thin film solar cells at an early stage and to reduce their cost.

Sodium thiosulfate ( $\text{Na}_2\text{S}_2\text{O}_3$ ) and tin sulfate ( $\text{SnSO}_4$ ) were used as raw materials for the electrolyte. Each was diluted with pure water to prepare a 0.1 M (0.1 mol/L) electrolyte. As anode and cathode electrodes a platinum (Pt) plate and a Mo/glass substrate, respectively, were used. SnS thin films were deposited for 30 min with constant potential pulses between electrodes. Furthermore, the as-deposited SnS thin films were heat treated in  $\text{N}_2$  atmosphere in order to improve the crystallinity.

The surface morphologies of as-deposited SnS thin films prepared at various redox potentials by electrodeposition is shown in Fig. 1. SnS thin film prepared at -0.5 V showed large irregularities and inhomogeneous particle size. On the other hand, the SnS films prepared at -0.7 V and -1.0 V showed uniformity and smoothness in particle size. From the results of

chemical composition analysis by EDX, SnS thin film prepared at -1.0 V had a stoichiometric composition (Sn:49.8 at%, S:50.2 at%). It was concluded that SnS thin films prepared at -1.0 V and  $\text{pH}=2.7$  have a good quality with a stoichiometric composition, and an improved crystallinity.



a) b) c)  
Fig.1. Surface morphology of SnS thin films prepared at various redox potentials: a) -0.5 V; b) -0.7 V; c) -1.0 V.

### **PAMS-P: Fabrication and characterization of inkjet-printed carbon nanotube-based transistor**

R. S. Singh<sup>1,2</sup>, K. Takagi<sup>2</sup>, T. Aoki<sup>2</sup>, J. Moon<sup>2</sup>, Y. Neo<sup>2</sup>, H. Mimura<sup>2</sup>, D. Moraru<sup>2</sup>

<sup>1</sup>Graduate School of Science and Technology, <sup>2</sup>Research Institute of Electronics, Shizuoka University, Japan

The miniaturization of electronics pushes the dimensions of the key devices, Si transistors, well into the nanoscale [1], posing several fundamental challenges. Carbon nanotubes (CNTs), particularly single-walled CNTs (SW-CNTs), have been widely considered for future electronics due to their excellent transport properties, nanoscale dimensions, and flexibility [2]. SW-CNTs can be made more compatible with CMOS platforms by using appropriate deposition methods.

CNTs are typically grown or deposited by solution processing on the substrate, which does not allow adequate control of CNT density and/or local positioning. We look into the possibility of using an emerging technology called inkjet printing technology to deposit low-density SW-CNT bundles locally, intending to fabricate CMOS-compatible CNT-devices. In this work, we investigated the fabrication and electrical characterization of CNT-FETs with discrete CNT-bundles as channels at low density and with precise location.

First, we optimized the homogeneity and dispersion conditions of SW-CNTs using dimethylformamide (DMF) solvent for inkjet printing. It is well understood that obtaining a stable solution for a suitable dispersion is critical because van der Waals attractive forces between the CNTs can form nano-bundles, ropes, or agglomerates [3]. Long-time sonication was done to achieve good solution homogeneity on Si/SiO<sub>2</sub> surface. The objective of device fabrication is to deposit individual CNTs or CNT bundles between Al electrodes on SiO<sub>2</sub> to form a transistor structure. In order to accomplish this, Al electrodes (approx. 100 nm thick) with gaps of 300-5000 nm were fabricated using a lift-off method. The CNTs were deposited in the gap between Al electrodes by inkjet printing.

Figure 1(a) Shows FE-SEM images a CNT-FET containing a few CNT bridges deposited in the nano-gaps. Figure 1(b) shows room temperature output IV characteristics for the same devices. Although reference devices with connected metal electrodes exhibit high currents, the low-density CNT bridges deposited by inkjet printing in the nano-gaps of the CNT-FETs allow current to flow only at low level [4].

With further optimization of the deposition and device fabrication, inkjet printing can be expected to allow precise

control of CNTs deposition on a CMOS-compatible platform. This study can open new pathways for hybrid nano-electronics.

- [1] M. M. Waldrop, *Nature* **2016**, 530, 144-147.
- [2] R. Saito *et. al*, "Physical Properties of Carbon Nanotubes", Imperial College Press, London **1998**.
- [3] R. P. Tortorich and J. W. Choi, *Nanomaterials* **2013**, 3, 453-468.
- [4] R. S. Singh, K. Takagi, T. Aoki, J. Moon, Y. Neo, F. Iwata, H. Mimura and D. Moraru, *Materials* **2022**, 15, 4935.

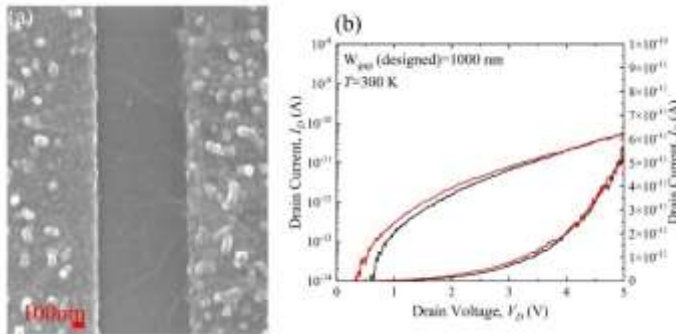


Fig. 1 a) FE-SEM image of a CNT-bridge network deposited by inkjet printing in a gap (designed gap = 1000 nm) between Al source and drain electrodes. b) Room-temperature ( $T=300$  K)  $I_D$ - $V_D$  characteristics for a CNT-FET, exhibit low current via one or a few CNT-bridge(s).

## PAMS-P: TiO<sub>2</sub> based composite materials with antifouling properties for aquaculture applications

111

M. Orfanou<sup>1</sup>, A. Bouranta<sup>1</sup>, I.V. Tudose<sup>1,2</sup>, L. Georgescu<sup>1</sup>, N. R. Vrithias<sup>2,4</sup>, G. Kenanakis<sup>3</sup>, E. Sfakaki<sup>5</sup>, N. Mitrizakis<sup>5</sup>, G. Strakantounas<sup>5</sup>, N. Papandroulakis<sup>5</sup>, C. Romanitan<sup>6</sup>, C. Pachiou<sup>6</sup>, O. Brincoveanu<sup>6</sup>, L. Barbu -Tudoran<sup>7</sup>, M. P. Sucnea<sup>1,6</sup>, E. Koudoumas<sup>1</sup>

<sup>1</sup>Center of Materials Technology and Photonics, Hellenic Mediterranean University, Heraklion 71410, Greece

<sup>2</sup> Chemistry Department, University of Crete, Heraklion, Greece,

<sup>3</sup>Institute of Electronic Structure and Laser, Foundation for Research & Technology-Hellas, Heraklion 70013, Greece

<sup>4</sup>Department of Materials Science and Technology, University of Crete, Heraklion 70013, Crete, Greece

<sup>5</sup>Institute of Marine Biology, Biotechnology and Aquaculture, Hellenic Centre for Marine Research, Heraklion 71500, Greece

<sup>6</sup>National Institute for Research and Development in Microtechnologies (IMT-Bucharest), Bucharest 023573, Romania

<sup>7</sup>Electron Microscopy Center "Prof. C. Craciun", Faculty of Biology & Geology, "Babes-Bolyai" University, 400006 Cluj-Napoca, Romania

Current technology for preventing biofouling is based on the use of toxic, biocide-containing materials, which can be a serious threat to marine ecosystems, as they affect both the targeted organisms and the environment around them. Then, it is important to fabricate new less toxic materials with antifouling properties. The purpose of this research is to develop alternative materials, which should be environmentally friendly and combine low cost, durability, ease of production and efficiency for aquaculture applications.

In recent years, there has been a strong interest in photocatalytic materials, such as TiO<sub>2</sub>, because of their support to antifouling, self-cleaning and antibacterial applications. TiO<sub>2</sub> seems to be one of the most active materials for photocatalytic action, as it also shows great stability due to its good resistance to corrosion. This



presentation reports on the preliminary results on new composite materials for aquaculture nets, using High-Density Polyethylene (HDPE)/TiO<sub>2</sub> and Cu:TiO<sub>2</sub> with different metal oxide contents. The sample nets were developed employing extrusion and 3D printing, and the obtained materials were characterized by SEM, XRD and Raman Spectroscopy, while, their antifouling properties were also evaluated. The antifouling response was determined by monitoring the prevention of growth of *Navicula* sp. diatoms and the monocellular algae *Chlorella* sp. on them. The results so far have shown that the HDPE/Cu:TiO<sub>2</sub> are promising candidates for antifouling nets.

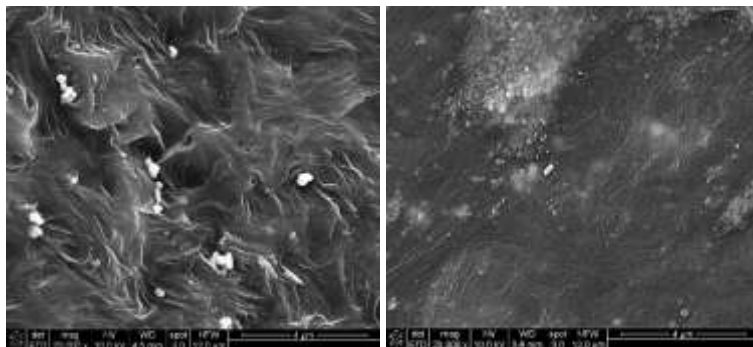


Fig. 1. Examples of SEM images of Cu:TiO<sub>2</sub>-HDPE composites a) with 5% metal oxide; b) with 15% metal oxide.

**Acknowledgement.** This work was funded by the Operational Program Fisheries and Maritime 2014–2020 in the framework of the project “Innovative materials for nets for fish farming with environmentally friendly antifouling action”, MIS 5029684. M.P.S. contribution was partially supported by the Romanian Ministry of Research, Innovation and Digitalisation thorough „MICRO-NANO-SIS PLUS” core Programme and MicroNEx, Contract nr. 20 PFE din 30.12.2021.

H. Ardeleanu<sup>1</sup>, I. Astefanoaei<sup>2</sup>, D. Creanga<sup>3</sup>

<sup>1</sup>*Alexandru Ioan Cuza University (Physics Faculty) Iasi, Romania,*

<sup>2</sup>*Alexandru Ioan Cuza University (Physics Faculty) Iasi, Romania*

<sup>3</sup>*Alexandru Ioan Cuza University (Physics Faculty) Iasi, Romania*

The aim of this work was to study cobalt ferrite magnetic nanoparticles (MNPs) that are used in tumor hyperthermia. We synthesized magnetic nanoparticles ( $\text{Co}_x\text{Fe}_{3-x}\text{O}_4$ ,  $x=0$ ,  $x=0.5$ ,  $x=1$ ) by applying the adapted chemical co-precipitation method [1]. Stabilization of MNP in water suspension was achieved by molecular coating with perchloric acid (PA) according to Laurent et al., (2008) [2].

Magnetic and microstructural characterization of MNP\_PA was performed by specific methods such as Scanning Electron Microscopy, X-ray Diffractometry, Vibrating Sample Magnetometry revealing good granularity, crystallinity and magnetic properties that were discussed depending on the cobalt content.

The heating of malignant tissue cells was studied hypothesizing magnetic nanoparticle injection into the tumor center. Mathematical modeling was carried out with focus on the previously considered cobalt ferrite nanoparticles. A spherical configuration composed of a liver malignant tissue having a radius  $R$  was considered in our simulations, with each type of  $\text{Co}_x\text{Fe}_{3-x}\text{O}_4$  nanoparticles placed into the O-center of the tissue. The most widely used thermal model is Pennes' bioheat equation model which was also utilized in our case. For each  $\text{Co}_x\text{Fe}_{3-x}\text{O}_4$  nanoparticle type the area of the magnetization

hysteresis loop was calculated aiming the final deducing of the theoretical temperature field,  $T=T(r)$ , centered on the source nanoparticle. Result discussion was done related to the cobalt content while further study was planned for the modeling of the heat transfer as function on the magnetic nanoparticle concentration. Also, nanotoxicity study in young plants will be analyzed since the nanoparticles released from human body after biomedical utilization are going to pollute water and soil.

- [1] A. Sathya, P. Guardia, R. Brescia, N. Silvestri, G. Pugliese, S. Nitti, L. Manna, T. Pellegrino, *Chem. Mater.* **2016**, 28, 6, 1769-1780.  
 [2] S Laurent, D. Forge, M. Port, A. Roch, C. Robic, L.V. Elst, R.N. Muller, *Chemical Reviews* **2008**, 108, 2064-2110.

### **PAMS-P: Radio frequency magnetron sputtering deposited ZnTe thin films physical properties study**

D. Manica<sup>1</sup>, V.A. Antohe<sup>1,2</sup>, A. Moldovan<sup>3</sup>, R. Pascu<sup>3</sup>, S. Iftimie<sup>1</sup>, L. Ion<sup>1</sup>, S. Antohe<sup>1,4</sup>

<sup>1</sup>*University of Bucharest, Faculty of Physics, 077125, Magurele, Romania D.M.*

<sup>2</sup>*Université catholique de Louvain (UCLouvain), Institute of Condensed Matter and Nanosciences (IMCN), Place Croix du Sud 1, B-1348 Louvain-la-Neuve, Belgium.*

<sup>3</sup>*National Institute for Laser, Plasma and Radiation Physics (NILPRP), P.O. Box MG-16, RO-77125, Magurele, Romania.*

<sup>4</sup>*Academy of Romanian Scientists, 3 Ilfov Street, 050044, Bucharest, Romania.*

Thin layers of zinc telluride (ZnTe) are used in various modern technologies, that are implemented in various micro and nano-structured devices such as: light emitting diodes, solar cells, photodetectors, etc Due to its characteristics depending on the deposition process such as: low resistivity, high transparency in the visible spectrum it has multiple uses. ZnTe is a sensitive material in the green spectral region with a bandgap of 2.26 eV

and a low electronic affinity of 3.53 eV, which can be used as a p-type buffer material in hetero-junction solar cells based on CdTe. [1]. It can be used also as back contact material to CdTe-based solar cells [1] in the multilayer device. It is a good material from an ecological point of view since it can be used as a replacement for the CdS window layer when obtained with n-type conductivity. ZnTe thin films were prepared by rf-magnetron sputtering, varying the deposition parameters. Depending on the selected growth conditions, an intermediate layer for the formation of junctions and the facilitation of electric charge transfer, which can be used directly in multilayer solar cells, was fabricated. In order to understand the ZnTe films structuring during growth, the investigation was centered on structure and surface morphology evolution and the surface characteristic parameters correlation with material optical properties and how these change depending on the deposition parameters. For this scope scanning electron microscopy (SEM), X-ray diffraction (XRD), atomic force microscopy (AFM), ellipsometry (spectroelipsometer-SE) and UV-Vis absorption spectroscopy, were used. Interesting information regarding correlation of film thickness with ZnTe structuring and surface morphology characteristic parameters was revealed. This study adds value to the existing knowledge regarding ZnTe thin films fabrication and their physical properties tailoring for the various applications. Fig 1 shows an example of AFM image of a ZnTe thin films.

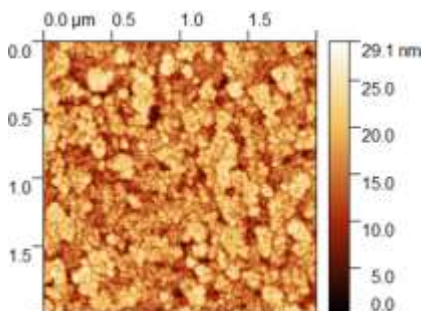


Fig. 1. Example of AFM image of a ZnTe thin film fabricated by RF magnetron sputtering.

[1] D. Manica, V-A. Antohe, A. Moldovan, R. Pascu, S. Iftimie, L. Ion, M. P. Sucheș, S. Antohe. *Nanomaterials*. **2021**; 11(9), 2286.

[2] O. Toma, L. Ion, S. Iftimie, V.A. Antohe, A. Radu, A.M. Raduta, D. Manica, S. Antohe, *Appl. Surf. Sci.* **2019**, ,478, 831-839.

### **PAMS-P: Hydrogel with hybrid structure designed for chemotherapeutic drug delivery obtained in situ by e-beam crosslinking**

M. Demeter<sup>1</sup>, A. Cimpean<sup>2</sup>, A. Negrean<sup>2</sup>, A. Scarisoreanu<sup>1</sup>, I. Calina<sup>1</sup>, M. Albu Kaya<sup>3</sup>

<sup>1</sup>*National Institute for Lasers, Plasma and Radiation Physics, Accelerators Laboratory, Magurele, Romania.*

<sup>2</sup>*Department of Biochemistry and Molecular Biology, Faculty of Biology, University of Bucharest, Bucharest, Romania*

<sup>3</sup>*Leather and Footwear Research Institute, Collagen Department, Bucharest, Romania*

Herein, bovine collagen, chitosan, carboxymethyl cellulose (CMC) poly(vinylpyrrolidone) (PVP), and poly(ethylene oxide) (PEO) three different hydrogels compositions were synthesized to be used as a new alternative for topical administration of

chemotherapeutic drugs. The hydrogel has been obtained in a single technological step (crosslinked and sterilized) without the addition of toxic chemical reagents, by irradiation with electron beams (e-beam) at 25 kGy.

The preliminary results of the CCK-8 test indicated that the 3 analyzed hydrogel compositions showed the ability to support the cell proliferation process both 24 h and 72 h post-seeding. A slight reduction in optical density values can be observed in the case of a hydrogel sample containing chitosan.

The fluorescence microscopy images revealed the presence of viable Vero cells on the 3 types of hydrogel compositions, predominantly on the surface of hydrogel samples containing collagen and CMC. A significant increase in the number of cells can also be observed with increasing incubation time, which suggests the ability of the samples to support the cell viability process.

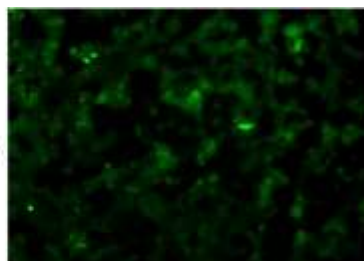
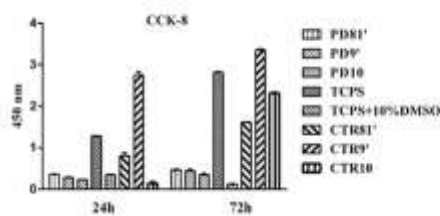


Fig. 1. The results of the CCK-8 test at 24h and 72h after seeding the VERO cells direct contact (on the surface of cross-linked hydrogels PD81'; PD9'; PD10) and indirect contact (the extraction media of non-cross-linked hydrogels CTR81'; CTR9'; CTR10). Negative cytotoxicity control - TCPS; cytotoxicity positive control - 10% DMSO.

The results regarding the non-crosslinked hydrogels showed the presence of contaminants in the cell culture, which

demonstrates the efficiency of the e-beam in terms of the final sterilization of the investigated hydrogels.

The biocompatibility results indicate the use of hydrogel composition based on collagen, CMC, PVP, and PEO for the formulation of hydrogel-containing chemotherapeutic drugs.

### **PAMS-P: Cellular response to low concentrations of AuNPs coated with lipid and chitosan**

Eliza Olteanu<sup>1</sup>, Anda Les<sup>1</sup>, Daniela A. Pricop<sup>1</sup>, Gabriela Vochita<sup>2</sup>, Iuliana Motrescu<sup>3</sup> Liviu Secarescu<sup>4</sup>, Dorina Creanga<sup>1</sup>

<sup>1</sup> Faculty of Physics, Alexandru Ioan Cuza University of Iasi, Iasi, Romania

<sup>2</sup> Department of Experimental and Applied Biology, Institute of Biological Research Iasi, branch of NIRDBS Iasi, Romania

<sup>3</sup> Ion Ionescu de la Brad University of Life, Iasi, Romania

<sup>4</sup> Petru Poni Institute of Macromolecular Chemistry of Romanian Academy, Iasi, Romania

Coupling liposomes with metal nanoparticles has generated interest due to low toxicity and signal amplification for LSPR (Localized Surface Plasmon Resonance) detection, but also for studying the interaction with cell membranes in living organisms. This work focuses on the analysis of the physico-chemical interactions of chitosan with liposomes loaded with simple and photoactivated gold nanoparticles (AuNP) in visible light, at physiological pH differences and on the toxicological effects on normal murine cells. Both the simulations based on mathematical models and the in vitro analysis showed the change in the level of lipid interaction with chitosan during the change in the pH of the digestive tract. The evaluation of the impact of nanoparticles on normal cells and the determination of cell morphology were carried out on the V-79 cell line, using the MTT viability test and respectively the observation technique through Fluorescence microscopy. As a result, cell

viability decreased with AuNPs concentration, the effect being more intense after 48 h of treatment. Comparing the two types of AuNPs, the irradiated ones show a stronger cytotoxic effect, with cell viability reaching 50.75% at the maximum concentration and after 48 hours of exposure. At the lowest concentration (0.01  $\mu\text{g/mL}$ ) cell viability varies between 91.01% (Au-Lip NPs) and 89.09% (Au-LipChi1% NPs), proving good biocompatibility. The subsequent study will focus on the analysis of the impact of coated nanoparticles at the lowest concentration on tumor cells.



Fig. 1. Two steps coating of AuNP with phosphatidylcholine and chitosan

[1] J. Nam, Y-T. Kim, A. Kang, K-H. Kim, K. R. Lee, W. S. Yun, Y. Ho, *Nanomaterials*, **2016**, 2860859, 7.



## PAMS-P: Fabrication and properties of pure and doped TiO<sub>2</sub> materials for potential agricultural applications

120

**L. Georgescu**<sup>1,2</sup>, P. Pascariu<sup>1,3</sup>, I.V. Tudose<sup>1,4</sup>, C. Romanitan<sup>5</sup>, I. Rosca<sup>3</sup>, L. Barbu-Tudoran<sup>6</sup>, M.P. Suchea<sup>1,5</sup>, E. Reditakis<sup>2</sup>, E. Koudoumas<sup>1,7</sup>

<sup>1</sup>Center of Materials Technology and Photonics, Hellenic Mediterranean University, Heraklion 71410, Greece,

<sup>2</sup>Department of Agriculture, Hellenic Mediterranean University, Heraklion 71410, Greece

<sup>3</sup>"Petru Poni" Institute of Macromolecular Chemistry, 700487, Iasi, Romania

<sup>4</sup>Chemistry Department, University of Crete, Heraklion, Greece

<sup>5</sup>National Institute for Research and Development in Microtechnologies - IMT Bucharest, Voluntari, Ilfov, Romania

<sup>6</sup>Electron Microscopy Center "Prof. C. Craciun", Faculty of Biology & Geology, "Babes-Bolyai" University, Cluj-Napoca, 400006, Romania

<sup>7</sup>Department of Electrical and Computer Engineering, School of Engineering, Hellenic Mediterranean University, 71410 Heraklion, Crete, Greece

In recent years, metal oxide nanoparticles have been used in agriculture as growth stimulators, nanofertilizers or as nanopesticides to prevent pest attack on crop, hence preventing the agricultural losses. The nanoparticles present either in the nanofertilizer or the nanopesticide can interact with plants through a variety of mechanisms and may have both a positive and negative impact. Due to photocatalytic properties of titanium dioxide nanoparticles (TiO<sub>2</sub> NPs), most of the studies where TiO<sub>2</sub> NPs were used at foliar level, have shown positive impacts on plants. When the phytotoxic response was reported, that was related to a decrease in plant growth, mitotic index, an increase in reactive oxygen species (ROS), antioxidant activity, and genotoxicity. But, in recent years, there is a worldwide effort on reducing the use of

nanoparticles in food-related products since their toxicity was proved. In this context, use of nanostructured materials in agriculture should be minimized in order to avoid nanoparticulate contamination.

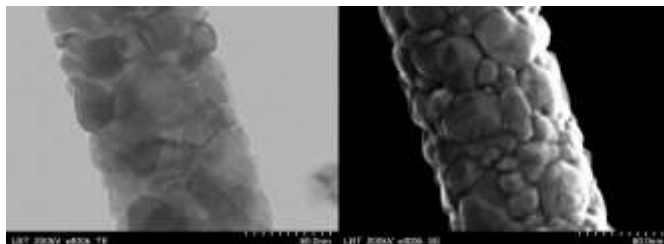


Fig. 1. Nanostructured doped  $\text{TiO}_2$  based microfiber a) STEM microstructure; b) STEM surface image.

The present work focuses on fabrication and properties of nanostructured pure and doped  $\text{TiO}_2$  based microstructures for potential use in agricultural applications. Pure and Cu, Ag and Ni doped  $\text{TiO}_2$  were fabricated by chemical and electrospinning-calcination methods and their structural and morphological properties were analysed using SEM, TEM, XRD, UV-Vis spectroscopy as well as their basic photocatalytic and antibacterial properties were tested. Results prove that nanostructured pure and doped  $\text{TiO}_2$  based microstructures with promising photocatalytic and germicide properties can be obtained for further use in agricultural applications.

Acknowledgments. PP contribution to this work was partially supported by a grant of the Romanian Ministry of Research, Innovation and Digitization, CNCS/CCCDI – UEFISCDI, project number PN-III-P1-1.1-TE-2019-0594, within PNCDI III, HMU contribution to this work was partially supported by NATO Science for Peace and Security Programme, grant G5868. M.P.S.

contribution was partially supported by the Romanian Ministry of Research, Innovation and Digitalisation thorough „MICRO-NANO-SIS PLUS” core Programme and MicroNEx, Contract nr. 20 PFE din 30.12.2021.

### **PAMS-P: Composite materials for electromagnetic shielding -fabrication and characterisation**

I.V. Tudose<sup>1,2</sup>, O. N. Ionescu<sup>3,4</sup>, C. Romanitan<sup>3</sup>, C. Pachiu<sup>3</sup>, O. Brincoveanu<sup>3</sup>, D. Stratakis<sup>5</sup>, M. P. Sucnea<sup>1,3</sup>, E. Koudoumas<sup>1,5</sup>

<sup>1</sup> *Center of Materials Technology and Photonics, Hellenic Mediterranean University, Heraklion 71410, Greece*

<sup>2</sup> *Chemistry Department, University of Crete, Heraklion, Greece*

<sup>3</sup> *National Institute for Research and Development in Microtechnologies (IMT-Bucharest), Bucharest, 023573, Romania*

<sup>4</sup> *Petroleum and Gas University of Ploiesti, 100680, Ploiesti, Romania*

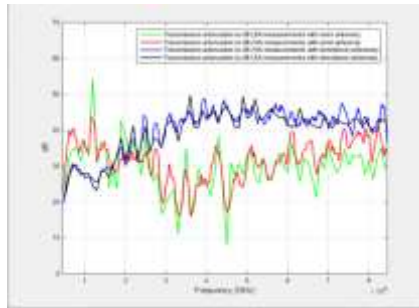
<sup>5</sup> *Department of Electrical and Computer Engineering, School of Engineering, Hellenic Mediterranean University, 71410 Heraklion, Crete, Greece*

Since EMI shielding materials are essential for reducing electromagnetic pollution in and from electronic devices, the necessity of conductive coatings rises, leading in an increase of the global EMI shielding materials share. There are various methods of protection against EM radiation, including the use of additional protective elements integrated into the design of electronic devices and in larger objects, such as residential buildings. Moreover, in order to solve the issue of human protection from the effects of EM radiation, the main idea is to use protective shielding materials, especially absorbents. In that respect, carbon allotrope nanomaterials-polymers composites have been fabricated by molten mixing methods, using different types of graphene nanoplatelets, and multiwall carbon nanotubes in polymeric matrices such as low density and high-density polyethylene [1, 2] and polypropylene. Early studies proved that a quite suitable polymeric matrix for the

desired applications would be polypropylene (PP) and MWCNTs-PP composite materials of different concentration were successfully fabricated as 1mm thick sheets and their properties were studied in the context of EMI shielding applications. Furthermore, the best method for achieving homogeneous composite MWCNTs-PP proved to be hot roll milling as described in [3].



a)



b)

Fig. 1. EMI shielding properties of MWCNT-PP composite a) experimental setup; b) comparative shielding results using a directional and an omni-directional antennas.

10% MWCNTs in PP was found having an electrical resistance of ~125 Ohm and exhibiting excellent EMI shielding performance at a wide range of frequencies. Further increasing of the MWCNTs concentration resulted in agglomeration and increased electrical resistance, leading in worse shielding performance.

**Acknowledgments.** This research has been partially co-financed by the European Union and Greek national funds through the Operational Program Competitiveness, Entrepreneurship and Innovation, under the call RESEARCH – CREATE– INNOVATE, project T1EDK-02784, with acronym POLYSHIELD. It was also funded in part by the NATO Science for Peace and Security Programme under grant G5477. IMT contribution was partially financed by the

Romanian Ministry of Research, Innovation and Digitization through “MICRO-NANO-SIS PLUS” core Programme and MicroNEx, Contract nr. 20 PFE din 30.12.2021

- [1] M. Sucheai, I. V. Tudose, P. Pascariu, E. Koudoumas, *Chapter 12*, Editor(s): Kuruvilla Joseph, Runcy Wilson, Gejo George, Materials for Potential EMI Shielding Applications, Elsevier, **2020**, 201-211,.
- [2] A. Maniadi, M. Vamvakaki, M. Sucheai, I. V. Tudose, M. Popescu, C. Romanitan, C. Pachiu, O. N. Ionescu, Z. Viskadourakis, G. Kenanakis, and E. Koudoumas., *Materials* 13, 21: 4776, 2020.
- [3] I.V. Tudose, K. Mouratis, O. N. Ionescu, C. Romanitan, C. Pachiu, O. Tutunaru, M. P. Sucheai and E. Koudoumas, *Nanomaterials*, **2022**, 12 (14) 2411.

### Invited Lectures (HALL 3)

#### **PAMS-IL: Phospholipid bilayers in drug delivery systems: from lamellar to cubic phases**

D. Uhríková

*Department of Physical Chemistry of Drugs, Faculty of Pharmacy, Comenius University Bratislava, Bratislava, Slovakia.*

Phospholipids are amphiphilic molecules. The addition of a solvent such as water hydrates selectively the hydrophilic (polar) part of each molecule, avoiding the hydrophobic region. Such phenomenon drives the molecules to self-assemble in order to minimize the contact of hydrophobic moieties with water. Hydrophobic effect and structural diversity of lipidic molecules result in a high variety of their supra-molecular assemblies [1]. Lipid in excess of water forms two phases system: a phase of lipid with a volume fraction of water trapped into its structure; and so-called “bulk” water. Fig. 1 illustrates a few structures of lyotropic liquid-crystalline mesophases formed by lipids: (a) one-dimensional lamellar phase known as multilamellar liposomes (onion-like structure); (b) two-

dimensional columnar hexagonal phase; (c) three-dimensional cubic phases of symmetries characterized by space groups. Multilamellar and unilamellar liposomes, formed by single lipid bilayer, frequently serve as a model system of lipid bilayer of biological membranes. Lipidic mesophases attract attention due to their capability to accommodate a drug into both the water phase and the hydrophobic matrix. The improved bioavailability of an anticancer drug entrapped in liposomes was introduced the first time in 1975 in an animal model [2]. A wide variety of lipidic drug delivery systems have been employed from that time. Small angle X-ray and neutron scattering (SAXS and SANS) are key techniques to study structural arrangement and polymorphic behaviour of lipid-based drug delivery systems. The structure is directly linked with bioavailability of the drug. We will review a few examples of functionality of lipid bilayers focusing on recent problems: antimicrobial mechanism of peptides that emerged as an interesting alternative of antibiotics to fight against infectious diseases; lipid-based delivery systems of genetic material (DNA, RNA) for gene therapy; and an exogenous pulmonary surfactant as a shuttle for additional drug aimed to combined therapy.

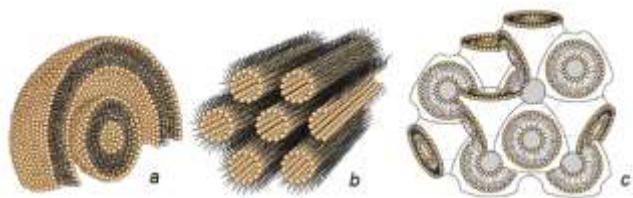


Fig. 1. Lyotropic liquid crystalline mesophases: a) multilamellar vesicle; b) inverted hexagonal phase; c) cubic phase.

Acknowledgement. Experiments were supported by projects APVV-17-0250, JINR 04-4-1121-2021/2025 and VEGA 1/0223/20.

- [1] J. N. Israelaschvili et al. J. Chem. Soc. Faraday Trans 2, Mol. Chem Phys **1976**, 72, 1525–1568.  
[2] T. Kobayashi et al. Gann **1975**, 66, 719–720.

## **PAMS-IL: Neutron Scattering for hard and soft condensed matter studies**

N. Kucerka

*Frank Laboratory of Neutron Physics at Joint Institute for Nuclear Research in Dubna and Faculty of Pharmacy at Comenius University in Bratislava*

Scientific research in general and condensed matter studies in particular have always benefited from the development of large-scale scientific infrastructures. Starting with the first X-ray tubes — coincidentally around the same time as Alzheimer's disease was identified — and all the way to modern synchrotron radiation sources, neutron sources, and powerful lasers, research approaches based on nuclear physics have been playing a significant role in the investigations of both hard and soft condensed matter. The peculiar properties of neutrons, power of synchrotrons, innovations in optical spectroscopy, including Raman, have their own niche in studies of the chemical composition and structure of condensed matter that possesses a high level of ordered or disordered — order that is the most important property of structure and disorder that is believed to be one of the foundations of life. The advances achieved over past decades developed to an extent that scattering approaches can successfully characterize the physical properties of various materials. The X-ray and neutron scattering methods are applied to elucidate the material properties previously thought to be the domain of other techniques, and even provide possibilities not present in

any other methods. In particular, neutron diffraction is utilized to determine the distribution of water or individual components through deuterium labeling. Its ability to isolate individual molecular groups at the atomic level of detail is unique among biophysical techniques and is directly comparable to molecular model simulations. The advantage of the joint refinement of X-ray and neutron scattering measurements is reflected in the improved robustness of structural models employed and in increased details made available through these advanced models. The structural studies of lipid membranes and their changes due to the environmental and compositional changes represent an important part of membrane biophysics that benefits in particular from the advancement of neutron scattering.

### **PAMS-IL: Scanning Probe Nanoimaging for Silicon and Graphene Nanoscale Devices**

Y. Tsuchiya

*Smart Electronic Materials and Systems (SEMS) Group, School of Electronics and Computer Science, University of Southampton, Southampton, UK*

Scanning Probe Microscopy (SPM) has been applied not only for studying local physical properties of materials but also for nanoscale device structures for in-depth understanding of their operational mechanism. This lecture will introduce two options of SPM; Kelvin Probe Force Microscopy (KPFM) and Tip-Enhanced Raman Spectroscopy (TERS) and will address how they are applied for investigation of silicon and graphene nanoscale device structures.

Figure 1 (a) shows a schematic diagram of KPFM that is specifically designed to be able to measure nanowire devices under operation. KPFM images of conductive silicon nanowires



under current flow taken either in vacuum or in ambient are shown in Fig. 1 (b) [1]. While the image taken in vacuum is almost identical to simulated potential profiles, characteristic hump and dip appear at the junctions between the nanowire channel and lead electrodes at either side. This anomolous fearure can be explained by considering surface charge redistribution [1]. This method also enables to investigate how the local potential profile is changed for back-gate and surface-exposed MOSFET devices under operation [2].

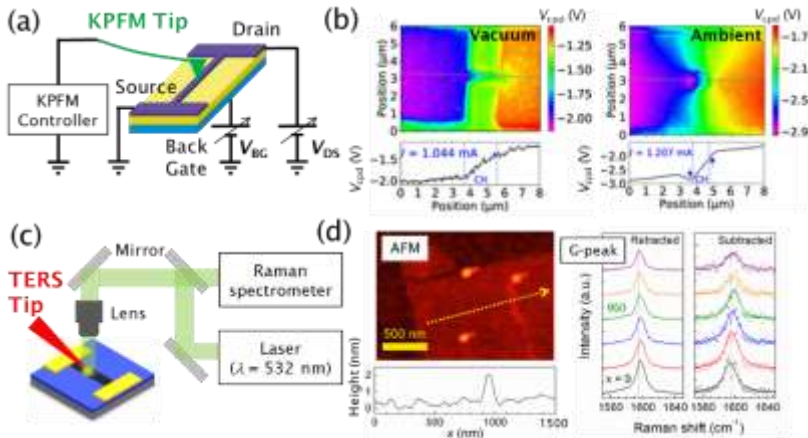


Fig. 1. (a) A schematic diagram of KPFM for devices under operation. (b) KPFM images of conductive silicon nanowires taken in vacuum and in ambient. Characteristic hump and dip appearing in ambient can be attributed to effects of surface charge redistribution [1]. (c) A schematic diagram of TERS for graphene nanostructures. (d) The AFM image shows the scanned trajectory across a wrinkle. The shift of the G-peak position has been observed only on subtracted TERS spectra [3].

Figure 1 (c) shows a schematic diagram of TERS applied for measuring graphene nanostructures. Near-field effect from Au particle on top to the TERS tip enhances Raman scattering intensity from the surface, so that high spatial resolution

exceeding laser diffraction limit is achievable. The AFM image and height profile of a graphene surface shown in Fig. 1 (d) suggest the scanned trajectory is across a wrinkle-like structure [3]. Compared with the left-hand-side spectra taken with the tip retracted, the right-hand-side subtracted TERS spectra clearly show the shift of the G-peak position along the trajectory. The analysis suggests this shift is due to modulation of doping around the wrinkle [3]. This method has been also applied for He-ion-irradiated graphene nanochannel structures to study effects of defect introduction on device characteristics [4].

[1] S. Ye, Y. Tsuchiya *et al.*, *Nanotechnology* **2021**, 32, 325206

[2] S. Ye, Y. Tsuchiya *et al.*, *MNE* **2015**.

[3] T. Iwasaki, Y. Tsuchiya *et al.*, *Carbon* **2017**, 111, 67.

[4] T. Zelai, Y. Tsuchiya *et al.*, *MNE* **2017**.

## Thursday, September 15, 2022

08:00	<b>Plenary Session</b> HALL 1-University of Dubrovnik
10:20	<b>Coffee break</b>
10:50	<b>Plenary and Invited Session</b> Hall 1
13:25	<b>Closing Ceremony</b> HALL 1
13:55	<b>Lunch</b>

**PL-online: Femtosecond laser micro- and nano-structuring of polymers for optical and thermal applications**

V. Mizeikis

*Research Institute of Electronics, Shizuoka University, Hamamatsu, Japan*

Ultrashort femtosecond and picosecond laser pulses are widely used for the fabrication of 2D and 3D structures in various materials using additive or subtractive local photomodification of the initial homogeneous material by a tightly focused laser beam [1]. Ultrafast laser structuring enables realization of maskless 3D lithography with very high spatial resolution, reaching deeply into the sub-micrometric region (Fig. 1(a)). This approach can be especially fruitful in organic photopolymerizable materials, where new optical and thermal functionalities can be created exclusively via laser structuring, i.e., without the need to tailor these cheap and abundant materials on the atomic or molecular level. Here we report on the fabrication of 3D micro- and nanostructures in hybrid organic-inorganic photoresist SZ2080[2] and organic photoresist SU-8[3]. Using tightly focused femtosecond laser beam, whose focal region is scanned in the bulk of the initial material along the desired trajectory, two-photon polymerization is induced at the focus, and fine 3D exposure patterns are created in the photoresist. Subsequently, they become transformed into 3D micro- and nanostructures using chemical development (Fig. 1(a)). We will describe several classes of polymeric structures exhibiting novel optical and thermal functionalities arising from the laser structuring: 3D

photonic crystals [1] (Fig. 1(b), electromagnetic metasurfaces [6] (Fig. 1(c), and environmental sensors [7] (Fig. 1(d)).

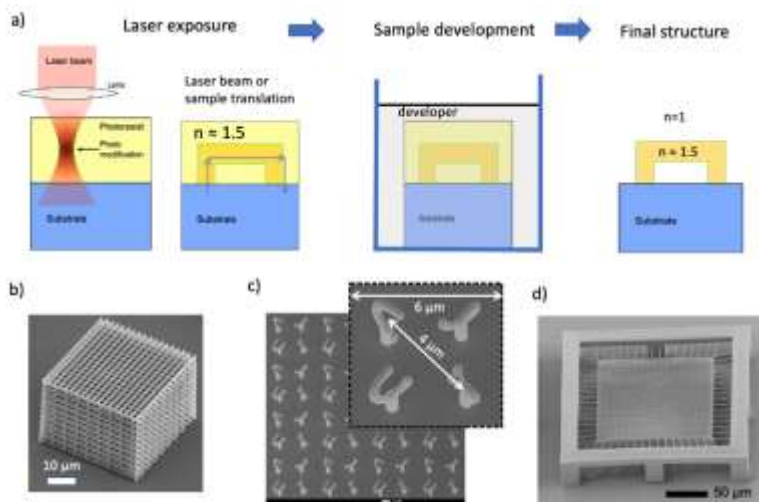


Fig. 1. Laser structuring and its applications: a) principle of laser fabrication based on two-photon polymerization, examples of various structures, b) photonic crystal, c) optical metasurface, d) environmental sensor structure.

- [1] M. Malinauskas et al., *Light: Sci.&Appl.* **5**, e16133 (2016).
- [2] A. Ovsianikov et al., *Las. Chemistry* **2008**, 493059 (2008).
- [3] <https://kayakuam.com/products/su-8-photoresists/>
- [5] M. Malinauskas et al., *Light: Sci.&Appl.* **2016**, 5, e16133.
- [6] I. Faniyeyu, V. Mizeikis, *Opt. Mater. Express*, **2017**, 7, 1453-1410 (2017).
- [7] S. Rekstyte, D. Paipulas, V. Mizeikis, *Opt. Lett.*, **2019**, 44, 4602-4604.

## **PL: Growth of metallic nanopatterns and superconducting nanodevices by Focused Ion Beam (FIB)**

J. M. De Teresa<sup>1,2</sup>, A. Salvador-Porroche<sup>1</sup>, A. T. Escalante-Quiceno<sup>1</sup>, F. Sigloch<sup>1</sup>, L. Herrer<sup>1</sup>, P. Orus<sup>1</sup>, S. Sangiao<sup>1,2</sup>, C. Magen<sup>1,2</sup>, P. Cea<sup>1,2</sup>, P. Philipp<sup>3</sup>

<sup>1</sup>*Instituto de Nanociencia y Materiales de Aragón (INMA, CSIC-Universidad de Zaragoza), Zaragoza, Spain,*

<sup>2</sup>*Laboratorio de Microscopías Avanzadas (LMA, Universidad de Zaragoza), Zaragoza, Spain,*

<sup>3</sup>*Advanced Instrumentation for Nano-Analytics (AINA), MRT Department, Luxembourg Institute of Science and Technology (LIST), Belvaux, Luxembourg*

Focused Ion Beam (FIB) techniques are very relevant to pattern materials down to the nanoscale, either through the local removal of material or through the change of physical properties produced by the ion beam. Moreover, in combination with precursors, the ion beam gives rise to the growth of nanomaterials, a technique known as Focused Ion Beam Induced Deposition (FIBID). Unfortunately, FIBID is a slow technique, which limits its applicability. In the first part of our contribution, two strategies that improve the throughput of FIBID by a few orders of magnitude will be shown. The first one is based on the condensation of precursors delivered through a gas injection system onto a cooled substrate (Cryo-FIBID) [1, 2]. The second one is based on the ion-induced dissociation of spin-coated metalorganic films, in particular Palladium Acetate films [3], as sketched below (Fig. 1). Both strategies have been applied to produce metallic nanopatterns with high lateral resolution and fast growth rate, and some applications will be shown. In the second part of the talk, our work on the growth of superconducting nanostructures by FIBID will be presented.

In particular, the use of the  $W(CO)_6$  precursor has been found to be very convenient to produce FIBID-based nanodevices [4].

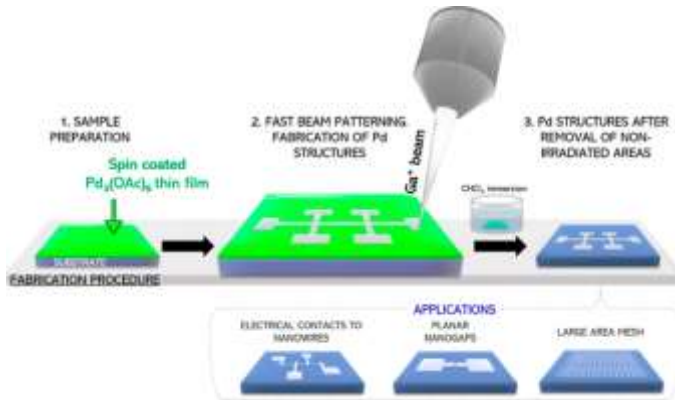


Fig. 1. Method for high-throughput growth of Pd micro- and nanostructures and the applications explored [3].

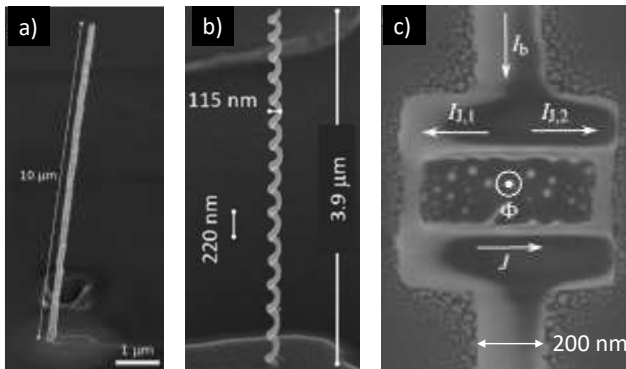


Fig. 2. W-C superconducting nanostructures by Focused Ion Beam Induced Deposition: a) using  $Ga^+$ -FIB [5]; b) using  $He^+$ -FIB [6]; c) nanoSQUID using  $Ga^+$ -FIB. [7].

Our recent efforts to grow out-of-plane superconducting nanostructures [5, 6] and in-plane nanoSQUIDs [7] will be presented and the potential applications will be discussed.

- [1] J. M. De Teresa et al., *Micromachines* **2019**, 10, 799.
- [2] A. Salvador-Porroche et al., *Nanoscale Advances* **2021**, 3, 5656
- [3] A. Salvador-Porroche et al., *ACS Appl. Mater. & Inter.* **2022**, 14, 28211
- [4] P. Orús et al., *Nanomaterials* **2022**, 12, 1367
- [5] P. Orús et al., *J. Solid State Chem.* **2022**, doi: 10.1016/j.jssc.2022.123476
- [6] R. Cordoba et al., *Nano Letters* **2019**, 19, 8597.
- [7] F. Sigloch et al., arXiv.: 2203.05278

### **PL: Silicene: a dream comes true**

P. Castrucci

*Department of Physics, University of Roma Tor Vergata, Roma, Italy*

Among graphene-like two-dimensional materials, silicene has been for a long time a dream for the scientific community for its theoretically predicted unique conductive properties due to its massless fermion carriers [1,2], the possibility to engineer its small energy bandgap by doping, applying electric or magnetic fields and to exploit its abilities in vertical and/or all metal (e.g. graphene/silicene) devices [1,3]. Due to Si inherent  $sp^3$  hybridization giving rise to no Si van der Waals (vdW) exfoliable structure, experimentally the only possibility to obtain silicene is through Si chemical or/and physical deposition methods. In this respect, substrate proved to play a fundamental role in the Si atom absorption process leading, in case of metal substrates, to a mixed phase formation [4-7] and, for vdW chemical inert substrates, to Si atom intercalation occurring even at room



temperature [8-12]. Such an intercalation has been recently associated to the presence of surface defects [11-12]. Lately, hundreds of nanometer area quasi-free standing silicene has been successfully reported to be grown on top an almost ideal epitaxial graphene layer synthesized on 6H-SiC substrate [13]. In the present talk, a review of the most recent studies on silicene formation on inert surfaces will be elucidated, providing an efficient and simple way to produce high quality and large-scale material on an inert and well-ordered surface.

- [1] M. Spenser, T. Morishita (Eds) *Silicene. Structure, Properties and Applications*, Springer, **2016**.
- [2] S. Cahangirov, M. Topsakal, E. Akturk, H. Sahin, S. Ciraci, *Phys. Rev. Lett.* **2009**, 102, 236804.
- [3] Y.Y. Wang, Z.Y. Ni, Q.H. Liu, R.G. Quhe, J.X. Zheng, M. Ye, D.P. Yu, J.J. Shi, J.B. Yang, J. Li, J. Lu, *Adv. Funct. Mater.* **2015**, 25, 68-77.
- [4] P. Vogt, P. De Padova, C. Quaresima, J. Avila, E. Frantzeskakis, M.C. Asensio, A. Resta, B. Ealet, G. Le Lay, *Phys. Rev. Lett.* **2012**, 108,155501.
- [5] Lin et al., *Phys. Rev. Lett.* **2013**, 110, 076801.
- [6] L. Meng, Y.L. Wang, L.Z. Zhang, S.X. Du, R.T. Wu, L.F. Li, Y. Zhang, G. Li, H.T. Zhou, W.A. Hofer, H.J. Gao, *Nano Lett.* **2013**, 13 685-690.
- [7] L. Huang, Y.F. Zhang, Y.Y. Zhang, W.Y. Xu, Y.D. Que, E. Li, J.B. Pan, Y.L. Wang, Y.Q. Liu, S.X. Du, S.T. Pantelides, H.J. Gao, *Nano Lett.* **2017**, 17, 1161-1166.
- [8] R. van Bremen, Q.R. Yao, S. Banerjee, D. Cakir, N. Oncel, H.J.W. Zandvliet, *Beilstein J. Nanotech.* **2017**, 8,1952-1960.
- [9] M. De Crescenzi, I. Berbezier, M. Scarselli, P. Castrucci, M. Abbarchi, A. Ronda, F. Jardali, J. Park, H. Vach, *ACS Nano*, **2016**, 10,11163-11171.
- [10] I. Kupchak, F. Fabbri, M. De Crescenzi, M. Scarselli, M. Salvato, T. Delise, I. Berbezier, O. Pulci, P. Castrucci, *Nanoscale* **2019**, 11, 6145-6152.

- [11] F. Ronci, S. Colonna, R. Flammini, M. De Crescenzi, M. Scarselli, M. Salvato, I. Berbezier, F. Jardali, C. Lechner, P. Pochet, H. Vach, P. Castrucci, *Carbon* **2020**, 158, 631-641.
- [12] F. Fabbri, M. Scarselli, N. Shetty, S. Kubatkin, S. Lara-Avila, M. Abel, I. Berbezier, H. Vach, M. Salvato, M. De Crescenzi and P. Castrucci, **2022** submitted to *Surfaces and Interfaces*
- [13] Z. Ben Jabra, M. Abel, F. Fabbri, J.-N. Aqua, M. Koudia, A. Michon, P. Castrucci, A. Ronda, H. Vach, M. De Crescenzi, I. Berbezier, *ACS Nano* **2022**, 16, 5920–5931.

## Plenary and Invited Session (HALL 1)

### T4-PL: Growth mechanisms and magnetic properties of ultrathin ferrite films

K. Kuepper, T. Pohlmann, J. Thien, J. Rodewald, K. Ruwisch, J. Wollschläger<sup>1</sup>

*University of Osnabrück, Department of Physics, Barbarastrasse, 7, 49076 Osnabrück, Germany*

Transition metal ferrites with (inverse) spinel structure are in the focus of current research due to a number of intriguing properties, including high Curie temperatures and significant magnetic saturation moments. Here magnetite,  $\text{Fe}_3\text{O}_4$  is one of the most frequently investigated materials due to its predicted half-metallic behavior with 100% spin polarization.

In the other hand, the magnetic insulator cobalt ferrite,  $\text{CoFe}_2\text{O}_4$ , is an interesting candidate due the so-called spin filter effect, which is a result of the exchange splitting of the energy levels in the conduction band that leads to different tunnel barrier heights for spin-up and spin-down electrons. However, the theoretical promises were never quite met experimentally

up to now. These drawbacks are associated to the structural properties of the ultrathin ferrite films at the interface between thin film and substrate such as antiphase boundaries (APBs) or other interface effects. Also the exact cationic distribution (degree of spinel inversion) at the interface and the surface of the thin films are of utmost importance.

Therefore, we performed a series of experimental works to investigate the growth mechanisms and the chemical and magnetic properties in depth. We performed time resolved x-ray diffraction and photoelectron spectroscopy of the growth of  $\text{Fe}_3\text{O}_4$  and  $\text{CoFe}_2\text{O}_4$  thin films in order to investigate the thickness-dependent evolution of Bragg reflections sensitive to the octahedral and tetrahedral sublattices of the inverse spinel structures [1,2]. The magnetic properties of magnetite thin films at the interface to the substrate and the surface were studied in detail employing a combination of x-ray magnetic circular dichroism and x-ray resonant magnetic reflectivity [3,4]. We also worked out an alternate pathway to form ultrathin  $\text{Co}_x\text{Fe}_{3-x}\text{O}_4$  films by interdiffusion of  $\text{Fe}_3\text{O}_4/\text{CoO}$  [5] and  $\text{CoO}/\text{Fe}_3\text{O}_4$  [6,7] bilayers instead of Co and Fe co-deposition.

- [1] T. Pohlmann et al., Phys. Rev. B **105**, 045412 (2022) .
- [2] K. Ruwisch et al., Materials **15**, 2377 (2022).
- [3] T. Pohlmann et al., Phys. Rev. B **102**, 220411(R) (2020).
- [4] T. Pohlmann et al., Phys. Rev. B **105**, 235436 (2022) .
- [5] J. Rodewald et al., Phys. Rev. B **100**, 155418 (2019).
- [6] J. Thien et al., J. Phys. Chem. C **124**, 23895 (2020).
- [7] J. Thien et al., Materials **15**, 46 (2022).

## **PL-online: Screen printed flexible thermoelectric generators (TEGs) for large-scale thermal energy harvesting**

139

L. Tzounis<sup>1,2</sup>, F. Simopoulos<sup>2,3</sup>, P. Mangelis<sup>2,3</sup>, E. Kymakis<sup>2,3</sup>, E. Koudomas<sup>2,3</sup>

<sup>1</sup>*Mechanical Engineering Department, Hellenic Mediterranean University, Estavromenos, 71004 Heraklion, Greece*

<sup>2</sup>*Center of Materials Technology and Photonics, Hellenic Mediterranean University, 71410 Heraklion, Crete, Greece*

<sup>3</sup>*Electrical and Computer Engineering Department, Hellenic Mediterranean University, Herakleio 71004, Greece*

Waste heat produced globally by the most common end-use sectors including transportation, industrial, commercial & residential as well as electricity generation on a global scale, it is estimated at 72% of the global primary energy consumption. In more detail, 63% of the aforementioned waste energy concerns temperatures below 100°C. Thermoelectric (TE) energy harvesting through the so-called thermoelectric generator (TEG) devices could be an emerging and promising technology of renewables in a wide range of applications

In this talk, highly efficient screen-printed flexible TEGs consisting of single walled carbon nanotubes (SWCNTs) will be discussed in detail regarding i.e. the SWCNT ink formulations, the screen printing parameters, the TEG device characterisation as well as practical applications powered-up by the TEG device [Fig. 1]. Namely, in our previous published articles [1], we have achieved the highest to date thermoelectric properties and efficiency of p- and n-type SWCNTs as well as the resulting TEG device that will be discussed in this presentation; i.e.  $S > 50 \mu\text{V/K}$  for p-doped and  $< -40 \mu\text{V/K}$  for n-doped CNT nanomaterials, electrical conductivity

$\sigma = 104 \text{ S/m}$  with power factors  $\text{PF} > 350 \text{ } \mu\text{W/mK}^2$  and  $300 \text{ } \mu\text{W/mK}^2$  for the p-type and n-type films (increased Power Factor by 10 times and  $\text{ZT}: 0.5\text{-}1.0$  reaching TEG device efficiency of  $\eta = 5\text{-}10\%$ ).

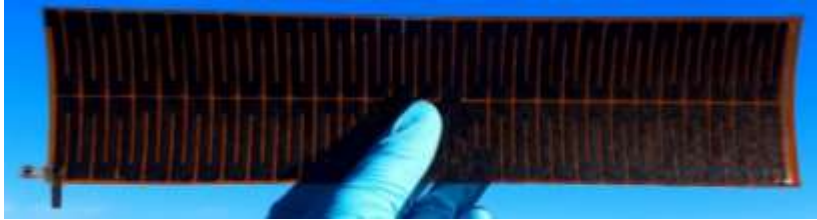


Fig. 1. TEG device (300mm length – 50mmwidth) screen printed onto a Kapton polymeric and flexible substrate, consisting of serially interconnected p- and n-type SWCNTs.

The TEGs presented herein would be highly scalable potentially to be fabricated in a continuous roll-to-roll (R2R) printing process, allowing the large-scale manufacturing/industrial production of highly efficient flexible TEGs and consequently large-scale thermal energy harvesting. In Figure 2, a TEG device is demonstrated, capable of powering-up a commercial step-up converter from body temperature- lost heat up to different thermal gradients, allowing potential practical applications e.g. self-powered IoT devices, wearable sensors, etc. This TEG device shown consists of p-type and n-type SWCNT films beyond  $308 \text{ } \mu\text{W/mK}^2$  and  $258 \text{ } \mu\text{W/mK}^2$  power factors, respectively, at  $\Delta T = 150 \text{ K}$  ( $T_{\text{HOT}} = 175^\circ\text{C}$ ) and outstanding stability in air without advanced and expensive encapsulation, while it delivers an open-circuit voltage  $\text{VOC} = 1.05 \text{ V}$  and short-circuit current  $\text{ISC} = 1.30 \text{ mA}$  at  $\Delta T = 150 \text{ K}$  ( $T_{\text{HOT}} = 175^\circ\text{C}$ ) with an internal resistance of  $R_{\text{TEG}} = 806 \text{ } \Omega$ , generating a maximum power output ( $P_{\text{max}}$ ) of  $342 \text{ } \mu\text{W}$ .

[1] Tzounis et. al. ACS Appl. Mater. Interfaces **2021**, 13, 9, 11151–11165.

**PL-online: Emerging 2-Terminal Memory Devices – Creation and Exploitation of Internal Electric Field for Realisation of Memory Devices**

S. Paul

*Emerging Technologies Research Centre, De Montfort University, Leicester, UK*

Intensive research is currently underway to exploit the highly interesting properties of nano-bits and/or sub-nano bits (“nano-sized particles, atoms and organic molecules”) for optical, electronic and other applications. Memory devices play an important role in the electronics arena and inspire advances in the technologies. There is always growing need to look for inexpensive, fast, high density and longer data retention time memory devices. This work describes the use of nano-bits and sub-nano bits in two terminal electronic memory devices. These devices show two electrical conductance states (“high” and “low”) when voltage is applied, thus rendering the structures suitable for data retention. These two states can be viewed as the realisation of non-volatile memory. The progress in the use of “nano/sub-nano-bits” in memory devices will be presented and invoke the conundrums that scholars of this field are currently faced with, such as questions about the electrical charging mechanism and stability of devices, proposed theories explaining the experimental data, contradictions in the published work by different groups.

[1] F. Paul, K. Nama Manjunatha, S. Paul, Materials. Advances, **2022**, 3, 5363 - 5374

[2] F. Paul, S. Paul, Small, **2022** 18 (21), 2106442.

[3] Paul, S. 2007, *IEEE Trans. Nanotechnol.*, **2007**, 6 (2) 191-195.

I. Salaoru

*Emerging Technologies Research Centre; De Montfort University, The Gateway, Leicester, LE1 9BH, United Kingdom*

Currently, the electronic memory elements are the important components of all electronic devices from computers to health monitors and from sensors to space, military and defence technologies. This is why these devices attract a huge interest from both the research and industry communities. Numerous candidates for emerging electronic memory technologies such as ferroelectric (FeRAM), phase-change random access memory (PCRAM), magneto-resistive (MRAM), resistive random-access memory (ReRAM) and organic memory have been proposed and investigated by a number of research groups worldwide [1,2]. On another hand, the current trend in electronics is to replace rigid substrates with flexible ones, supporting the development of flexible, bendable electronics. In this context of re-defining memory technology, organic materials are the best candidates to fulfill the current pathway in memory technologies and applications. It should be highlighted that the organic materials offer a large number of advantages such as: being able to be processed at a low temperature over large area on flexible substrates using wet-processing techniques, have low weight and great mechanical flexibility [3-5].

The organic memory devices can be fabricated either by depositing a polymer blend or a polymer composite (blend of polymer and small organic molecules or nanoparticles) between two metal electrodes.

We obtained organic (polymer blend and admixture of organic polymer, small organic molecules and nanoparticles) based two terminal non-volatile memories. The physical

switching/charging mechanism(s) along with experimental evidence are studied. Along with the electrical experimental results, we have also used the chemical characterization tools to further understand the operating mechanism that is also discussed.

**Acknowledgments** The author would like to thank the EPSRC (Grant #EP/E047785/1) for supporting this work.

- [1] S. Lee, S. Kim, and H. Yoo, *Polymers*, **2021**, 13(21), 3774.
- [2] S. Lombardo, B. de Salvo, C. Gerardi, and T. Baron, *Microel. Eng.*, **2004**, 72, (1–4), 388–394.
- [3] C.W. Tang, S.A. Vanslyke, *Appl. Phys. Lett.* **1997**, 51 (12), 913.
- [4] G. Yu, J. Gao, J.C. Hummelen, F. Wudl, A.J. Heeger, *Science* **1995**, 270, 1789.
- [5] F. Garnier, R. Hajlaoui, A. Yassar, P. Srivastava, *Science* **1994**, 265, 1684.

## **T5-I-online: III-V nanowires and nanostructures grown by HVPE**

Y. Andre<sup>1,2</sup>, E. Chereau<sup>1</sup>, G. Gabin<sup>1</sup>, H. Hijazi<sup>1</sup>, M. Zheghouane<sup>1</sup>, G. Avit<sup>1</sup>, C. Bougerol<sup>3</sup>, D. Paget<sup>4</sup>, V. Dubrovskii<sup>5</sup>, Ph. Shields<sup>6</sup>, N. I. Goktas<sup>2</sup>, R. R. LaPierre<sup>2</sup>, A. Trassoudaine<sup>1</sup>, E. Gil<sup>1</sup>

<sup>1</sup>*University of Clermont Auvergne, Clermont Auvergne INP, CNRS, Institut Pascal, F-63000 Clermont-Ferrand, France.*

<sup>2</sup>*Department of Engineering Physics, McMaster University, Hamilton, Ontario, Canada, L8S4L7*

<sup>3</sup>*University of Grenoble Alpes F-38000 Grenoble, France, CNRS, Institut Neel, F-38042 Grenoble*

<sup>4</sup>*Physique de la matiere condensee, Ecole Polytechnique, CNRS, Universite Paris-Saclay, 91128 Palaiseau, France*

<sup>5</sup>*Saint-Petersburg State University, Russia*

<sup>6</sup>*Department of Electronic & Electrical Engineering, University of Bath, Claverton Down, Bath BA2 7AY, UK*



III-V semiconductor materials enable a wide range of novel optic and spintronic devices. Nanometer-scale nitride semiconductor structures are often at the hearth of such applications. The performances of such devices are strongly dependent on the crystallographic, electronic and optical properties of the semiconductor material and thus on the growth processes used to synthesize the crystal structures.

Hydride Vapor Phase Epitaxy (HVPE) process exhibits unexpected properties when growing III-V and III-Nitride semiconductor micro- and nanostructures. With respect to the classical well-known methods such as Metal Organic Phase Epitaxy (MOVPE) and Molecular Beam Epitaxy (MBE), this near-equilibrium process is based on hot wall reactor technology, and the aim of this presentation is to investigate the potential of the versatile HVPE process implementing III- chloride precursors, and describe why it has been developed in the recent and last decades to grow III-Nitride and III-V semiconductor nanostructures and nanowires.

This presentation will address the growth through several regimes: selective area growth (SAG), vapor liquid solid growth (VLS) and self-catalyzed growth in the HVPE environment. In SAG, the chloride precursors are so volatile that they provide the most suitable environment for implementing selective and localized growth without any adsorption on the dielectric surface. The HVPE growth process is ruled by surface kinetics that is, by the intrinsic growth anisotropy of crystals. The facet growth rate can be set by varying the experimental parameters of temperature and vapor phase composition. In VLS-HVPE, under high mass input, the synthesis and doping are demonstrated for nanowires with a constant cylinder shape over unusual length and free of crystal defects with great

optical, quantum, spin and charge transport properties [1,2,3,4].

[1] D. Paget, et al., Phys. Rev. B, **2021**, 103, 195314

[2] G. Gabin, et al., CrystEngComm, **2021** 23 (2), 378-384

[3] H. Hijazi, et al., Nano Lett. **2019**, 7, 4498-4504

[4] G. Avit et al., Nano Lett. **2014**, 14, 2, 559-562.



interactions,  
complex phenomena and  
advanced materials  
society